

ANALYSIS OF SOIL ORGANIC CARBON STORAGE RESPONSES TO JUNIPER  
ENCROACHMENT INTO GRASSLANDS IN SEMI-ARID NORTHERN ARIZONA

By Olivia A. RoDee

A Thesis

Submitted in Partial Fulfillment  
of the Requirements for the Degree of  
Master of Science  
in Applied Geospatial Sciences

Northern Arizona University

May 2017

Approved:

Brian Petersen, Ph.D., Chair

Nancy Johnson, Ph.D.

Amanda Stan, Ph.D.

Erik Schiefer, Ph.D.

## ABSTRACT

Over the past 150 years, pinyon-juniper woodlands have increased in range and density in Northern Arizona, effectively encroaching into areas that were previously dominated by grassy vegetation. Woodland encroachment into grasslands is known to alter the soil organic content of the underlying soil and therefore carbon fluxes, which has profound implications for atmospheric carbon dioxide concentrations and thus climate. However, the effect of pinyon-juniper encroachment on soil carbon dynamics is less well understood for grasslands in semi-arid and arid regions, and no studies have undertaken the task of assessing soil organic carbon fluctuations resulting from juniper encroachment into grasslands in Northern Arizona. The objective of this study is to evaluate how soil organic carbon stocks and fluxes within soil are modified by juniper encroachment by quantifying soil organic matter and carbon content and the natural abundance of stable carbon and nitrogen isotopes in a study site characterized by a mosaic of juniper cover and grass cover. The spatial patterns of soil organic carbon driven by juniper trees across this study site will be analyzed using spatial interpolation techniques. The findings of this study will reveal the role of woodland encroachment into grasslands in the enhancement or reduction of carbon sequestration in the soil of a semi-arid region. In addition, this study will explore the spatial variability in soil organic carbon fluxes across a gradient of declining juniper influence and the accuracy of spatial interpolation techniques in illustrating this variability.

Key words: *soil science; soil organic carbon; stable carbon isotopes; stable nitrogen isotopes; vegetation change; spatial interpolation; carbon sequestration; plant-soil feedbacks*

## Acknowledgements

This thesis would have been impossible without the incredible, generous people who helped pave the way. First and foremost, thank you to my top-knotch advisor Dr. Brian Petersen for your constant support, kindness, and keen insights, and for re-directing me when I went adrift in my focus. Thank you to Dr. Nancy Johnson for showing me the complex microbial world living within the soil, for sharing your unique knowledge of plant-soil feedbacks, and for your undying enthusiasm. Thank you to Dr. Erik Schiefer for your sharp understanding of statistical analyses in earth/environmental sciences, for your openness to any and all questions, and for opening your laboratory doors to me so I could explore and run laboratory analyses with flexibility and peace. Thank you to Dr. Amanda Stan for your valuable perspectives of vegetation patterns, your guidance in preparing for field work, and taking the pressure of Teaching Assistant duties off so I could wholeheartedly dive into my study. Thank you to Dana Mandino for arranging the transportation to my field site and for your endless patience with my million questions and requests related to the logistics of my thesis and the Masters program in general. Thank you to Katherine Whitacre for mentoring me in multiple laboratory analyses and cheering me on through long hours of laboratory work. Thank you to Dr. Nick McKay for teaching me how to wield R to find meaning in seas of data. Thank you to Kara Gibson for patiently showing me how to prepare samples for particle size analysis. Thank you to Dr. Pete Fulé for sharing your field equipment with me and teaching me how to measure the diameter of tree trunks. Thank you to Emily Yurich for sharing your soil corer with me and not minding when I totally bent it. Thank you to Dr. Matt Bowker for welcoming me into your lab space and to Dustin Kebble for instructing me in the laboratory procedure for texture and pH analyses and helping me troubleshoot issues with the pH meter. Thank you to my spirited, hard-working field assistants, Christopher RoDee, Enrique Ruiz Soto, Lorna Thurston, and Julia Vogel for tirelessly helping me set up my sampling transects and drill into the soil until the sun drifted below the horizon (and trusting me to drive you even though I only just acquired my driver's license). Thank you to Ehren Moler for early morning whiteboard-brainstorming parties and for bringing my awareness to the magic in science. Lastly, thank you to my family for encouraging me to maintain a healthy perspective in difficult moments and for thinking (or at least saying) my thesis topic is cool.

**Table of Contents**

Chapter One: Introduction	1
1.1 Problem Statement	3
1.2 Research Objectives	4
Chapter Two: Literature Review	5
Chapter Three: Methods	18
3.1 Study Area	19
3.2 Field Methods	23
3.3 Laboratory Methods	32
3.4 Statistical Analysis	35
3.5 Geostatistical Analysis	38
Chapter Four: Results	40
Chapter Five: Discussion	74
Chapter Five: Conclusions	89
References	92
Appendix A	102

## List of tables

Table 1: Coordinates and trunk diameters of the five juniper trees .....	24
Table 2: Chemical characteristics of leaf litter from selected juniper trees.....	40
Table 3: Analysis of variance between samples from different distances from juniper trees .....	46
Table 4: Analysis of variance between samples under juniper trees of different trunk diameters .....	46
Table 5: Analysis of variance between samples under juniper canopies from different compass direction .....	60
Table 6: Root-mean-squared-error in predictions of multiple variables generated using Empirical Bayesian Kriging.....	62
Table 7: Summary of Model A results.....	75
Table 8: Accuracy assessment of Model A.....	75
Table 9: Summary of Model B results .....	76
Table 10: Accuracy assessment of Model B .....	76

## List of figures

Figure 1: Blue Chute field site (Photo credit: Christopher RoDee) .....	19
Figure 2: Supervised land cover classification of the study area .....	22
Figure 3a: Tree #1 (A.K.A Zhaad) .....	25
Figure 3b: Tree #2 (A.K.A. Elijah) .....	25
Figure 3c: Tree #3 (A.K.A. Larry) .....	26
Figure 3d: Tree #4 (A.K.A. Athena) .....	26
Figure 3e: Tree #5 (A.K.A. Borris) .....	27
Figure 4: Establishment of radial transects within the site (Photo credit: Christopher RoDee).....	28
Figure 5: Soil corer .....	30
Figure 6: Map of sampling points within the study area .....	31
Figure 7: Histogram of organic matter content (%) across the field site .....	41
Figure 8: Histogram of carbon content (%) across the field site .....	41
Figure 9: Histogram of nitrogen content (%) across the field site .....	42
Figure 10: Histogram of moisture content (%) across the field site.....	42
Figure 11: Histogram of pH across the field site .....	43
Figure 12: Histogram of clay content (%) across the field site .....	43
Figure 13: Histogram of silt content (%) across the field site.....	44
Figure 14: Histogram of very fine sand content (%) across the field site .....	44
Figure 15: Histogram of fine sand content (%) across the field site .....	45
Figure 16: Histogram of medium sand content (%) across the field site .....	45
Figure 17: Average soil organic matter content with increasing distance from juniper trees for two depth increments .....	47
Figure 18: Soil organic matter content below juniper canopies with increasing tree age.....	48
Figure 19: Average stratification ratio of $\delta^{13}\text{C}$ with increasing distance from juniper trees .....	48
Figure 20: Average soil carbon content with increasing distance from juniper trees for two depth increments .....	49
Figure 21: Soil carbon content with increasing tree age .....	49
Figure 22: Average natural abundance of $^{13}\text{C}$ with increasing distance from juniper trees for two depth increments .....	50
Figure 23: Average natural abundance of $^{13}\text{C}$ with increasing tree age .....	51
Figure 24: Average soil C:N with increasing distance from juniper trees for two depth increments .....	52
Figure 27: Average soil nitrogen content with increasing distance from juniper trees for two depth increments .....	53
Figure 28: Soil nitrogen content with increasing tree age .....	54
Figure 29: Average natural abundance of $^{15}\text{N}$ with increasing distance from juniper trees for two depth increments .....	54
Figure 30: Soil $\delta^{15}\text{N}$ stratification ratios with increasing distance from juniper trees .....	55
Figure 31: Soil $\delta^{15}\text{N}$ under juniper canopies with increasing tree age .....	56
Figure 32: Correlations between selected soil properties and soil organic matter content .....	56
Figure 33: Correlations between selected soil properties and soil carbon content .....	58

Figure 34: pH with increasing distance from juniper trees.....	59
Figure 35: The effect of direction from juniper tree and depth on soil moisture .....	60
Figure 36: : Surface soil organic matter map .....	63
Figure 37: Subsurface soil organic matter map .....	64
Figure 38: Surface soil carbon map .....	65
Figure 39: Subsurface soil carbon map .....	66
Figure 40: Surface soil $\delta^{13}\text{C}$ map .....	67
Figure 41: Subsurface soil $\delta^{13}\text{C}$ map .....	68
Figure 42: Surface soil nitrogen map.....	69
Figure 43: Subsurface soil nitrogen map .....	70
Figure 44: Surface soil $\delta^{15}\text{N}$ map .....	71
Figure 45: Subsurface soil $\delta^{15}\text{N}$ map .....	72
Figure 46: Surface soil moisture map .....	73
Figure 47: Subsurface soil moisture map .....	74
Figure 48: Map of predicted soil organic matter content using multivariate linear regression and Empirical Bayesian Kriging.....	77

## Chapter One: Introduction

In the past century, woodland encroachment into grasslands has been occurring in regions across the globe, including the South African savannahs and parts of western North America (McCulley et.al., 2004; Parker et.al., 2009; Yusuf et.al., 2015). This current encroachment is unmatched in intensity and extent compared to any other time within the Holocene epoch (Johnson and Miller, 2006). Woodland encroachment, defined as an increase in range, canopy cover, and biomass of woody plant species, is especially prevalent in arid and semi-arid areas (Yusuf et.al., 2015). This encroachment consists of three phases (Johnson and Miller, 2006). In the first phase, shrubs and herbaceous plants are the prevailing vegetation, however woody plants have taken root. The second phase is characterized by the presence of both vegetation types, however neither one dominates over the other. In the third and final phase, woody plants have gained dominion over shrubs and herbaceous plants. When this final phase is reached, the reversal of woody encroachment becomes difficult. This transition from phase two to phase three is marked by a shift in resource availability, ecological interactions, and ecosystem processes.

The majority of woodland encroachment can be attributed to human interference and disturbances, including grazing, alterations in fire regimes, elevated atmospheric carbon dioxide concentrations, shifts in the deposition of nitrogen, human settlement, and climate change (Bragazza et.al., 2014; McCulley et.al., 2004; Parker et.al., 2009; Yusuf et.al., 2015). Woodland encroachment into grasslands has important implications involving net primary productivity of ecosystems, physical and chemical properties of soil, nutrient fluxes into and from the soil, climate change, and biodiversity and biomass, both above-ground and below-ground (Chen,

2015; Hess and Austin, 2014; Manning et.al., 2015; McCulley et.al., 2004; Norton et.al., 2012; Overby et.al., 2015, Yusuf et.al., 2015). In particular, woodland encroachment into grasslands is associated with alterations in the amount of organic carbon stored in soil (Fang et.al., 2015; McCulley et.al., 2004; Overby et.al., 2015; Throop et.al., 2013; Yusuf et.al., 2015). The purpose of this study will be to characterize the impact of juniper encroachment into the semi-arid grasslands of Northern Arizona on spatial patterns of soil organic carbon and on soil organic carbon sequestration.

Pinyon-juniper woodlands have increased in range in density during the past 150 years as a result of climate change and anthropogenic activities (Brockway et.al., 2002). These woodlands have moved into grassland areas, resulting in shifts in vegetation ecotones (Brockway et.al., 2002). Vegetation plays a powerful role in steering pedogenesis and soil transformations (Jobbagy and Jackson, 2003). Plant species composition is controlled largely by the local climate, specifically temperature and precipitation gradients, and changes in the dominant vegetation type in an area affect carbon and nitrogen content and dynamics in soil (Hess and Austin, 2014). Considering plant species composition changes can result in increases and decreases in soil carbon stocks and considering plant community composition controls the ability of soil to store carbon (Manning et.al., 2015), juniper encroachment has likely changed the carbon content of the underlying soil. The dynamics of carbon exchanges between soil and the atmosphere, the role of climate change in influencing carbon fluxes in soil, and the environmental conditions that control soil carbon stock gains or losses are still uncertain (Kucuker et.al., 2015; Winowiecki, 2015), however interest in soil carbon stocks and the climate change mitigation potential of soil has increased since the year 2000 (Xiang et.al., 2015). The effect of vegetation change on biogeochemical cycling in semi-arid and arid regions has yet to be

fully understood (McCulley et.al., 2004; Throop et.al., 2013), but researchers expect the woody plant encroachment has re-shaped the carbon cycle in North America through alterations in ecosystem structure, function, and climate (Scott et.al., 2006). Limited research has been conducted on the effect of climate change on carbon budgets in grasslands in the United States (Wagle et.al., 2015). Previous studies of woodland encroachment into grasslands and within semi-arid and arid regions indicate a high level of uncertainty regarding the effect of this vegetation change on carbon and nitrogen fluxes (McCulley et.al., 2004; Parker et.al., 2009; Yusuf et.al., 2015), which is why the information presented in this study of woodland encroachment in semi-arid areas may be beneficial to land managers and to fellow researchers.

### ***1.1 Problem Statement***

Climate, vegetation, and soil are all key determinants of carbon dioxide fluxes and the spatial variability of those fluxes (Chen et.al., 2015). Researchers have yet to fully understand the effect of climate change and alterations in temperature and precipitation on soil processes in arid ecosystems and in grasslands (Zelikova et.al., 2012). Quantifying the changes in soil carbon stock resulting from shifts in vegetation patterns will allow researchers to improve our understanding of the role of soils in storing or releasing carbon and of how woody encroachment will contribute to or hamper the ability of soils to mitigate climate change through carbon sequestration (Throop et.al., 2013). The high variability in environmental conditions and soil properties across very small spatial and temporal scales increases the difficulty in gauging soil carbon stocks (Kucuker et.al., 2015). Significant levels of uncertainty regarding variations in soil carbon stock are a result of this variability and the paucity of soil carbon data that is

available (Kucuker et.al., 2015).

### ***1.2 Research Objectives***

The objective of this study is to understand how juniper encroachment into grasslands has altered soil organic carbon fluxes. A site characterized by mixed vegetation cover of juniper trees and grasses within the Colorado Plateau was selected to capture the nature in which junipers modulate soil organic carbon fluxes in comparison to nearby grasses exposed to the same soil-forming factors. Soil was sampled along radial transects extending outward from juniper trees to encapsulate soil responses to juniper encroachment along a gradient of decreasing juniper influence. Collected soil was tested for soil organic matter and soil carbon to quantify existing soil organic carbon stocks and analyzed for the natural abundance of stable carbon isotopes and stable nitrogen isotopes to quantify rates of soil organic carbon turnover. The second objective of this study is to utilize interpolation techniques in Geographic Information Science to produce a map of soil organic carbon for the three study sites, which will visualize how soil organic carbon content varies spatially among different relative abundances of grassy and woody species. The interpolation techniques used in this study will be analyzed to determine the accuracy of these methods in capturing spatial variability of soil organic content across a continuous area. The four questions that will be interrogated in this study are:

1. Has juniper encroachment into grasslands in Northern Arizona enlarged or reduced soil organic carbon stocks?
2. Has juniper encroachment hastened or decelerated rates of soil organic carbon turnover?
3. Has juniper encroachment modified the soil carbon sink strength of soil in Northern Arizona?

4. How accurate are interpolation techniques in accurately capturing the spatial variability of soil carbon in a juniper-grassland area on the landscape scale?

## **Chapter Two: Literature Review**

Woodland encroachment into grasslands has been occurring over the last 150 years in regions across the globe and is particularly prominent in arid and semi-arid regions, in high latitude regions, and in areas with high elevation (Bragazza et.al., 2014; Brockway et.al., 2002; McCulley et.al., 2004; Parker, 2009; Throop et.al., 2013; Yusuf et.al., 2015). The majority of alterations of vegetation patterns today involve shifts in the abundances and spatial distributions of woody plant species and herbaceous plant species (McCulley et.al., 2004). Grasslands, which conduct about a third of the net primary production of terrestrial regions and hold about a third of the Earth's soil organic carbon store, are losing ground to woody species across the globe (McCulley et.al., 2004). Depending on the area, woodland encroachment can be due to elevated concentrations of carbon dioxide in the atmosphere, changes in nitrogen deposition, climate change, the introduction of non-native species, and human interference (Brockway et.al., 2002; McCulley et.al., 2004; Parker, 2009; Throop et.al., 2013; Yusuf et.al., 2015). Woody encroachment in semi-arid and arid regions is of particular concern because these dryland regions comprise about 40% of the global land surface area (Throop et.al., 2013). Therefore, a change in the characteristics and properties of these regions can have significant global repercussions in terms of carbon flows between terrestrial ecosystems and the atmosphere (Throop et.al., 2013).

Over the last 150 years in the Flagstaff, Arizona, area, junipers have been spreading into lands previously dominated by grassy vegetation as a result of increased human activity and

changes in climatic conditions (Koepke et.al., 2010; Parker, 2009). The Colorado pinyon pine (*Pinus edulis*), the Utah juniper (*Juniperus osteosperma*), and the one-seed seed juniper (*Juniperus monosperma*) typically comprise pinyon-juniper woodlands in Northern Arizona (Parker, 2009). Pinyon-juniper woodlands, which are classified as a mid-elevation, semi-arid vegetation type, are usually found in an elevational range below ponderosa pine forests and above grasslands on the Colorado Plateau (Parker, 2009). However, a combination of climatic and anthropogenic factors has caused pinyon-juniper woodlands to move to lower slopes, into valleys, and into other areas originally characterized as grasslands (Parker, 2009). In the Flagstaff area, the spread of these species into grasslands, a phenomenon termed pinyon-juniper encroachment, is due to increased grazing following European settlement, fire suppression, and climate change (Parker, 2009). Grazing resulted in a depletion of grassland populations, thereby decreasing the competitive pressure on woody species which previously maintained the boundary between grasslands and woodlands (Parker, 2009). Prior to human interference, fires held the Flagstaff area in a transition zone, which was beneficial to the growth of grassy species (Parker, 2009). Lastly, the alteration of precipitation and temperature patterns due to climate change has created an environment conducive to the growth of woody species (Parker, 2009). These anthropogenic and environmental factors have resulted in this documented shift in vegetation patterns in the Flagstaff area (Parker, 2009). As a result of these influences, understory grassland vegetation population and biodiversity has decreased (Parker, 2009). Loss of grasslands and increase in canopy cover in the area has resulted in a decrease in grassland bird populations and pronghorn antelope populations (Parker, 2009). However, the effect of this vegetation shift in Northern Arizona on the carbon content of the underlying soil has yet to be determined.

The terrestrial biosphere is a key regulator of global carbon cycling and the concentration of carbon dioxide present in the atmosphere (Wißkirchen et.al., 2013). Soil carbon plays a key role in the regulation of the global carbon budget, as soil can serve as a source or as a sink of carbon (Kucuker et.al., 2015), thereby producing positive or negative feedbacks to climate change (He et.al., 2016). Soil carbon fluxes must be measured to determine the prevailing direction of the flow of carbon between the terrestrial ecosystem and the atmosphere (Johnson and Curtis, 2001). The concentration of atmospheric carbon dioxide is reduced when carbon dioxide is removed from the atmosphere and stored in the soil as soil organic carbon or soil inorganic carbon (Lal, 2004; Olson and Al-Kaisi, 2015; Xiang et.al., 2015). Soil inorganic carbon is carbon that is not of organic origin and includes primary and secondary carbonates (Chatterjee et.al., 2009). Soil organic carbon is carbon that is derived from organic material such as plant residues and animal residues (Stockmann et.al., 2013). When these residues are partially decomposed by microbes in soil, they become soil organic matter, which includes sugars, proteins, lignin, tannins, lipids, and organomineral complexes (Chatterjee et.al., 2009; Stockmann et.al., 2013). Approximately 58% of soil organic matter is soil organic carbon (Stockmann et.al., 2013; Zhang et.al., 2015). Soil organic carbon plays a key role in the productivity of the terrestrial biosphere (de Paul Obade and Lal, 2013) and its storage in soil has profound implications for the climate (Croft et.al., 2012; Stockmann et.al., 2013; Throop et.al., 2013).

The quantity of soil organic carbon stored in soil is a function of the amounts and chemical characteristics of organic matter inputs to soil and the rate of decomposition of these inputs (Tiwari and Iqbal, 2015). The type and density of aboveground foliage as well as environmental conditions influence the chemical composition of the plant residues and how

much organic material and therefore nutrients are incorporated into the soil profile (Fontaine et.al., 2007; Hess and Austin, 2014; Manning et.al., 2015; McCulley et.al., 2004; Norton et.al., 2012; Overby et.al., 2015; Stockmann et.al., 2013; Tiwari and Iqbal, 2015; Zhang et.al., 2015). As the carbon to nitrogen ratio (C:N), lignin content, and the lignin to nitrogen ratio of plant litter increase, decomposition slows and the accumulation of organic material and therefore soil carbon increases (Stockmann et.al., 2013). The litter of woody plants often has a lower C:N ratio than grasses, which can hasten microbial decomposition (McCulley et.al., 2004). In addition, the biomass of roots of woody species is higher than the biomass of roots of grassy species and is distributed farther down in the soil profile (McCulley et.al., 2004; Throop et.al., 2013), which can induce microbial activity in deeper soil layers (Stockmann et.al., 2013). Alternatively, woody encroachment may not alter total carbon stocks in the encroached region at all, but rather adjust its spatial patterns of abundance (McCulley et.al., 2004).

Vegetation change is associated with changes in microbial community composition and activity (Manning et.al., 2015; Stockmann et.al., 2013). Microbes in soil, through their community structures, anatomy and physiology, and activity levels, define nutrient fluxes in the terrestrial biosphere and the fate of carbon in soil (Bragazza et.al., 2014). About two-thirds of soil carbon loss in terrestrial ecosystems is due to microbial decomposition, the rate of which is being impacted by climate change (Nie et.al., 2013). Root respiration and microbial decomposition are responsible for the majority of carbon dioxide release from the soil surface (Davidson and Janssens, 2006). The amount of soil organic carbon in the soil, in addition to soil temperature and moisture, leaf area and chlorophyll content, plant biomass, and the total amount of nitrogen in soil, influences the rate of soil respiration (Huang et.al., 2014). Soil respiration, which is performed by soil microbes and in the roots of plants, is the process by which organisms

consume organic matter, resulting in a release carbon dioxide (Huang, et.al., 2014) and the incorporation of organic material into their biomass (Accoe et.al., 2002). The more active the microbes, the greater the rate of carbon emissions from soil, except when microbial processing converts the carbon into a stable form that is chemically inaccessible to microbes (Manning et.al., 2015). Microbial processing of soil organic matter transforms residues into humus, which is partially decomposed organic material with slow turnover rates (Stockmann et.al., 2013).

A change in vegetation cover will resonate through the entire belowground world of microorganisms through its effect on species types and abundances and the cycling of energy and matter (Bragazza et.al., 2014; Chen, 2015; Overby et.al., 2015). Many plants form symbiotic associations with soil microorganisms in order to enhance their ability to extract nutrients from soil, and each plant species forms its own types of associations (Johnson et.al., 2010; Overby et.al., 2015; Stockmann et.al., 2013). For example, mycorrhizal fungi form attachments to the roots of some plant species and supply the plants with the mineral nutrients they have gathered with their hyphae (Johnson et.al., 2010). In return, the mycorrhizae receive photosynthates from the plants (Johnson et.al., 2010). Plant species composition alters microorganism species composition, and increased plant species diversity spurs microbial growth and respiration and increases the prevalence of fungi and therefore nutrient uptake (Chen, 2015; Johnson et.al., 2010; Overby et.al., 2015). In addition, microbial biomass will shift to accommodate different litter qualities (Fontaine et.al., 2007). Nutrient abundances, which are influenced by vegetation type and plant litter chemical composition, affect what symbioses are formed (Fontaine et.al., 2007; Johnson et.al., 2010).

Furthermore, the physical structure of plants impacts microbial activity, enzyme activity, and the abundance of substrate available to microbes, and thus soil carbon content and turnover

through its effect on soil moisture and temperature (Erhagen et.al., 2013; Nie et.al., 2013; Hess and Austin, 2014; Koepke et.al., 2010; Norton et.al., 2012; Zhang et.al., 2015). Vegetation regulates the reception of precipitation at the ground interface (Hess and Austin, 2014). Soil moisture is a key control of microbial activity and the rate of carbon mineralization (Norton et.al., 2012). The arrangement of branches and the shape of leaves influences the quantity of and rate at which precipitation reaches the soil (Norton et.al., 2012). Vegetation further alters soil water content through evapotranspiration and its effects on surface runoff and the amount of water the soil can physically hold (Norton et.al., 2012). Woody encroachment can elevate soil moisture through stem flow and by inhibiting the transmission of solar radiation to the soil surface (McCulley et.al., 2004). The effect of precipitation on microbial activity and carbon turnover is moderated by vegetation influences (Hess and Austin, 2014; Norton et.al., 2012). The structure of the vegetation canopy regulates the flow of energy to and from the soil surface (Koepke et.al., 2010). Increased temperatures result in increased microbial activity, therefore increased rates of decomposition of plant litter and soil organic matter (Erhagen et.al., 2013; Nie et.al., 2013), however the rate is also a function of the structure of the organic compounds being decomposed (Erhagen et.al., 2013). In summary, vegetation plays a significant role in the regulation of matter and energy fluxes to and from the soil surface (Erhagen et.al., 2013; Nie et.al., 2013; Hess and Austin, 2014; Koepke et.al., 2010; Norton et.al., 2012).

The distribution of soil organic carbon varies vertically throughout the soil profile as a result of the depth of plant root penetration, plant productivity, and microbial activity (Stockmann et.al., 2013). Globally, the top three meters of soil contains 2344 Gigatons (Gt) of organic carbon, the top one meter of soil contains 1500 Gt of organic carbon, and the top 20 centimeters of soil contains 615 Gt of organic carbon (Stockmann et.al., 2013). Similarly, the

mean residence time of carbon changes with depth (Fontaine et.al., 2007; Stockmann et.al., 2013). In deep soil layers, carbon is bound to soil minerals, making it inaccessible to decomposers and therefore incorporating it into the passive fraction of the soil carbon pool (Fontaine et.al., 2007). Microbial activity is minimized deeper in the soil profile due to reduced oxygen levels and decreased root biomass (Fontaine et.al., 2007; Stockmann et.al., 2013) and is maximized at the surface where the incorporation of new carbon into the soil profile is most rapid, thereby stimulating microbial activity (Garten and Cooper, 2000). Typically, the deeper the carbon in the soil profile, the stronger the stability of soil organic matter (Accoe et.al., 2002) and the longer the carbon will remain in the soil (Fontaine et.al., 2007; Stockmann et.al., 2013).

Effective carbon sequestration relies on the storage of atmospheric carbon dioxide in stable pools and within stable microaggregates (Lal, 2004). Soil carbon turnover rates depend on the fraction to which the soil carbon belongs (Manning et.al., 2015). Three carbon pools exist, each with their own turnover rate: active, intermediate, and passive (Stockmann et.al., 2013). Carbon stocks in the active fraction, which consist of large particles of carbon, root exudates, and quickly decaying plant litter, turn over in months to a few years and are therefore responsible for the majority of soil carbon fluxes (Manning et.al., 2015; Stockmann et.al., 2013). Moderate-size carbon particles, which consist of humified organic matter, turn over in tens of years and belong to the intermediate fraction of carbon. Small soil particles and stabilized organic matter constitute the stable or passive fraction of carbon, and turn over in centuries to millennia, making this fraction essential in soil carbon sequestration. The length of time in which carbon remains stabilized in soil depends on soil aggregate size and soil depth (Fang et.al., 2015). Organic matter that is encased in soil aggregates has a slower rate of decomposition compared to organic

matter that exists outside of aggregates, because soil aggregates form a protective layer around organic matter that physically separates the organic matter from decomposers and from environmental factors that would accelerate its decomposition (Fang et.al., 2015).

Stable carbon isotopes can be used to trace the journey of carbon through the soil (Busari et.al., 2016; Yonekura et.al., 2012; Zhang et.al., 2015). When carbon transforms from one phase to another, the ratios of carbon and nitrogen isotopes in soil shift, which is called isotope fractionation (Busari et.al., 2016). The natural abundance of  $^{13}\text{C}$  ( $\delta$ ) in soil indicates the stage of soil organic matter in the decomposition and humification process (Zhang et.al., 2015) and the turnover rate of soil organic carbon (Yonekura et.al., 2012). As microbial processing of soil organic matter intensifies, the natural abundance of  $^{13}\text{C}$  increases (Busari et.al., 2016). The natural abundance of  $^{13}\text{C}$  diminishes as fresh carbon is incorporated into the soil and is negatively correlated with soil organic carbon content (Busari et.al., 2016). Temperature, nitrogen availability, litter C:N, and microorganisms all drive the rate of  $^{13}\text{C}$  fractionation (Garten, 2006). Enrichment in  $\delta^{13}\text{C}$  can also be reflective of the residence time of organic matter and the inherent  $\delta^{13}\text{C}$  of incoming plant litter (Accoe et.al., 2002; Garten, 2006). Stable carbon isotopes are a useful metric for measuring soil carbon turnover and distinguishing fresh carbon inputs from old carbon inputs following woodland encroachment (Busari et.al., 2016; Yonekura et.al., 2012; Zhang et.al., 2015).

Similar to the natural abundance of  $^{13}\text{C}$ , the natural abundance of  $^{15}\text{N}$  indicates the degree of microbial processing of organic matter (Craine et.al., 2015). Microbes preferentially consume  $^{14}\text{N}$  and discriminate against  $^{15}\text{N}$ , resulting in an enrichment in  $^{15}\text{N}$  as decomposition progresses (Craine et.al., 2015). Increased denitrification, nitrification, and ammonia volatilization are evidenced by increased nitrogen isotope fractionation (Craine et.al., 2015). The natural

abundance of  $^{15}\text{N}$  also provides an image of nitrogen cycling over large time spans within ecosystems, making it a useful index for analyzing the flow of nitrogen into, out of, and within ecosystems, as well as the health of ecosystems (Craine et.al., 2015; Bekele and Hudnall, 2005; Garten, 2006).

The encroachment of woody species into grasslands in arid and semi-arid areas in the United States is suspected to alter soil carbon pools (Throop et.al., 2013). Woodland encroachment typically results in an increase in aboveground carbon storage, however the effect of woodland encroachment on belowground carbon stores and soil carbon dynamics is less well understood (Throop et.al., 2013). In previous studies, researchers observed that changes in plant species composition and in spatial patterns of vegetation have resulted in alterations of carbon and nitrogen content of soils and of carbon and nitrogen fluxes between the soil and the atmosphere (Fang et.al., 2015; McCulley et.al., 2004; Overby et.al., 2015; Throop et.al., 2013; Yusuf et.al., 2015). According to a study by Throop et al. (2013), the encroachment of the creosote bush, a C<sub>3</sub> plant, onto grasslands of C<sub>4</sub> species resulted in increased soil organic carbon storage. One prevailing theory regarding the effect of woody encroachment on soil organic carbon content is that “islands of fertility” develop around woody species due to the structure and chemical composition of woody plant tissues, which differs from that of the surrounding grassland species (Throop et.al., 2013). Soil organic content and soil nutrients are more abundant in the soil underneath the woody species due to increased biomass input and due to differing decomposition rates of woody plant material (McCulley et.al., 2004; Throop et.al., 2013). Soil organic carbon responses to woodland encroachment are prolonged and can result in continuing enrichment of soil organic carbon over long periods of time (Throop et.al., 2013).

Woody plants and grasses steer the pathways of nutrient cycling in different ways

because they have different nutrient requirements and methods of obtaining nutrients, channel the flow of nutrients into their aboveground components and belowground components with different intensities and proportions, and return nutrients to the soil at different rates depending on the structure of their leaves and roots and the ambitions of the microbes residing below (Bekele and Hudnall, 2005). Woody plants instigate enhanced nutrient cycling, including the movement of calcium, magnesium, and potassium, in the surface layers of soil (Bekele and Hudnall, 2005). Nitrogen, a limiting resource, drives ecosystem function and plays a critical role in modifying organic matter fluxes (Craine et.al., 2015; Garten, 2006). An increase in nitrogen can stimulate rapid organic matter turnover on short timescales, however elevated nitrogen levels over time can increase the sink strength of soil organic carbon pools through the stabilization of organic matter, reduction in soil respiration, inhibition of lignolytic enzymes, changes in microbial communities, and the deceleration of microbial processing of organic matter in the stable fraction (Craine et.al., 2015; Garten, 2006).

Woody encroachment modifies the pH of soil, usually resulting in an elevation in the concentration of hydrogen ions and an associated depression in pH values (Bekele and Hudnall, 2005; Bekele and Hudnall, 2006; Jobbagy and Jackson, 2003). Soil pH regulates microbial activity, decomposition rates, and the ability of soil to retain key nutrients, for example calcium, magnesium, and iron (Bekele and Hudnall, 2006; Manning et.al., 2015). Soil pH readily responds to a change in vegetation and can become highly variable following woody encroachment (Bekele and Hudnall, 2006). Bekele and Hudnall (2006) observed soil acidification and an intensification of pH variability following the encroachment of red cedar into grasslands in Louisiana. Considering woody encroachment strongly influences soil pH and pH drives nutrient availability and cycling, the spatial patterns of pH within encroached sites can

serve as an indication of how woody encroachment impacts nutrient dynamics.

McCulley et. al. (2004) reported an enhancement in soil organic carbon and total nitrogen following woodland encroachment in subtropical grasslands. This effect was especially pronounced in the top 20 centimeters of soil. Despite the growth of microbial biomass following the increased plant inputs to the soil, which resulted in accelerated carbon and nitrogen mineralization rates, soil organic carbon and total nitrogen still accumulated. This led to the deduction that with woodland encroachment, additions of carbon exceed losses of carbon through decomposition. In this study area, woodland encroachment has heightened the strength of the carbon sink over the last two centuries as a result of this positive net balance of carbon as well as the magnification of the stable soil carbon pool (McCulley et.al., 2004), which has very slow turnover rates (Stockmann et.al., 2013). The increased residence time of much of the added carbon indicates that in this instance, woody plant litter was of poor quality and therefore took longer for microbes to consume (McCulley et.al., 2004). However, if the carbon to nitrogen ratio (C:N) of the tissue of the encroaching woody species is lower than the C:N of the tissue of the original grassy species, then woodland encroachment may excite microbial activity and microbial biomass growth (McCulley et.al.,2004).

In another study, reforestation expanded the soil carbon pool through inputs of biomass (Fang et.al., 2015). In addition, according to Overby et al. (2015), the reduction of tree stand density can hasten decomposition, therefore the opposite may be true in the case of tree stand densification. However, according to Fontaine et.al. (2007), the addition of new organic carbon to the soil can spur microbial activity, thereby increasing the decomposition rate of organic matter and instigating the release of carbon from soil. This amendment to the soil can initiate the decomposition of stable carbon in deep soil layers, which has long mean residence times and

slow turnover rates (Fontaine et.al., 2007). Furthermore, woody encroachment increases the biomass of roots, and the roots of woody plant species generally reach deeper into the soil profile (Stockmann et.al., 2013). This increased biomass and depth of root penetration instigates the priming effect, in which the addition of carbon in deep soil layers paves the way for microorganisms to survive and thrive at depth and consume carbon that was previously untouched by soil microorganisms (Stockmann et.al., 2013). This heightened microbial activity and the decomposition of carbon that previously belonged to the stable carbon pool can alter the net carbon balance in soil (Stockmann et.al., 2013). Although the growth of pinyon-juniper trees may benefit carbon storage through the incorporation of carbon into their tissues, plant mortality in grasslands could result in the release of stored carbon and increased carbon emissions through decomposition (Kucuker et.al., 2015), as the decomposition of dead vegetation can put carbon back into the atmosphere (Hurteau et.al., 2011).

Soil is the second strongest sink of carbon dioxide after the ocean (Stockmann et.al., 2013). Researchers estimate that soil stores twice as much carbon as the atmosphere and biosphere (de Paul Obade and Lal, 2013). At this moment in time, when carbon emissions from anthropogenic sources are rising at steadily increasing rates and when carbon dioxide has been identified by the United Nations Framework Convention on Climate Change as the most impactful greenhouse gas in terms of climate change, the preservation of the soil carbon pool is becoming increasingly important (de Paul Obade and Lal, 2013; Stockmann et.al., 2013). A small decrease in the soil carbon pool and the subsequent release of carbon from the soil can result in a spike in atmospheric carbon dioxide levels (Croft et.al., 2012; Stockmann et.al., 2013). Likewise, the increased storage and maintenance of carbon in soil is a form of climate mitigation (Lal, 2004; Stockmann et.al., 2013). The flux of carbon dioxide from the soil rivals the flux of

carbon dioxide to the atmosphere from fossil fuel emissions (Throop et.al., 2013).

Interpolation is a tool in spatial analysis that has been implemented in previous studies to visualize soil organic carbon variations over space and to estimate soil organic carbon content in unsampled areas (de Paul Obade and Lal, 2013; Miller et.al., 2016; Wang et.al., 2015). Spatial interpolation involves converting discrete points of known attributes into continuous areal surfaces by predicting the values in the spaces between the points (de Paul Obade and Lal, 2013; Miller et.al., 2016). The small-scale variability in soil properties means that the sample pool used to construct interpolations must be comprehensive in terms of the number of sampling points and the density of its areal coverage (Bekele and Hudnall, 2006). Interpolation is a method in geostatistics that allows for the maximization of data obtained through expensive and time-consuming field sampling and laboratory analysis (Lark, 2012) and allows for the visualization of spatial trends and patterns (Wang et.al., 2015). The spatial patterns of soil properties captured in interpolated surfaces are essential to uncover what mechanisms are driving soil characteristics and how those mechanisms vary over space (Bekele and Hudnall, 2006), however the internal variability of soil and the simplification of spatial phenomena into equations can introduce uncertainties in predictions generated through interpolation (Kumar et.al, 2012; Malone et.al., 2009). Spatial interpolation techniques include inverse distance weighting, regression, proximity polygons, trend surface modeling, and kriging (de Paul Obade and Lal, 2013). Spatial interpolation relies on the assumption that the data under analysis is spatially autocorrelated (Miller et.al., 2016). This study will employ inverse distance weighting and kriging to produce maps of soil organic carbon content for the study sites. Inverse distance weighting assigns values to unsampled points by following the rule that as spatial proximity increases, values come closer together numerically (de Paul Obade and Lal, 2013). Kriging uses a variogram of distance

and variability to estimate values of unsampled points (de Paul Obade and Lal, 2013). Soil organic carbon varies on small spatial scales and in response to vegetation species composition and spatial patterns (Miller et.al., 2016; Manning et.al., 2015). A spatial analysis of soil organic carbon content will improve our understanding of soil organic carbon dynamics in response to woodland encroachment.

### **Chapter Three: Methods**

### 3.1 Study Area

The intention of this research was to explore the effects of juniper encroachment on soil carbon fluxes in a semi-arid ecosystem within Arizona. A study area was sought within the semi-arid Colorado Plateau to realize this goal as well as to ensure the accessibility of the site. Specifically, a site characterized by the presence of juniper trees as well as large grassy areas with minimal topographic variability was sought with the intention of using the heterogeneity in vegetation to represent both a juniper woodland and a grassland while keeping other variables that can influence soil organic carbon content constant. A field site that met this criteria was found within the Southwest Experimental Garden Array, which is a collection of research stations funded through the National Science Foundation and Northern Arizona University (Northern Arizona University, 2014).



Figure 1: Blue Chute field site (Photo credit: Christopher RoDee)

The site, named Blue Chute, is a pinyon-juniper woodland within Babbitt Ranches. Blue Chute is located at 35.58 degrees North and -111.97 degrees West and is about 40 minutes

northwest of Flagstaff, Arizona (Northern Arizona University, 2014). The site was previously a part of grazing lands for cattle before it was designated through the Landsward Foundation as an ecological research site (Northern Arizona University, 2014). As a result of this designation, the site could be utilized for this study in a timely manner, which was essential given the compressed timeline of this study. Trampled ground and cow manure is visible evidence of its previous use. The entire research area covers about 1.2 hectares, but only the southernmost part of the area was selected for use in this study to avoid the disturbance of other ongoing research projects and to avoid patches of compacted ground indicative of human activities. The study area for this research covered about 12,260 square meters. The small extent of the study area ensured small-scale soil carbon variability could be represented with the sampling scheme, which will be discussed in the Field Methods section of this chapter.

At 6332 feet in elevation, the site receives about 478 millimeters of precipitation annually (Northern Arizona University, 2014). The annual mean air temperature ranges from 0.889°C to 18.6°C (Northern Arizona University, 2014), and the average weighted slope for the soil map unit is 6.7% (United States Department Agriculture, 2016). The site experiences a monsoon season from June to September. To determine the percent canopy cover of trees in the study area, a supervised image classification analysis was performed on 2015 aerial imagery obtained from the U.S. Department of Agriculture's National Agriculture Imagery Program (United States Department of Agriculture, 2016). This classification was performed using the Image Classification toolbar in the ArcGIS Spatial Analyst extension of ArcMap. Groups of pixels visually determined as grasses were manually selected from the 2015 aerial imagery, designated as grass cover, and used to inform the software's automated identification of grassy areas. The same procedure was used to delineate juniper tree cover. According to the results of this

analysis, percent canopy cover of the study area is about 21%. A map of the results of the supervised land cover classification is shown in Figure 2. The site is characterized by the Oneseed Juniper (*Juniperus monosperma*) and the Two-needle Pinyon Pine (*Pinus edulis*), as well as numerous grass species including grasses belonging to the genera *Bouteloua* and *Aristida* (United States Department Agriculture, 2016). Junipers of various heights and sizes dot the landscape, and are often accompanied by pinyon pines. Tall grasses, prickly pear cacti, and some wildflowers lie between trees. Large junipers appear to serve as nurseries for young junipers, young pinyon pines, small leafy vegetation, and wildflowers. A thick layer of undecomposed juniper leaves rests under most juniper trees.

Bare soil occurs in patches, and is often covered by rocks or large ant hills. When the weather is dry, cracks appear in the bare soil, which is reddish-brown to brown to grayish brown in color. The top layer of soil does not have a cohesive structure and disintegrates easily when cored. The site is underlain by basalt and limestone, and the soil contains carbonates (Northern Arizona University, 2014). According to the Web Soil Survey data produced by the Natural Resources Conservation Service, a part of the United States Department of Agriculture, the soil belongs to the class Aridic Calcicustolls, the order Mollisols, and the Suborder Ustolls (United States Department of Agriculture, 2016).

### Supervised Land Classification of the Study Area



Aerial imagery available from the U.S. Geological Survey.

Figure 2: Supervised land cover classification of the study area

### **3.2 Field Methods**

The experimental design involves a “space for time” approach, which is explained in Bragazza et.al. (2014) and McCulley et.al. (2004) as a way to simulate different periods of time using different spaces as representations of each time. With this approach, two times can be brought temporally coincident through spatial variations. In other words, one area resembling the conditions of one time can be used to represent the past, while another area resembling projected future conditions can represent the future. Instead of using a grassland site to represent the time before juniper encroachment and a juniper-dominated site as an example of time after encroachment, one site was selected to minimize the effect of other controlling factors of soil carbon not under scrutiny. For example, soil thickness and soil organic carbon vary across a slope gradient, with the majority of soil organic carbon present at the top and at the base of slopes (McCulley et.al., 2004; Olson and Al-Kaisi, 2015). Soil type and climatic conditions must also be held constant, as different soil classes have inherently different carbon content (Stevens et.al., 2010) and temperature and precipitation affect soil carbon content and organic matter decomposition rates (Hess and Austin, 2014; Stockmann et.al., 2013; Zhang et.al., 2015). In addition, season has a profound impact on soil carbon content (Norton et.al., 2012), therefore sampling in all areas must be carried out within the same season. All samples were taken in the autumn between October 14, 2016, and October 17, 2016. All four days were characterized by minimal cloud cover, no precipitation, and strong winds.

The presence of juniper trees of various ages and sizes as well as the wide swaths of grass between trees made the site an ideal environment to explore how junipers modify the spatial distribution and dynamics of soil carbon. The impact of juniper encroachment on soil properties was expected to be most prominent close to junipers trees, with diminishing effects with

increasing distances. The southeast half of the research site was utilized for this study because it showed no visible signs of human activity and compaction. The study area was bound in the southwest, southeast, and northwest direction by a metal fence, and the extent of the study area in the northeast direction was delineated using flags. The northeastern edge of the area was set with the intention of creating a buffer between my research area and the area in use by other researchers. The length and width of the study area were measured, resulting in a length of 110 meters and a width of 65 meters. Five parallel transects perpendicular to the long dimension of the area were established at 20-meter intervals.

These five transects were established to find the five trees serving as the anchor points for soil sampling transects and as the post-woodland encroachment representations of vegetation. Along each transect, a juniper tree was selected. In some transects, only one tree was intercepted, but in other transects, more than one tree was present. In these cases, the tree standing in isolation, the tree farthest from other selected trees, and/or the tree with different dimensions than other selected trees was chosen. The goal of juniper selection was to obtain maximum coverage of the study area and to select trees across a wide range of ages and sizes.

Table 1 below shows the coordinates and trunk diameters for the five selected trees.

*Table 1: Coordinates and trunk diameters of the five juniper trees*

<b>Tree</b>	<b>Latitude</b>	<b>Longitude</b>	<b>Diameter</b>
1	35 deg. 35.231'	111 deg. 58.187'	14.4 cm
2	35 deg. 35.210'	111 deg. 58.176'	69.6 cm
3	35 deg. 35.172'	111 deg. 58.161'	32.9 cm
4	35 deg. 35.180'	111 deg. 58.151'	118.6 cm
5	35 deg. 35.19'	111 deg. 58.158'	5.4 cm



Figure 3a: Tree #1 (A.K.A Zhaad)



Figure 3b: Tree #2 (A.K.A Elijah)



Figure 3c: Tree #3 (A.K.A Larry)



Figure 3d: Tree #4 (A.K.A Athena)



Figure 3e: Tree #5 (A.K.A. Borris)

For each tree, the radius of the canopy in each compass direction was estimated and recorded. Soil organic carbon content is known to vary within study sites at small spatial scales (Miller et.al., 2016), therefore 50 sampling points were used to represent this landscape-scale variability (Cihacek et.al., 2015). A large number of observations is also required to produce an accurate map illustrating soil organic carbon content across vegetation gradients (Miller et.al., 2016). In each compass direction, a soil sample was taken halfway between the juniper trunk and the dripline of the canopy, and another sample was taken five meters from the trunk. Samples under the tree represent the strongest influence of juniper encroachment on soil properties, and samples five meters from the tree indicate soil properties in inter-canopy spaces. These samples were used to represent soil carbon characteristics after encroachment. In a randomly selected compass direction, additional samples were taken fifteen meters from the tree and thirty meters from the tree. These samples taken fifteen and thirty meters from the junipers were intended to represent soil with minimal to no juniper influence. The directions of these extended transects were selected at random, however if the 30-meter transect extended past the study area or terminated close to another juniper, a different direction was randomly

selected. Due to the spatial distribution of juniper trees, 15-m and 30-m sampling points occasionally were located less than 15 meters or 30 meters from other unselected juniper trees. To get an accurate distance from sampling points to nearby junipers, the coordinates of all nearby junipers were collected. A map of all of the sampling points is shown in Figure 6.



*Figure 4: Establishment of radial transects within the site (Photo credit: Christopher RoDee)*

At each sampling point, fallen juniper leaves were brushed aside, and three soil cores were taken. The depth to which soil is sampled must be carefully selected, because soil organic carbon varies with depth and generally decreases with depth (Jobbagy and Jackson, 2000; Olson and Al-Kaisi, 2015; Stockmann et.al., 2013; Winowiecki, 2015; Zhang et.al., 2015) and insufficient sampling depth can produce inaccuracies when quantifying soil organic carbon stock alterations (Zhang et.al., 2015). According to Throop et.al. (2015), only the top 20 cm of soil is affected by woody encroachment in terms of soil carbon content in semi-arid and arid areas, and the top 10 cm of the soil profile shows the most pronounced change in response to woody encroachment. Zhang et.al. (2015) asserts that 20-cm is the minimum sampling depth for representing soil organic carbon stocks, and Fang et.al. (2015) states that the top 20 cm of soil

contains the highest carbon concentration and the top 10 cm of soil contains the highest concentration of soil organic carbon and the largest mass of litter inputs. Although deeper soil contains the majority of the passive fraction of carbon (Fang et.al., 2015), a 20-cm sampling depth was selected to maximize vegetation-dependent alterations in soil carbon. In order to capture some of the variability in soil carbon with depth and to expand the study into the third dimension, each core was split into two depth increments: 0-10 cm and 10-20 cm. Due to the loose structure and fine texture of the soil, obtaining a cohesive core was difficult, and much of the surface soil could not be captured with the corer. To ensure enough soil for all laboratory analyses was captured in the top ten cm of soil, a shovel was used to scoop some of the surface soil. As a result, the 0-10 cm samples may better represent properties of shallower depths, therefore from here onward, these samples will be referred to as “surface samples” and samples in the 10-20 cm depth increment will be referred to as “subsurface samples”. Surface samples from each sampling point were incorporated into the same sample and 10-20 cm samples for each sampling point were joined together and stored separately. With fifty sampling points and two depth increments, a total of one hundred samples were collected across the study site.



*Figure 5: Soil corer*

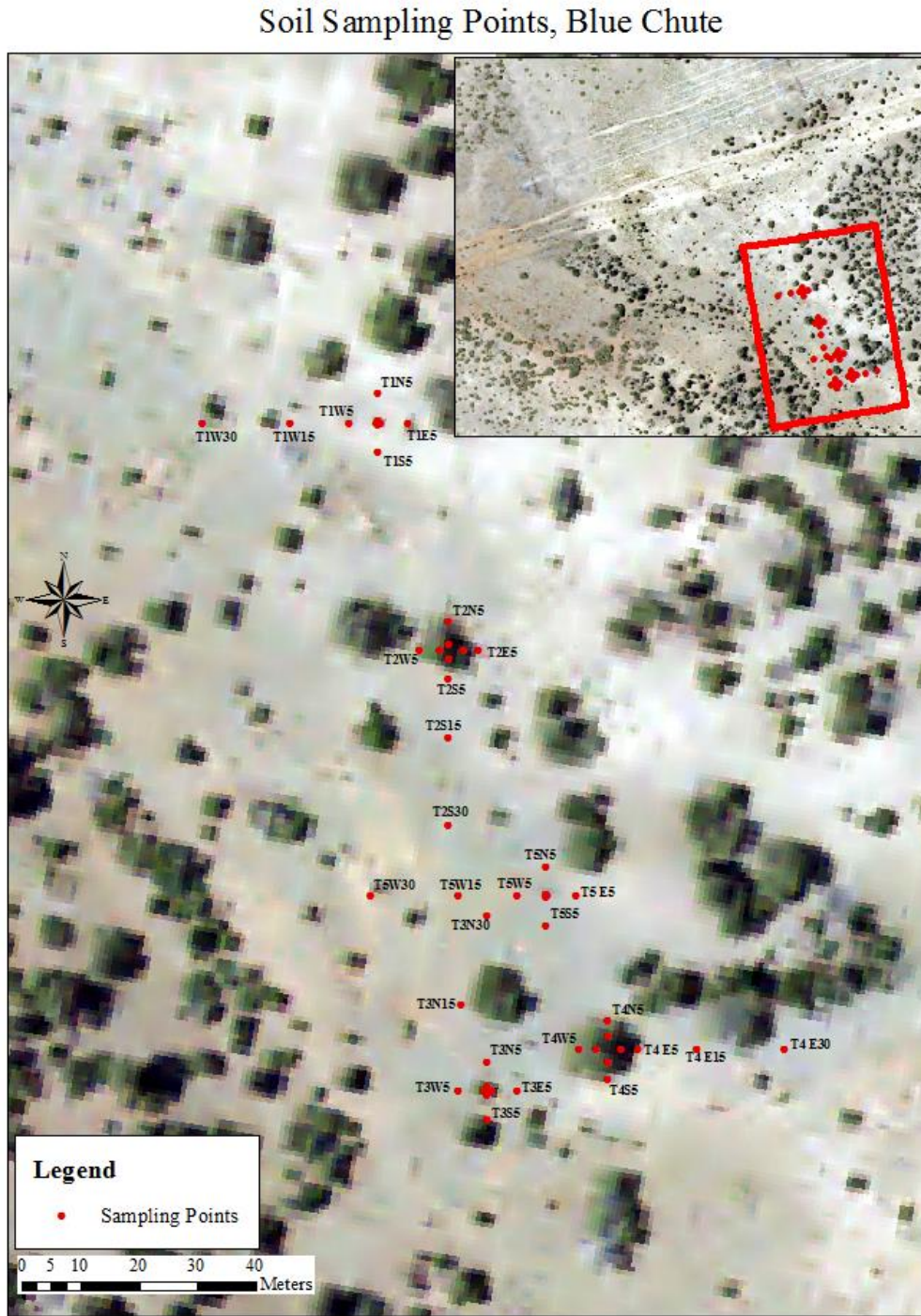


Figure 6: Map of sampling points within the study area

### ***3.3 Laboratory Methods***

All soil samples were sieved using a 2-mm sieve to remove all coarse particles, most roots, and large pieces of leaf litter. Sieved samples were used for all analyses. Due to the compression of the 10-20 centimeter samples and the inability to obtain a cohesive core of the surface soil, the calculation of bulk density was removed from this study. As a result, all analyses are on a per mass basis, as bulk density measurements are required to convert values to a per volume concentration (de Paul Obade and Lal, 2013) or to a per area concentration (Chatterjee et.al., 2009; IPCC, 2003; Tiwari and Iqbal, 2015). Subsamples for each analysis were collected by shaking the sample bags by hand and taking small portions of soil from sections of the bag until the required mass of sample was obtained. This method was used to obtain a fraction of soil that was reasonably representative of the entire sample.

To determine how juniper encroachment modifies the carbon and nitrogen content of soil and alters carbon and nitrogen microbial processing and dynamics, %C, %N, C:N ratios, and the natural abundance of stable carbon and nitrogen were measured at the Colorado Plateau Isotope Laboratory. To prepare the samples for the analyses, small subsamples of 5 g were taken from each soil sample and each leaf litter sample and dried in an oven for 24 hours at 55°C. The spoon used to scoop the subsamples was cleaned using alcohol wipes between samples to prevent cross-contamination. Soil subsamples were then ground to a fine powder using a mortar and pestle and transported to the Colorado Plateau Stable Isotope Laboratory. At the Colorado Plateau Stable Isotope Laboratory, leaf litter subsamples were ground using a ball mill. Soil subsamples were acid washed to remove carbonates because the presence of carbonates can result in inaccurate stable isotope readings, according to the Colorado Plateau Stable Isotope Laboratory. Trials were run prior to analysis to determine the appropriate mass of soil and leaf

litter needed to obtain accurate measurements. A small amount of material from each subsample was packaged in foil and analyzed for carbon and nitrogen content and the abundance of stable carbon and nitrogen isotopes using an elemental analyzer.

Water content of soil is one of the factors regulating microbial activity and therefore the rate of decomposition of organic material in soil (Manning et.al., 2015). Therefore, gravimetric soil moisture of the samples was determined to explore how the presence of junipers alters soil moisture and how strongly soil moisture controls carbon fluxes in soil. Gravimetric soil moisture content was measured by drying approximately 10 g of soil per sample for 24-48 hours in an oven set to 105°C. Samples were weighed before and after drying to attain a value for the mass of water in each subsample. After drying, samples were placed in a desiccator to cool prior to weighing to inhibit the acquisition of ambient moisture. Gravimetric soil moisture was calculated using the following equation adapted from Yahaya et.al. (2016):

$$\text{Gravimetric soil moisture} = (\text{Wet soil weight} - \text{dry soil weight}) / \text{dry soil weight}$$

To determine how juniper encroachment modifies the spatial distribution of organic matter in soil and alters soil organic carbon stocks, the weight loss on ignition (LOI) method was implemented (Chatterjee et.al., 2009; de Paul Obade and Lal, 2013; Tiwari and Iqbal, 2015; Zhang et.al., 2015). This method involves predicting the soil organic matter content by calculating the weight difference after exposure to high temperature and converting this value to a soil organic carbon content (Chatterjee et.al., 2009; de Paul Obade and Lal, 2013; Zhang et.al., 2015). For each sample, a subsample of about 1.5 grams of soil (roughly 1 cm<sup>3</sup>) was weighed on a microscale in a small cylinder of tin foil. Tin foil weights were recorded before this step so weights could be adjusted to represent only soil. Subsamples were dried at about 90°C for 24 hours to remove water, placed in a desiccator to cool, and weighed to determine the pre-ignition

weight of soil. Subsamples were then placed into glass vials and ignited in a furnace at 550°C for five hours. Glass vials were burned for one hour at 550°C prior to ignition to clean them. After the five-hour burn, the glass vials containing the sample packets were cooled in a desiccator to prevent the addition of moisture to the samples. Once the samples were cooled, they were weighed using a microscale. The mass lost with ignition represents the mass of organic matter present in the subsample. The following equation was used to determine the percent of organic matter present in each soil sample:

$$\text{Percent organic matter} = (\text{Pre-ignition soil weight} - \text{post-ignition soil weight}) / \text{pre-ignition soil weight} * 100$$

Soil pH affects the activity levels of microbes in soil and the rate at which organic matter is decomposed in soil (Manning et.al.,2015). To determine the pH of each sample, 10 g of each sample was mixed by hand with distilled water to create a shiny paste. A glass electrode pH meter was inserted into the paste and the resulting pH value was recorded.

Texture influences microbial communities and influences how encroachment affects soil organic carbon (Yusuf et.al., 2015). To measure the texture of each sample, an LS 230 Coulter particle size analyzer was utilized. Initially, the hydrometer method was attempted to determine the texture of each sample, however, this method proved to be unrealistic given time constraints and the number of samples to be processed. To prepare samples for particle size analysis, about 0.4 grams (0.35-0.45 grams) of each sample was weighed into 50-mL centrifuge tubes. Organic matter was removed by adding 30% hydrogen peroxide to the tubes, mixing the soil and hydrogen peroxide using a shaker table, and allowing the sample and hydrogen peroxide to react for 4-6 hours in a 50°C water bath. 15 mL of reagent grade water was added to the centrifuge

tubes. Tubes were centrifuged at 3400 revolutions per minute (rpm) for 15 minutes, and then liquid at the top of the centrifuge tube was decanted. 30 mL of reagent grade water was added to the centrifuge tubes, and samples were centrifuged at 3400 rpm for another 15 minutes. The reagent grade water was removed using a pipette. 5-15 mL of 5% sodium hexametaphosphate solution, the particle dispersing agent, was added to each centrifuge tube, and tubes were shaken on a shaker table on high for two hours. Samples were then transferred to tubes for analysis and analyzed using the particle size analyzer to determine the relative abundance of soil in each particle size category.

### ***3.4 Statistical Analysis***

RStudio was used for all data analyses. Histograms were generated from the organic matter, carbon, nitrogen, moisture, pH, and particle size fraction data to depict the range and distribution of the data and to characterize the field site in the context of these soil properties. Stratification ratios based on depth increment were calculated for  $\delta^{13}\text{C}$  and  $\delta^{15}\text{N}$  to determine the role of juniper encroachment in creating or eliminating differentiation in isotope enrichment vertically. ANOVAs were performed to determine if distance from juniper trees, direction from juniper trees, and age of juniper trees can individually manifest significant variability in the following soil properties: organic matter content, carbon content, nitrogen content,  $\delta^{13}\text{C}$ ,  $\delta^{15}\text{N}$ ,  $\delta^{13}\text{C}$  stratification ratios,  $\delta^{15}\text{N}$  stratification ratios, moisture, pH, clay content, silt content, very fine sand content, fine sand content, and medium sand content.

To determine whether juniper encroachment modifies spatial patterns of organic matter fluxes and soil chemistry, the averages of organic matter content, carbon content,  $\delta^{13}\text{C}$ ,  $\delta^{13}\text{C}$

stratification ratios, nitrogen content,  $\delta^{15}\text{N}$ ,  $\delta^{15}\text{N}$  stratification ratios, soil C:N, and pH were calculated for the surface soil and subsurface soil for three areas: below juniper canopies, juniper dripline to five meters distance from the trees, and over five meters from the tree. These classes were built to reflect the actual distances of soil samples from juniper trees, rather than estimated distances. Actual distances were found using the coordinates of the soil sampling points and NAIP aerial imagery provided by the United States Department of Agriculture. The soil below juniper canopies represents soil most strongly influenced by juniper encroachment; the soil from the dripline to five meters from the juniper trees represents intercanopy soil; and soil over five meters from juniper trees represents soil prior to juniper encroachment. For the resulting graph of averages and for all graphs to follow, error bars indicate the standard error.

To determine how juniper encroachment alters organic matter fluxes and soil chemistry over time, the averages of organic matter content, carbon content,  $\delta^{13}\text{C}$ , nitrogen content,  $\delta^{15}\text{N}$ ,  $\delta^{15}\text{N}$  stratification ratios, soil C:N, and litter C:N were calculated for the surface soil and subsurface soil for each tree. These averages were graphed against increasing tree age. Tree trunk diameter served as a proxy for tree age for this analysis, with larger tree trunks representing older trees.

To explore the strength of all factors excluding soil carbon and organic matter content in shaping carbon stocks in soil, the correlations between these potential explanatory variables and soil organic matter and carbon were measured. Correlation coefficients and p-values were calculated for each combination and graphed. A multivariate linear regression, hereafter referred to as Model A, was performed to determine the role and strength of distance and direction from juniper trees, canopy diameter, and depth in shaping soil organic matter content in the study site. Canopy diameter was calculated prior to this regression analysis using the canopy radii

measurements collected in the field. A second multivariate linear regression, hereafter referred to as Model B, was performed to create a model that could be integrated with geostatistical analyses to predict surface soil organic matter at unsampled, **randomly** selected points in the study area, which could then be used to create an **interpolated** surface map of soil organic carbon in the study area. For this analysis, **only surface samples** were used to generate the model, since this model was used to create a map of organic matter only in surface soil. Canopy areas were used in lieu of canopy diameter because canopy areas can be easily calculated using GIS. These canopy area values were derived for each tree using the GIS layers produced in the supervised land cover classification. The resulting coefficients from Model B were then used to construct an equation to predict soil organic matter at **randomly** selected, unsampled points in the study area, which will be discussed in Section 3.5 of this document. Compass direction was removed as a predicting variable for this analysis because this variable weakened the strength of the final model and was found to be insignificant (p-value >0.1). In both multivariate linear regression analyses, organic matter content and distance were log-transformed because this dependent variable and independent variable both have skewed distributions. Only the results of these two analyses are mentioned in this study, however multiple combinations of factors and transformations were tested. Akaike information criterion values were calculated for each model and considered in conjunction with knowledge of soil-plant feedbacks to select these final two models.

A copy of the scripts used is included in Appendix A of this document.

### ***3.5 Geostatistical Analysis***

To determine the ability of geostatistical methods in GIS to capture the spatial variability of soil carbon content and factors related to soil carbon storage, the table of soil data was joined to plotted soil sampling points in ArcMap 10.3.1. Different methods of spatial interpolation were conducted using tools within the Interpolation toolset of the Geostatistical Analyst Tools toolbox in ArcMap 10.3.1. Inverse Distance Weighting, Ordinary Kriging, Simple Kriging, and Empirical Bayesian Kriging were tested and the Geostatistical Wizard in ArcMap was used to measure the accuracy of predicted soil properties at unsampled points. Multiple variations of Kriging were used because this method has been extensively applied by researchers seeking to evaluate the spatial variability of soil properties because this method modifies the strength of observed points in influencing predicted values at unsampled points to reflect underlying patterns in the data (Simón et.al., 2013). The interpolation method with low root-mean-squared error that captured the variability in soil properties between juniper trees and grassy areas was selected to produce final interpolated raster datasets. Final interpolated surfaces were clipped to the extent of the study area.

To improve soil organic predictions in unsampled areas far from sampled points, the equation for predicting soil organic matter content derived through the multivariate linear regression was combined with interpolation methods, resulting in a higher resolution, model-based map of soil organic matter. To create a series of points at which soil organic matter would be estimated, the Create Fishnet tool in the ArcGIS Data Management toolbox was utilized. This tool generates a grid over a selected area of interest given specified cell dimensions and places points at the centerpoint of each cell. The grid was set to the extent of the study area and the cell size was set to 1 m<sup>2</sup> to create a high-density point surface. To determine the distance

from each of these random points to its closest tree, points were created at the centroid of each tree canopy using the Feature to Point tool in the Data Management toolbox. The Near tool in the Analysis toolbox was then applied to find the closest tree from each point and to calculate the distance of each point from its closest tree. The canopy area for each closest tree was joined to the point feature class. The table for this point layer, which included the identifications of each point, the distances between each point and its closest tree, and the canopy area of the closest tree to each point, was exported from ArcMap and imported into Microsoft Excel. In Excel, data values for each point were applied to the following model equation: EXP(1.836-  
0.095\*ln(Distance)+0.003\*Canopy Area). The predicted organic matter values were imported back into ArcMap and joined to the point layer, resulting in an array of points across the study area with predicted organic matter values. Empirical Bayesian Kriging to create a continuous surface of predicted organic matter values using these predicted values at points to inform estimates of organic matter content in spaces with unknown soil organic carbon content.

## Chapter Four: Results

Percent carbon, percent nitrogen, the natural abundance of  $^{13}\text{C}$  and  $^{15}\text{N}$  isotopes, and C:N values of plant litter from each of the five trees are shown in Table 2 below. Tree 2 and Tree 4 were the largest trees within the site (Table 1). The litter samples from these two trees have the largest  $\delta^{13}\text{C}$  values as well as the largest percent carbon and C:N values (Table 2). Percent nitrogen and the abundance of  $^{15}\text{N}$  do not show a clear trend with tree age.

*Table 2: Chemical characteristics of leaf litter from selected juniper trees*

Sample	$\delta^{13}\text{C}$ (‰)	$\delta^{15}\text{N}$ (‰)	%C	%N	C/N
Tree 2	-23.93	0.26	49.17	1.03	47.86
Tree 3	-24.10	0.91	42.11	1.01	41.53
Tree 4	-23.22	0.68	47.12	0.99	47.52
Tree 5	-24.71	-0.87	42.23	1.02	41.54

Organic matter content within the field site ranges between 2% and 12%, with a few higher values reported (Figure 7). Carbon content typically lies in the range of 0% to 4% (Figure 8), and nitrogen content typically ranges between 0% and 0.3% (Figure 9). Most soil moisture values lie between 5% and 20% (Figure 10). Most soil within the site is alkaline, with a large proportion of pH values between 7.25 and 8.25 (Figure 11). Clay content ranges from 16-30% (Figure 12), silt content ranges from 55%-75% (Figure 13), very fine sand is in the range of 4%-16% (Figure 14), fine sand is in the range of 0-8% (Figure 15), and medium sand is in the range of 0-6% (Figure 16).

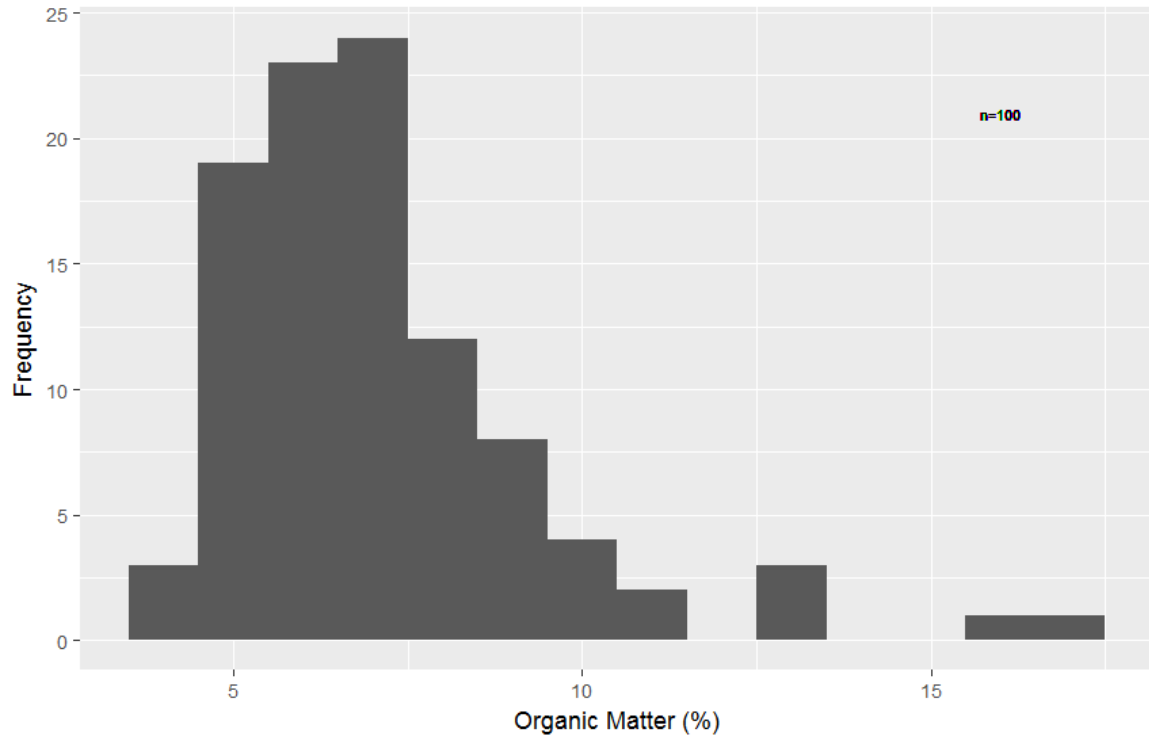


Figure 7: Histogram of organic matter content (%) across the field site

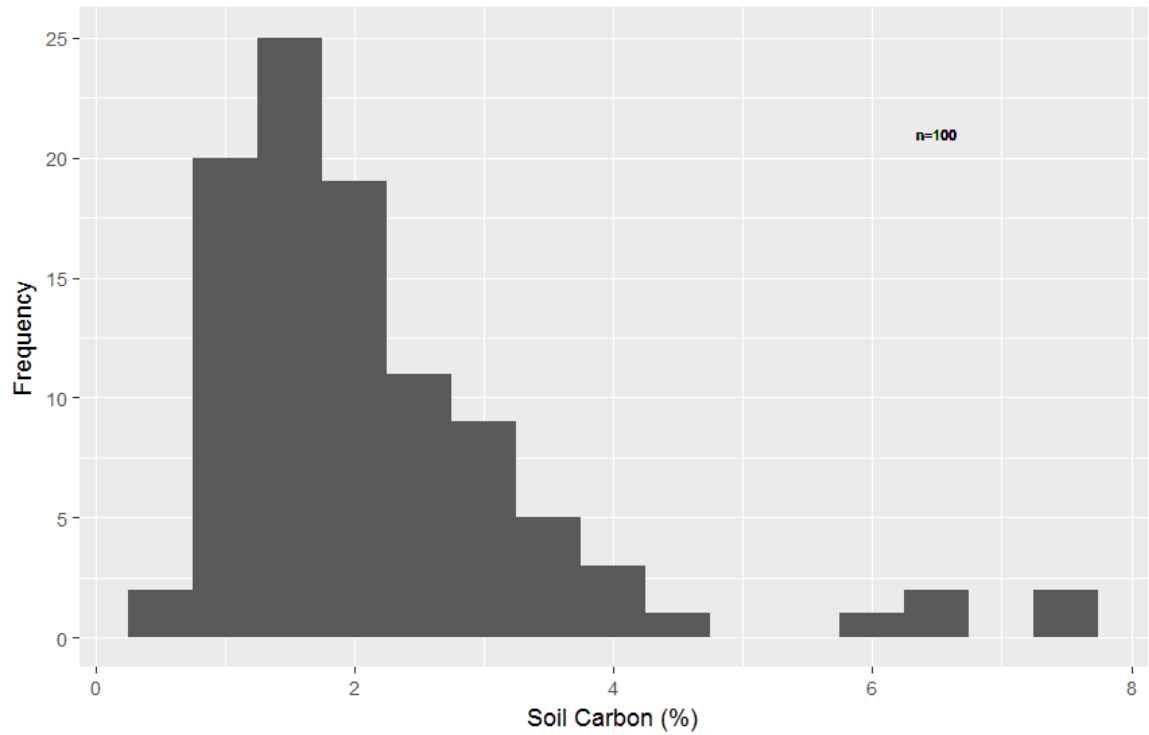


Figure 8: Histogram of carbon content (%) across the field site

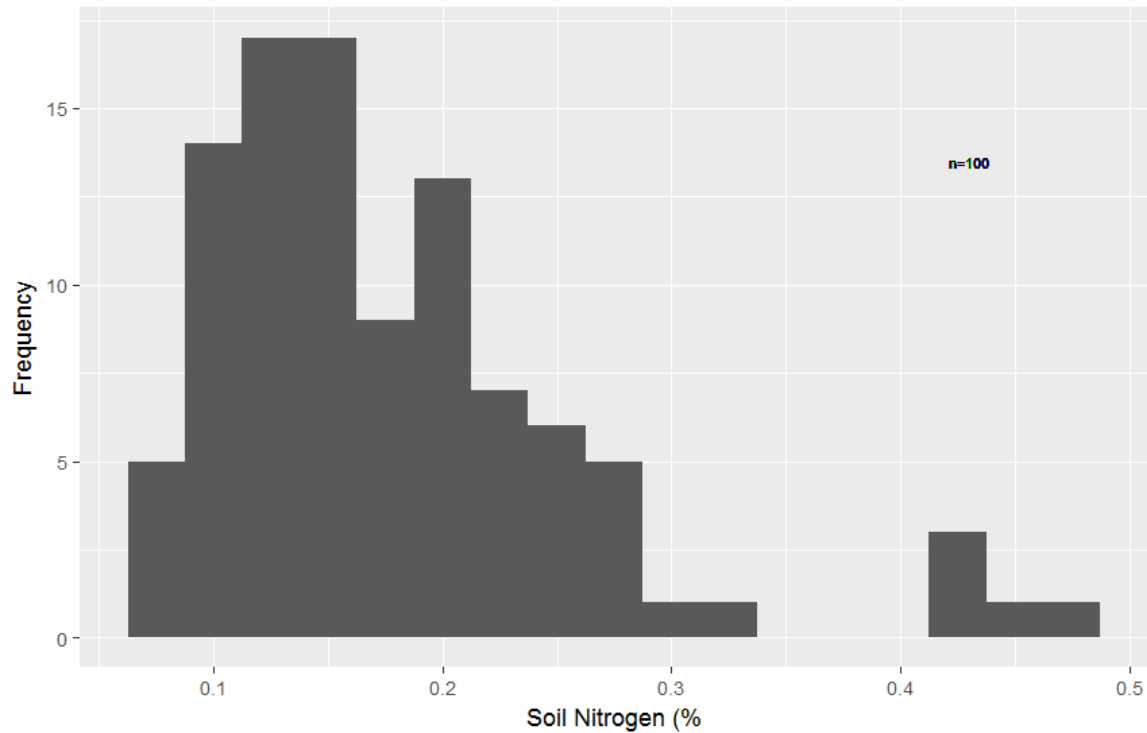


Figure 9: Histogram of nitrogen content (%) across the field site

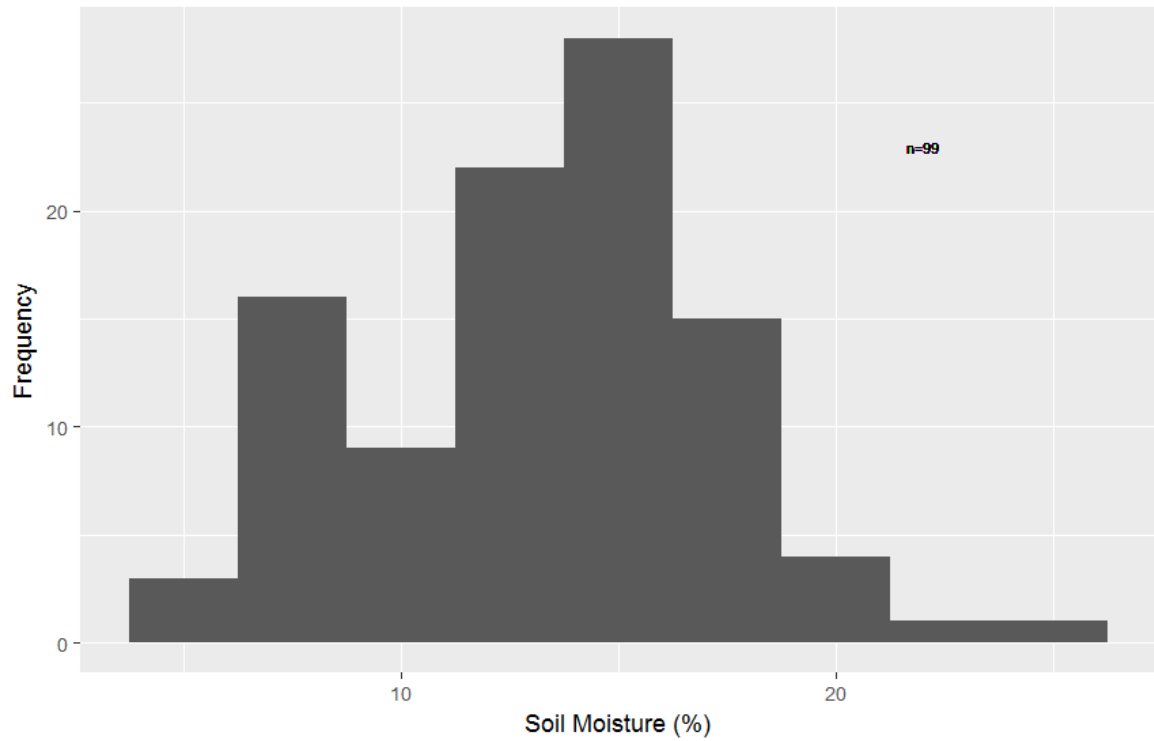


Figure 10: Histogram of moisture content (%) across the field site

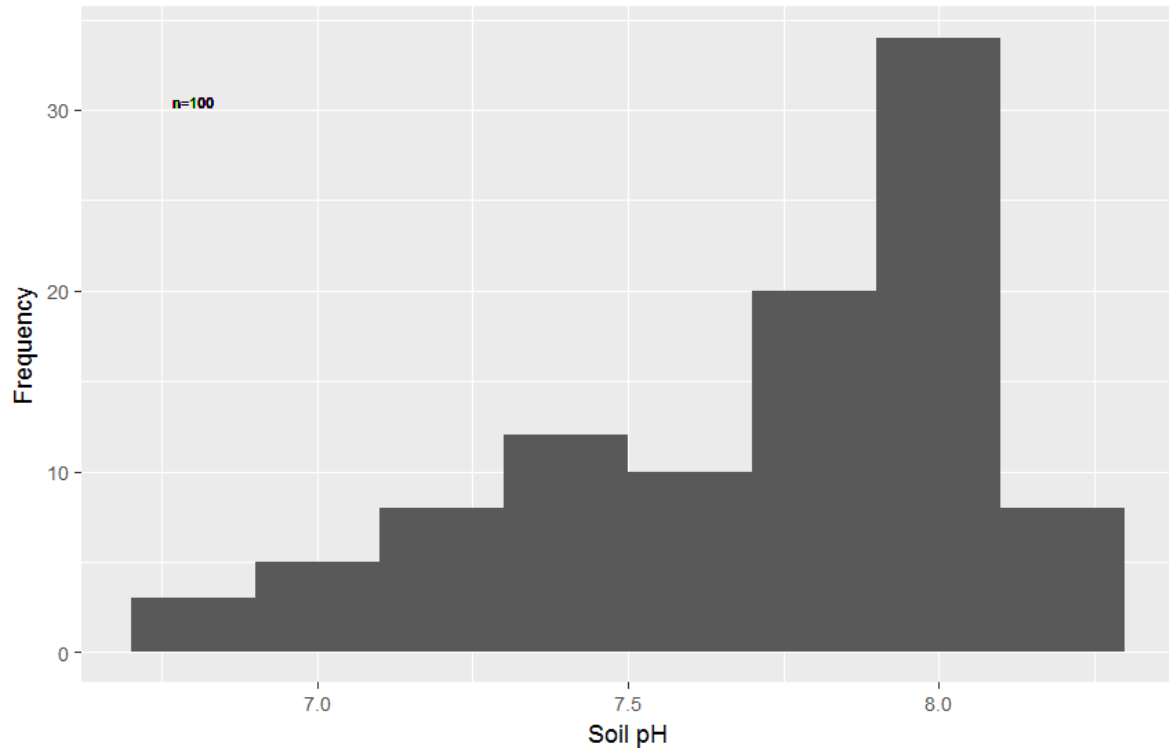


Figure 11: Histogram of pH across the field site

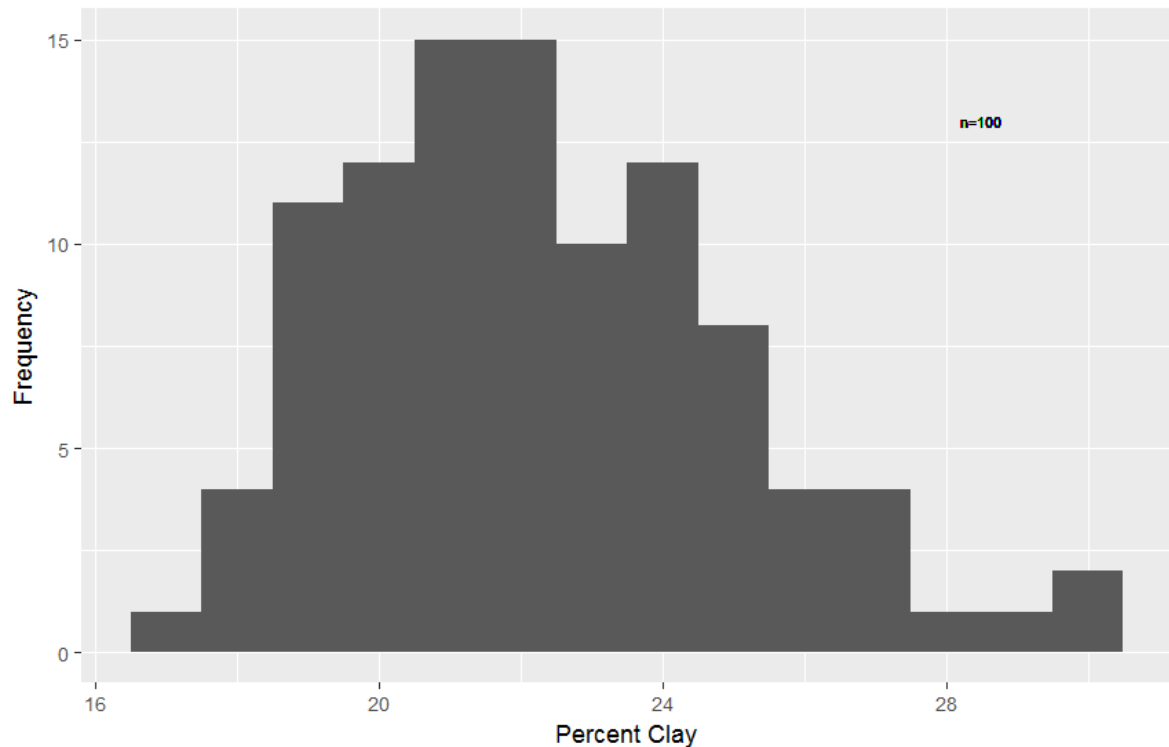


Figure 12: Histogram of clay content (%) across the field site

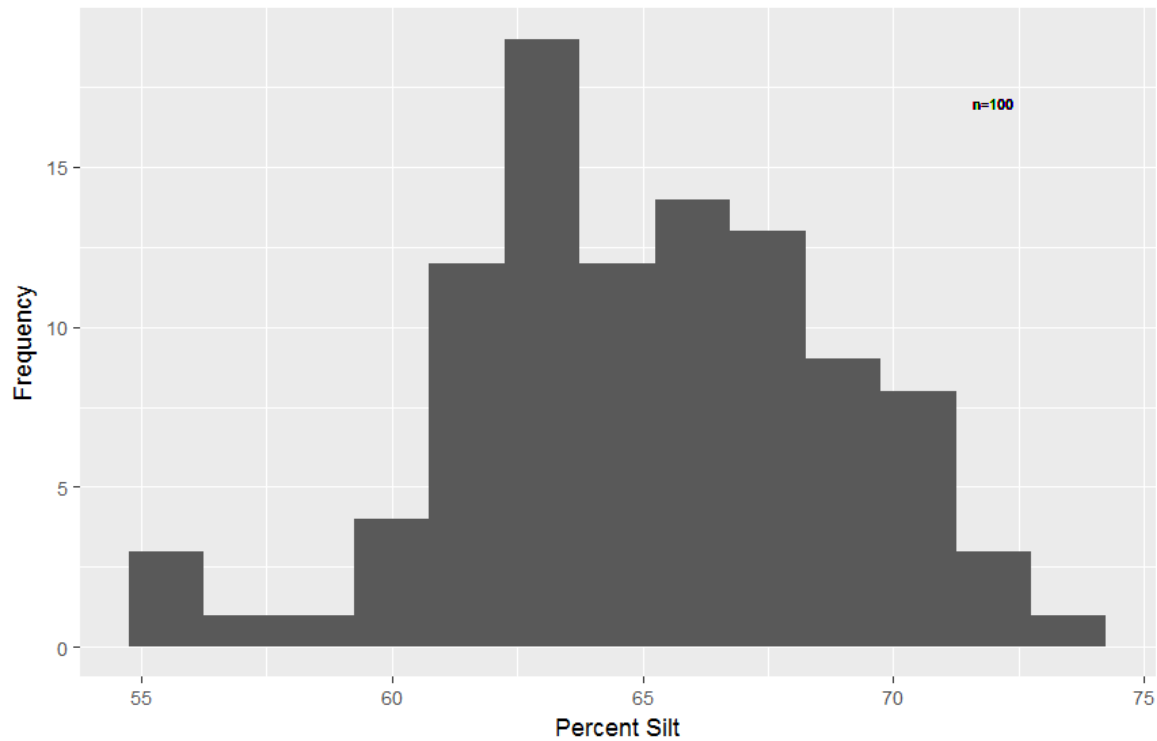


Figure 13: Histogram of silt content (%) across the field site

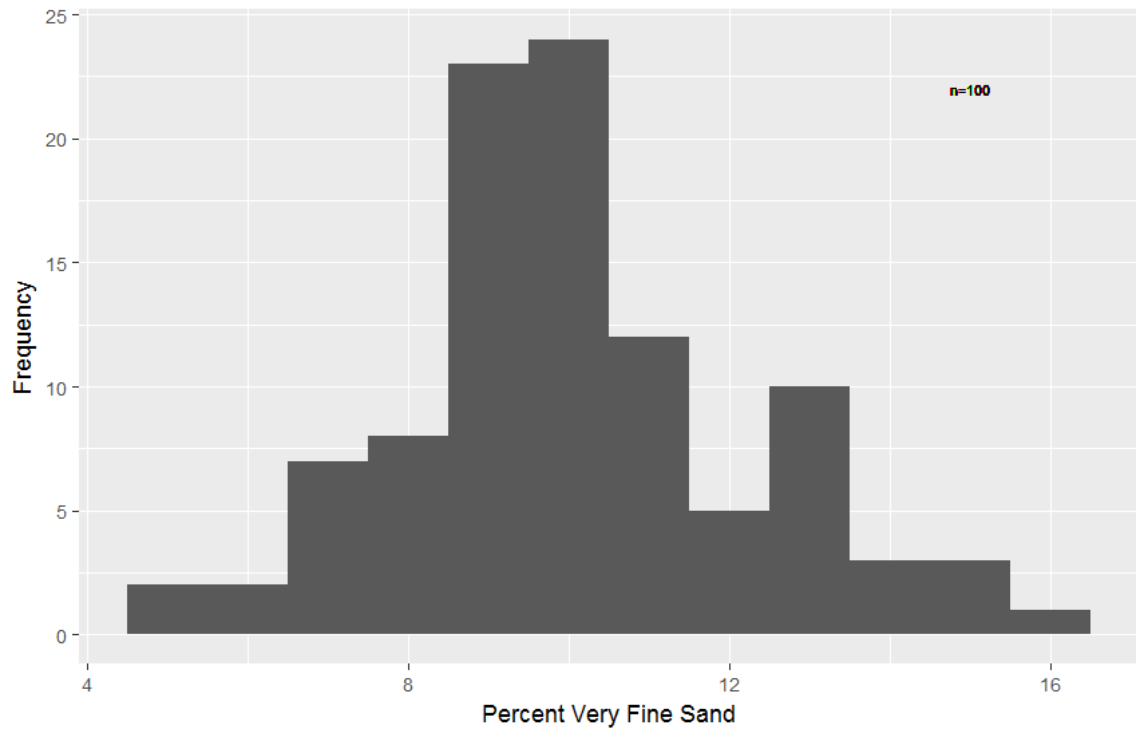
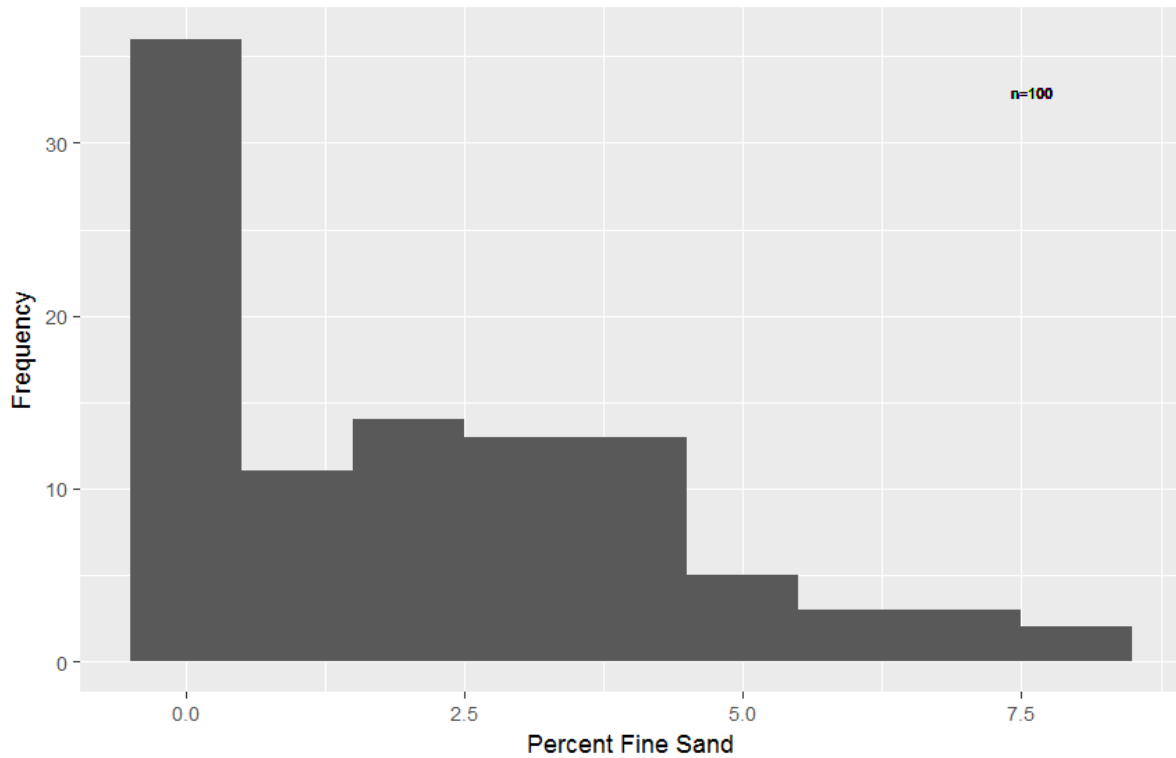
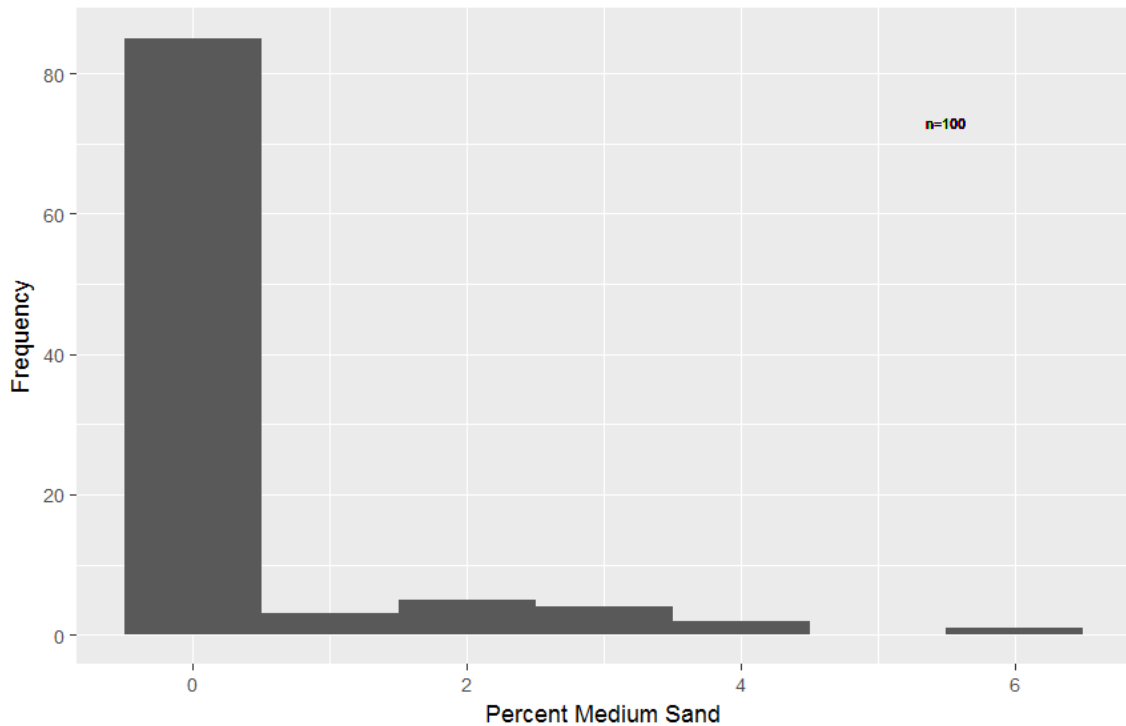


Figure 14: Histogram of very fine sand content (%) across the field site



*Figure 15: Histogram of fine sand content (%) across the field site*



*Figure 16: Histogram of medium sand content (%) across the field site*

Distance from juniper trees, and by extension vegetation cover, produces significantly

different soil organic matter content, carbon content, nitrogen content,  $\delta^{13}\text{C}$ ,  $\delta^{15}\text{N}$ ,  $\delta^{15}\text{N}$  stratification ratios, and percent very fine sand content (Table 3). Juniper age, which is represented by juniper trunk diameter, causes recognizable variations in soil organic matter content, carbon content, nitrogen content,  $\delta^{13}\text{C}$ ,  $\delta^{15}\text{N}$  stratification ratios, pH, and very fine sand content (Table 4).

*Table 3: Analysis of variance between samples from different distances from juniper trees (Degrees of freedom = 37)*

Dependent Variable	F-statistic	p-value
Organic matter	10.62	0.000227
Carbon	11.6	0.000123
Nitrogen	10.35	0.000269
$\delta^{13}\text{C}$	10.04	0.000329
$\delta^{15}\text{N}$	6.001	0.00553
$\delta^{13}\text{C}$ stratification ratio	1.291	0.301
$\delta^{15}\text{N}$ stratification ratio	10.48	0.00108
Moisture	1.396	0.261
pH	0.18	0.836
Clay	0.308	0.737
Silt	0.7	0.503
Very fine sand	3.508	0.0403

*Table 4: Analysis of variance between samples under juniper trees of different trunk diameters (Degrees of freedom = 38)*

Dependent Variable	F-statistic	p-value
Organic matter	10.78	0.00221
Carbon	8.708	0.0054
Nitrogen	7.43	0.00965
$\delta^{13}\text{C}$	5.193	0.0284
$\delta^{15}\text{N}$	1.053	0.311
$\delta^{13}\text{C}$ stratification ratio	0.619	0.442
$\delta^{15}\text{N}$ stratification ratio	5.234	0.0345
Moisture	1.632	0.209
pH	12.08	0.00129
Clay	1.63	0.21
Silt	0.627	0.433
Very fine sand	9.391	0.004

Organic matter content declines with increasing distance from juniper trees (Figure 17).

This decline is more pronounced in the surface soil compared to the subsurface soil. The highest organic matter concentrations are found below juniper canopies, while the lowest organic matter concentrations are found over five meters from juniper trees. Under the juniper canopies, organic matter content is slightly higher in the surface soil compared to the subsurface soil (Figure 18). Soil over five meters from juniper trees was lowest in organic matter content. As juniper age increases, soil organic matter content below the tree canopy also increases (Figure 18).

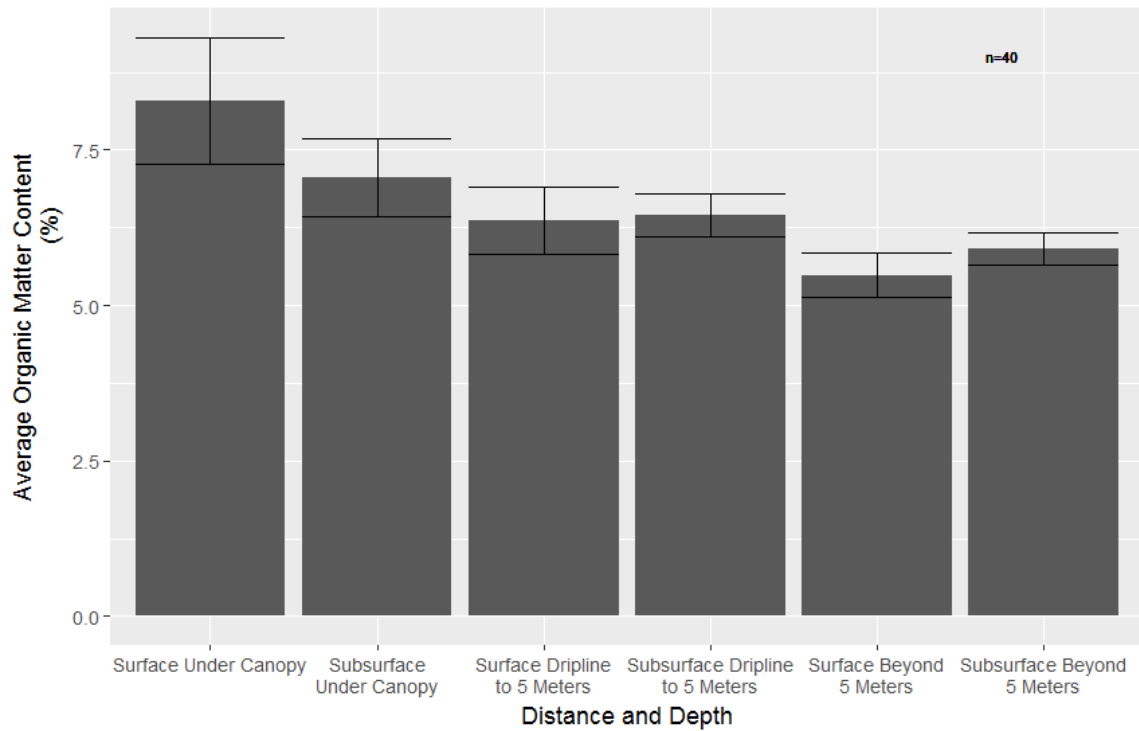


*Figure 17: Average soil organic matter content with increasing distance from juniper trees for two depth increments*

Interestingly, subsurface soil beyond juniper canopies had higher organic matter concentrations compared to surface soil (Figure 17). Although the soil under juniper trees exhibited a decline in organic matter content with depth and the soil under grasses exhibited a magnification in organic matter content with depth,  $\delta^{13}\text{C}$  stratification ratios show little variation

over distance (Figure 19).

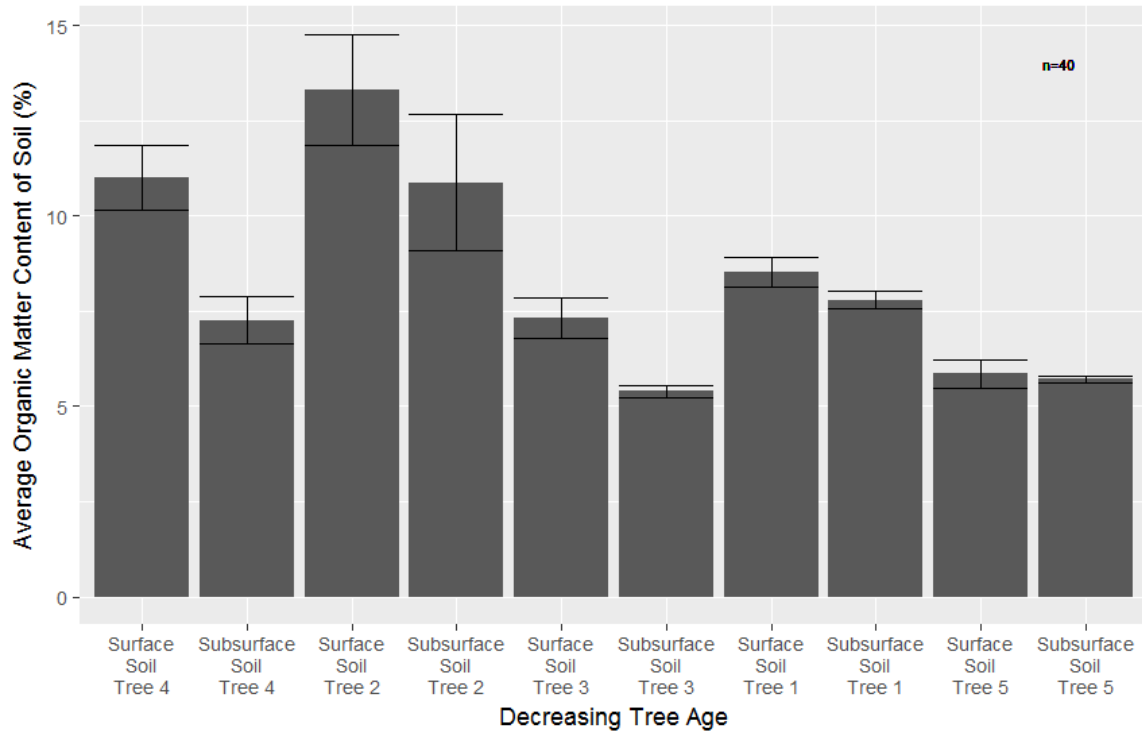


*Figure 18: Soil organic matter content below juniper canopies with increasing tree age*

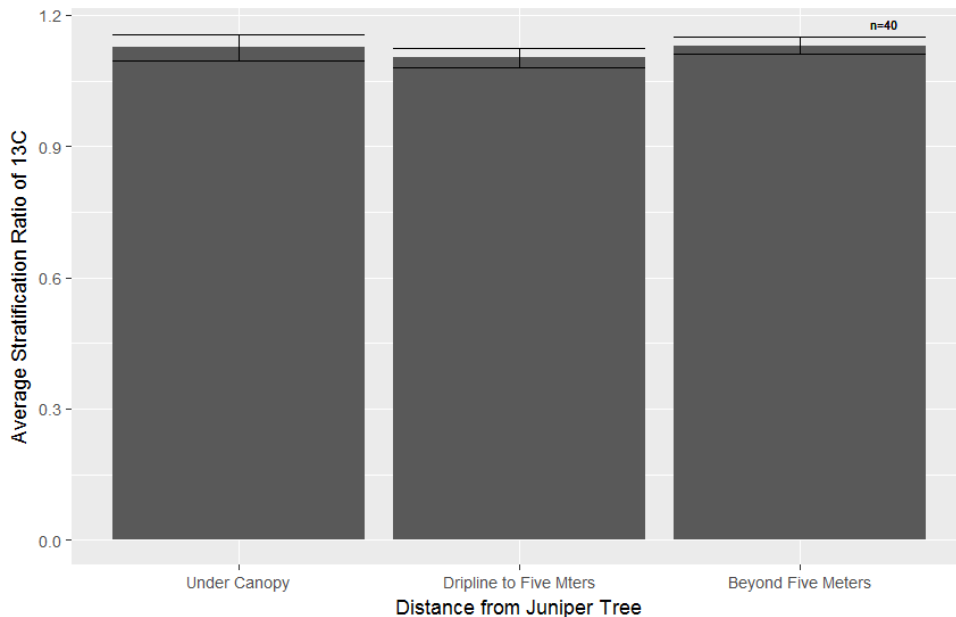


*Figure 19: Average stratification ratio of  $\delta^{13}\text{C}$  with increasing distance from juniper trees*

Soil carbon content is consistently elevated in surface soil compared to subsurface soil

across all distances from juniper trees (Figure 20). Similar to observed patterns in soil organic matter content, soil carbon content declines with increasing distance from juniper trees and increases as trees become more established on the study site (Figure 21).

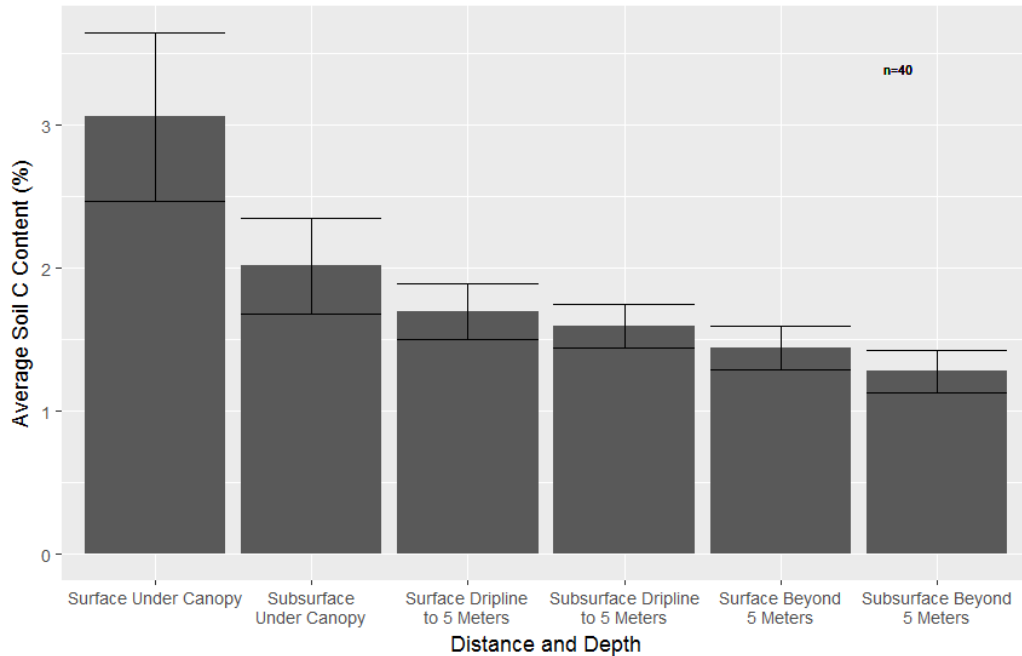


*Figure 20: Average soil carbon content with increasing distance from juniper trees for two depth increments*

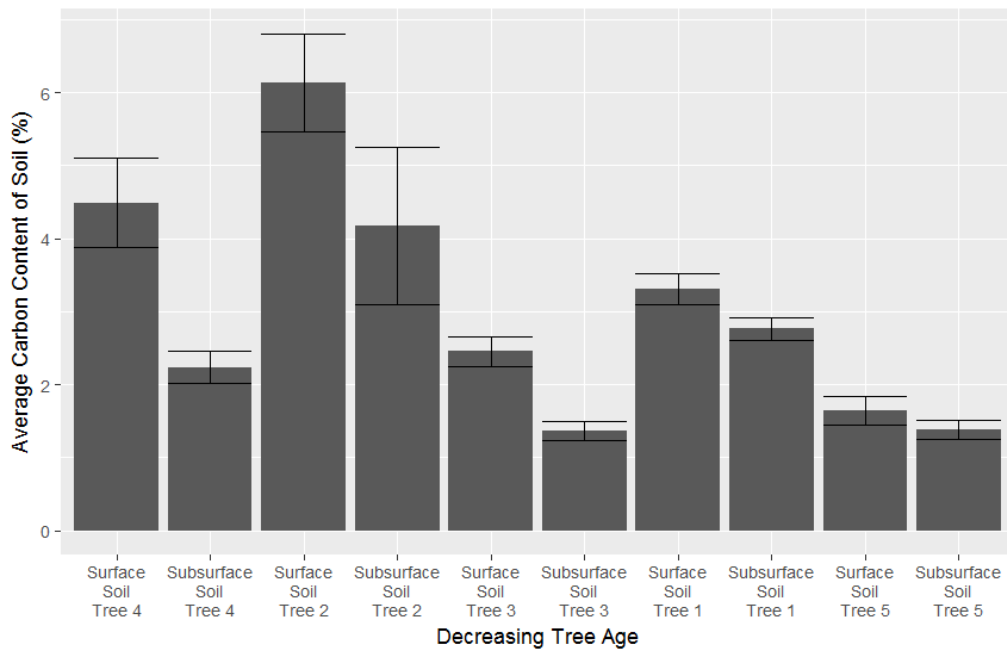


*Figure 21: Soil carbon content with increasing tree age*

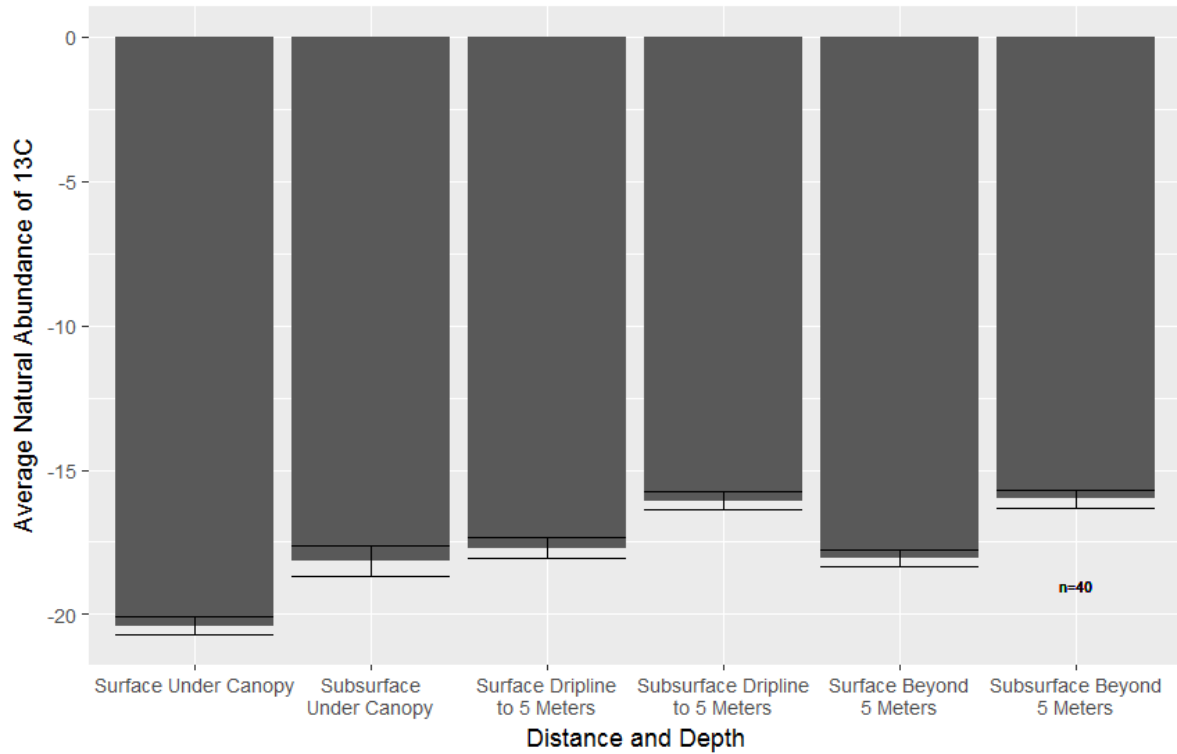


*Figure 22: Average natural abundance of  $^{13}\text{C}$  with increasing distance from juniper trees for two depth increments*

As distance from juniper trees increases,  $\delta^{13}\text{C}$  values become less negative (Figure 22).

The transition from juniper trees to grasses is accompanied by an enrichment in soil  $\delta^{13}\text{C}$ . At all distances, subsurface soil is more enriched in  $\delta^{13}\text{C}$  compared to its corresponding surface soil (Figure 22). The  $\delta^{13}\text{C}$  values of soil below juniper trees is slightly lower than the  $\delta^{13}\text{C}$  values of the juniper leaf litter (Figure 23; Table 2), showing a transformation of litter as it is incorporated into the soil profile. A decrease in tree age corresponds with an enrichment in soil  $\delta^{13}\text{C}$  below the canopy (Figure 23).

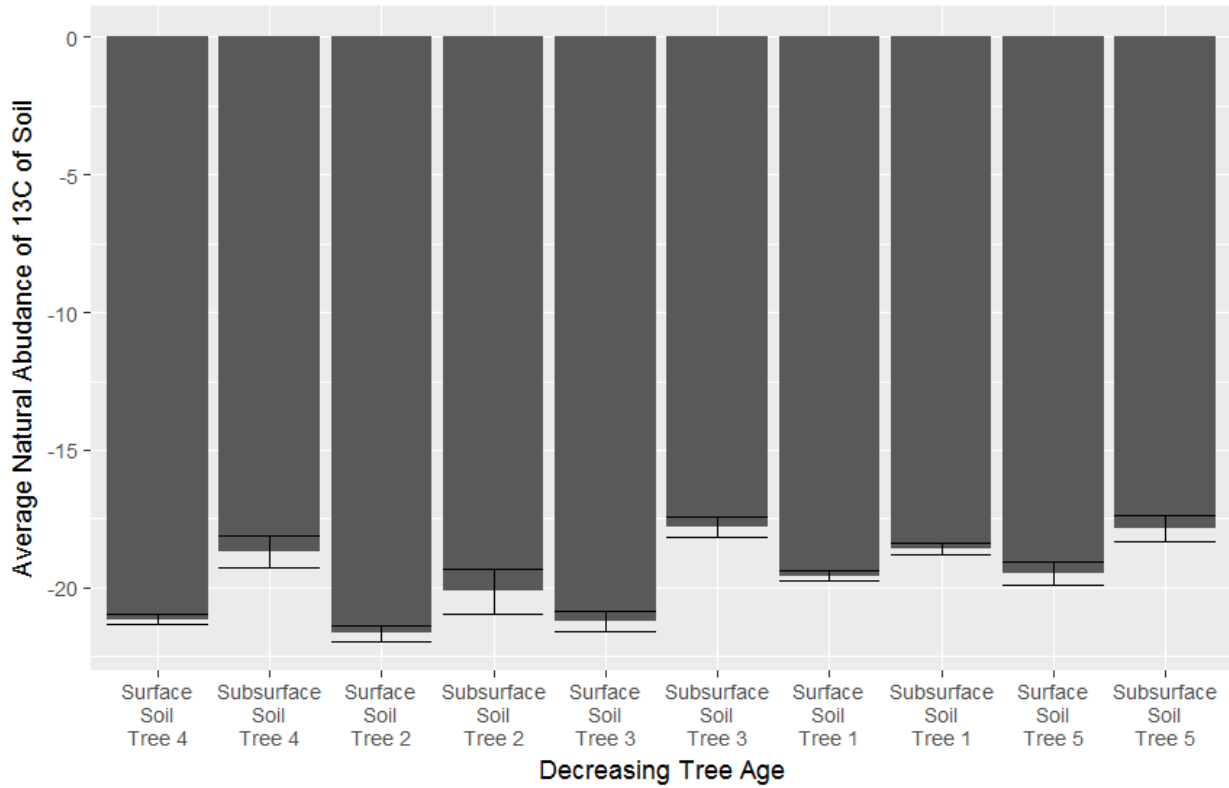


*Figure 23: Average natural abundance of  $^{13}\text{C}$  with increasing tree age*

The C:N of soil is higher under juniper canopies compared to adjacent intercanopy and grassy areas (Figure 24). Beyond the juniper canopies, soil C:N varies little with increasing distance from juniper trees. At all sampled points within the site, soil C:N is slightly lower in the subsurface soil relative to the surface soil. Juniper litter C:N rises with increasing tree age (Figure 25). This relationship is mirrored in the soil, where soil C:N under juniper canopies rises as trees grow and mature (Figure 26).

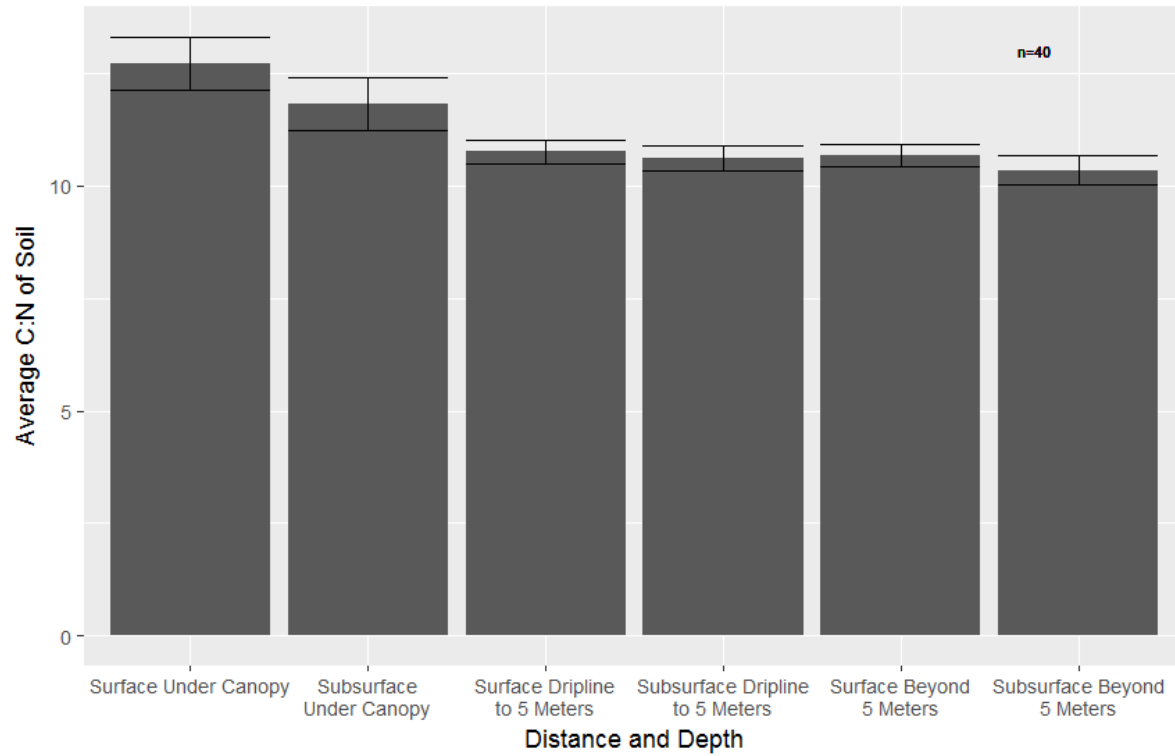


*Figure 24: Average soil C:N with increasing distance from juniper trees for two depth increments*

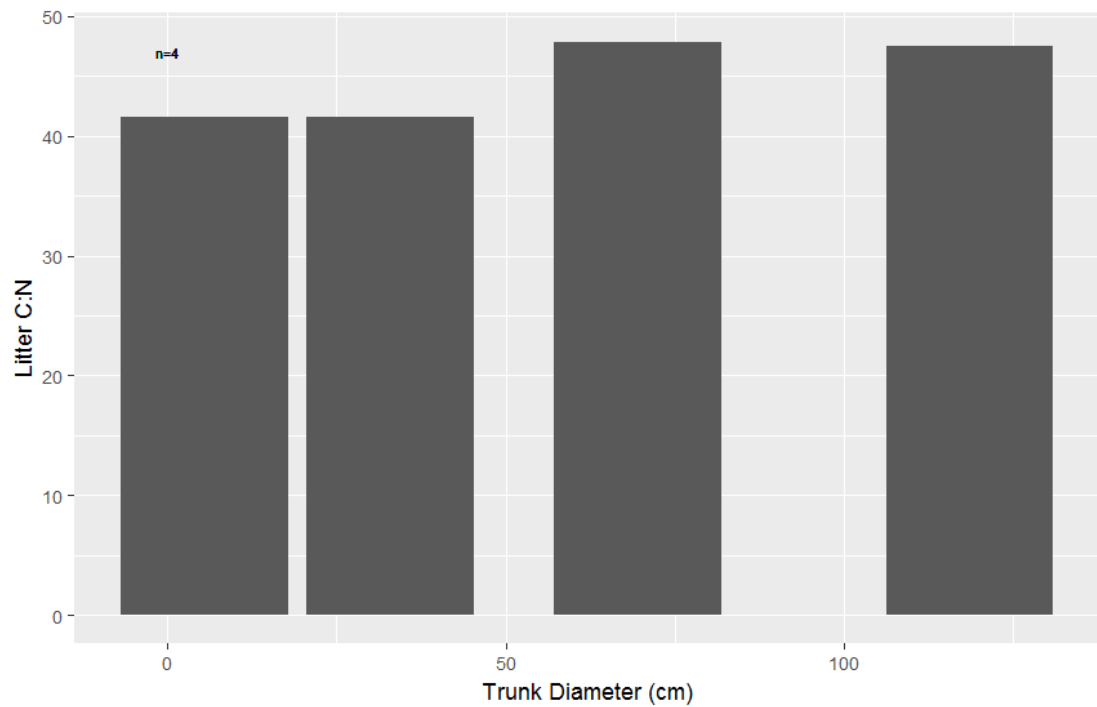


*Figure 25: Litter C:N with increasing tree age*

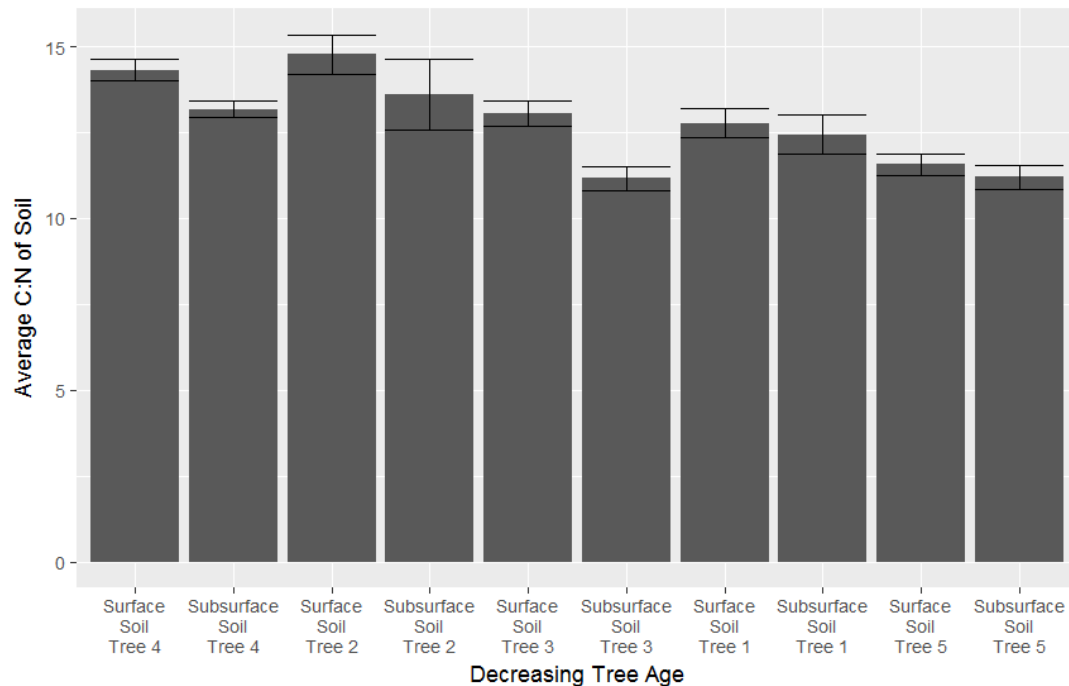


Figure 26: Soil C:N under juniper canopies with increasing tree age

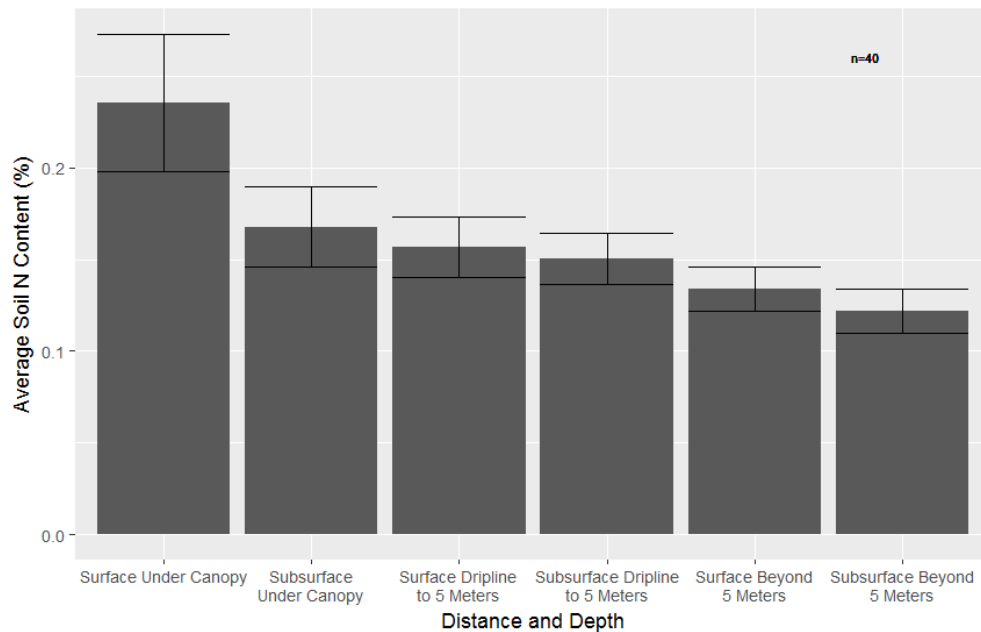


Figure 25: Average soil nitrogen content with increasing distance from juniper trees for two depth increments

Soil nitrogen content is highest in the surface soil below juniper canopies (Figure 27). As distance from juniper trees increases, soil nitrogen content decreases. As tree age increases, soil

nitrogen in surface soil increases (Figure 28); however, there is not a significant relationship between tree age and subsurface soil nitrogen ( $r=0.23, p= 0.25$ ).

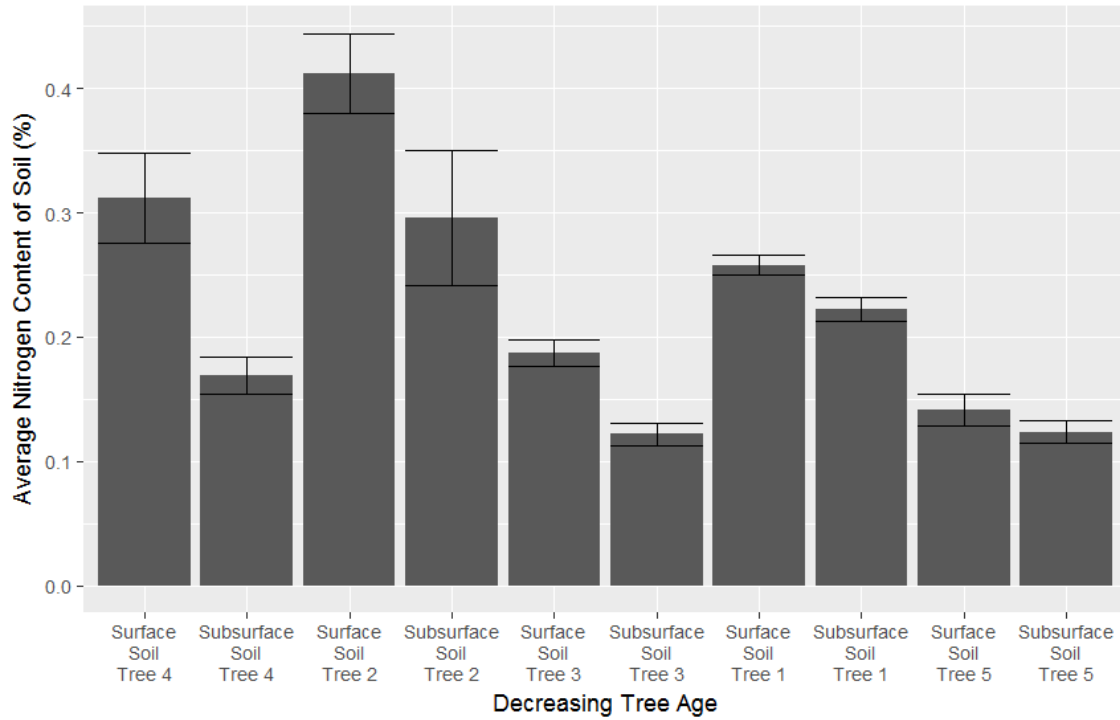


Figure 26: Soil nitrogen content with increasing tree age

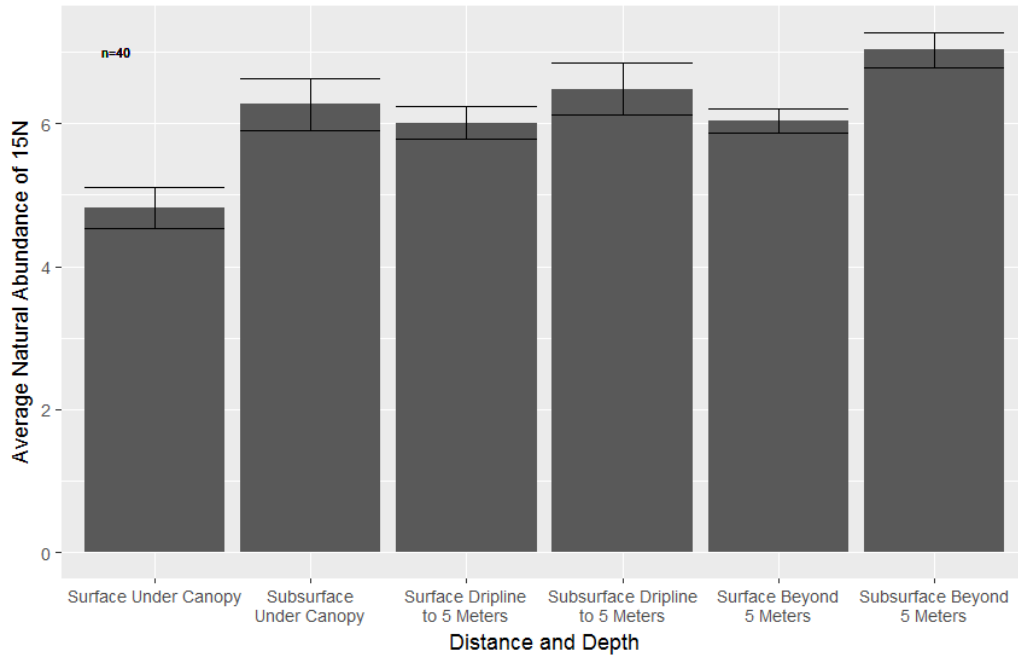


Figure 27: Average natural abundance of  $^{15}\text{N}$  with increasing distance from juniper trees for two depth increments

At all distance increments, subsurface soil is more enriched in  $\delta^{15}\text{N}$  compared to surface soil (Figure 29). As the distance from juniper trees increases, an enrichment in soil  $\delta^{15}\text{N}$  occurs. Stratification ratios of  $\delta^{15}\text{N}$  across depth are closer to a value of 1 in soil beyond the juniper canopy (see Figure 30). As tree age increases, the C:N of the soil under the tree canopy increases (Figure 25), however tree diameter and  $\delta^{15}\text{N}$  of the underlying soil are not significantly correlated for surface samples or subsurface samples, as shown in Figure 31 ( $r_{surface} = -0.45$ ,  $p_{surface} = 0.075$ ;  $r_{subsurface} = -0.025$ ,  $p_{subsurface} = 0.47$ ).

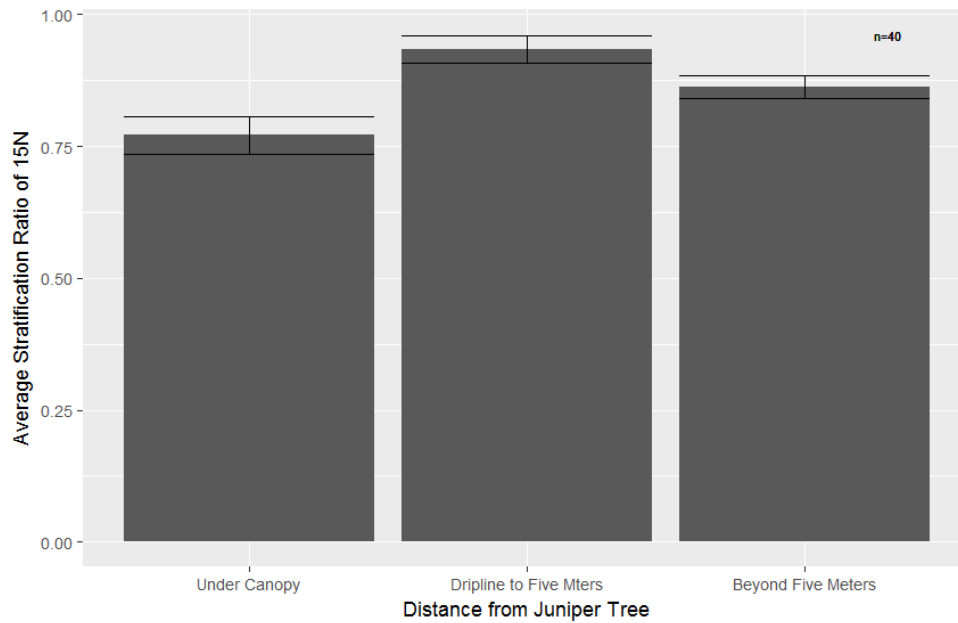


Figure 28: Soil  $\delta^{15}\text{N}$  stratification ratios with increasing distance from juniper trees

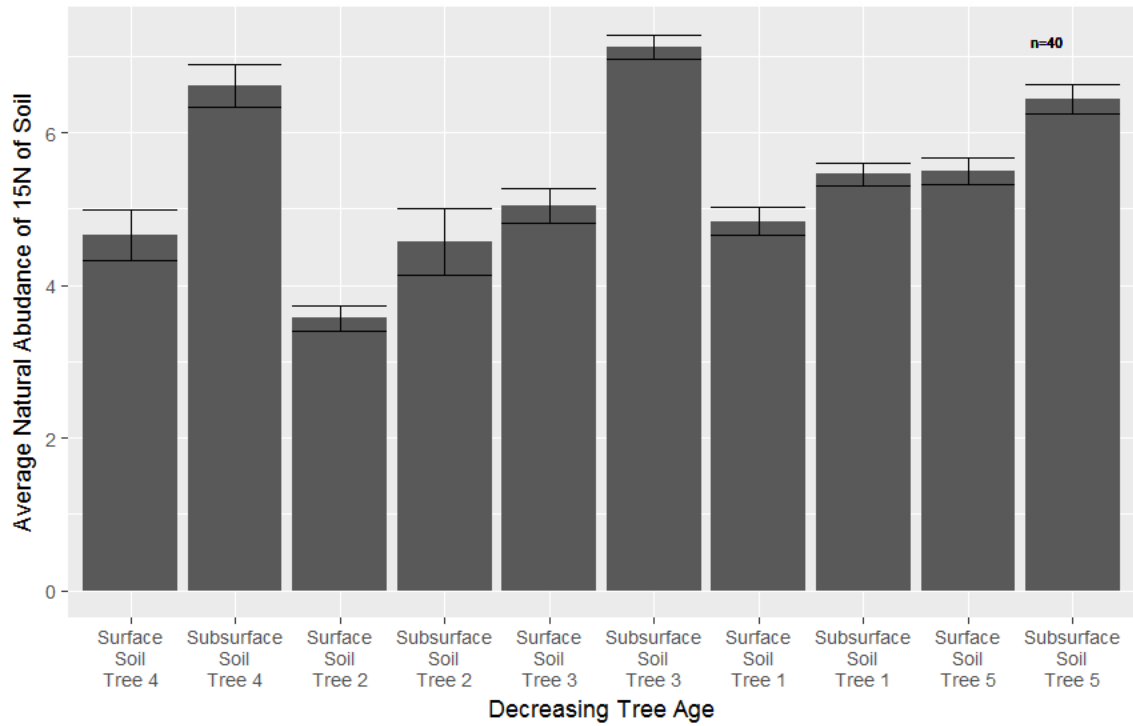


Figure 29: Soil  $\delta^{15}\text{N}$  under juniper canopies with increasing tree age

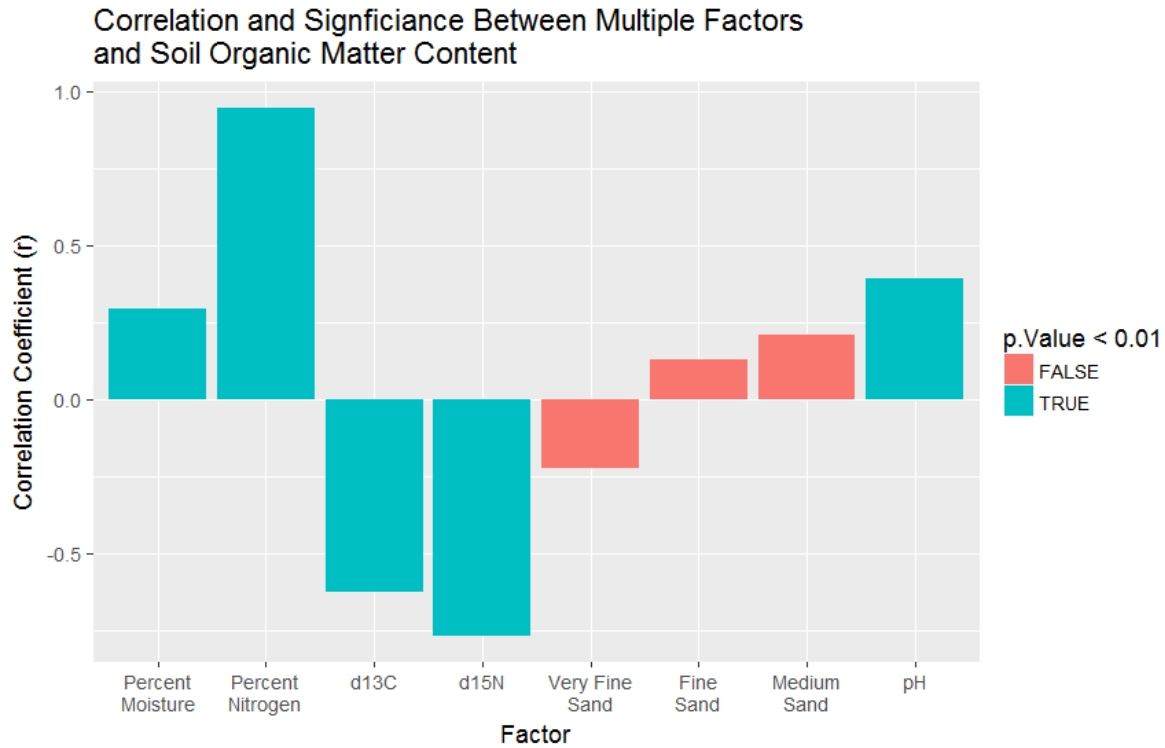
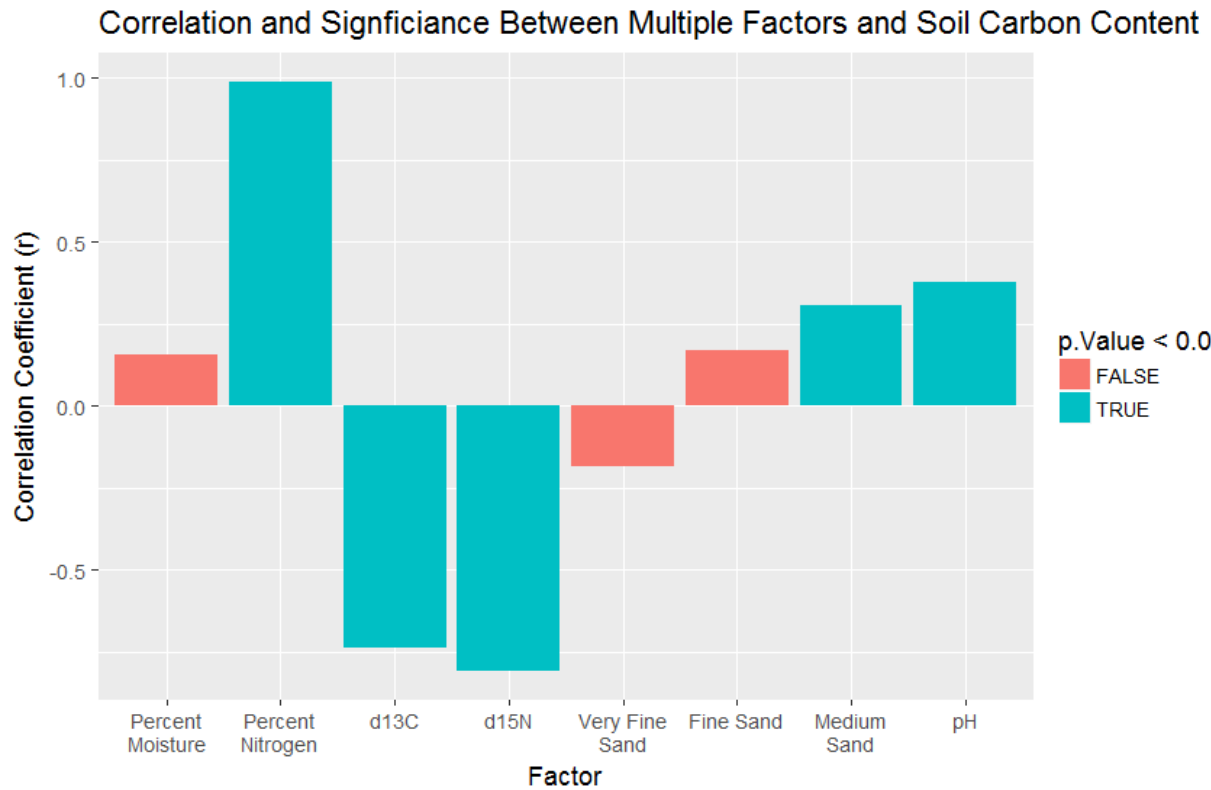


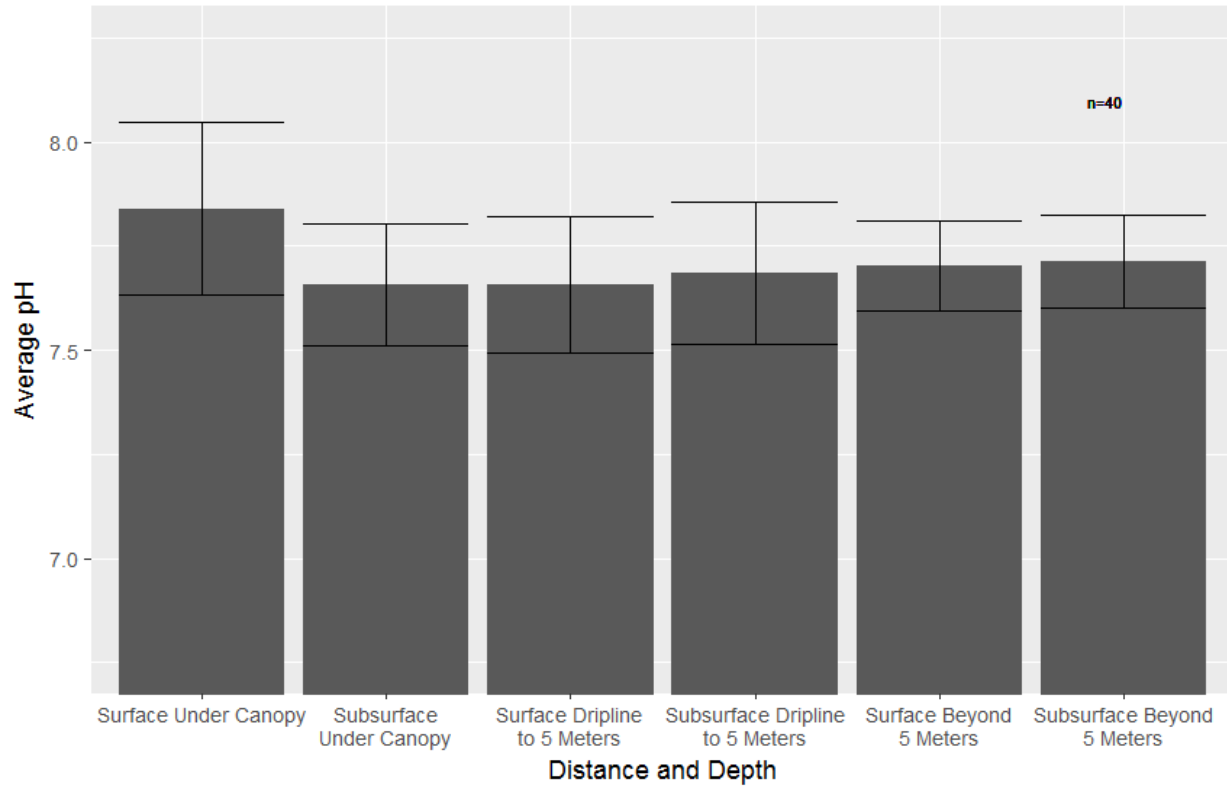
Figure 30: Correlations between selected soil properties and soil organic matter content

Figure 32 above shows the correlations between potential determinants of soil organic matter content and organic matter content. Among factors tested, percent moisture, percent nitrogen,  $\delta^{13}\text{C}$ ,  $\delta^{15}\text{N}$ , and pH show the highest correlations with organic matter content with high significance ( $p < 0.01$ ). Percent nitrogen is most correlated with organic matter content ( $r=0.95$ ), which is expected given nitrogen availability influences organic matter decomposition (Garten, 2006). As nitrogen content and moisture content increase and soil becomes more alkaline, organic matter content increases. The percentage of particles in very fine sand fraction, the fine sand fraction, and the medium sand fraction are correlated with organic matter content, but not significantly so. The plethora of fine particles in the soil may have obscured the particles above, including the fine sand particles, causing these particles to go undetected by the laser in the particle size analyzer. Therefore, the proportion of fine sand and medium sand in the samples is underestimated. No particles above medium sand were detected, however sieving of some of the samples indicated that such particles were present, but in very small numbers. The percentage of particles in the clay fraction and the silt fraction had  $r$ -values less than 0.1. These factors were excluded from further study of soil organic matter determinants.



*Figure 31: Correlations between selected soil properties and soil carbon content*

As shown in Figure 33, nitrogen content, pH,  $\delta^{13}\text{C}$ ,  $\delta^{15}\text{N}$ , and the percentage of medium sand are positively and significantly correlated with carbon content ( $p<0.01$ ). These correlations between soil carbon and these variables are similar to those in Figure 33; however, medium sand is not significantly correlated with organic matter content but is correlated with carbon content. Medium sand particles may contain high concentrations of inorganic carbon, however given the underestimation of the medium sand fraction of soil for this study area, this information may not be accurate. Despite the correlation between organic carbon content and pH, pH does not show a linear trend with increasing distance from juniper trees, however pH is slightly more alkaline in the surface soil below juniper canopies (Figure 34).



*Figure 32: pH with increasing distance from juniper trees*

No significant difference in soil properties among compass directions was detected through the ANOVAs (Table 5). However, contradictory to the results of the ANOVA tests, surface and subsurface soil moisture is highest on the north side of trees and surface soil moisture is lowest on the southern sides of juniper trees (Figure 35). In this instance, the results of ANOVA tests should be discussed in conjunction with other analyses to ensure spatial patterns in soil properties are not overlooked.

*Table 5: Analysis of variance between samples under juniper canopies from different compass directions (Degrees of freedom = 36)*

Dependent Variable	F-statistic	p-value
Organic matter	1.031	0.39
Carbon	0.857	0.472
Nitrogen	0.58	0.632
$\delta^{13}\text{C}$	0.464	0.709
$\delta^{15}\text{N}$	0.3	0.825
$\delta^{13}\text{C}$ stratification ratio	0.942	0.444
$\delta^{15}\text{N}$ stratification ratio	0.997	0.419
Moisture	0.531	0.664
pH	0.131	0.941
Clay	0.551	0.651
Silt	0.433	0.433
Very fine sand	0.367	0.777

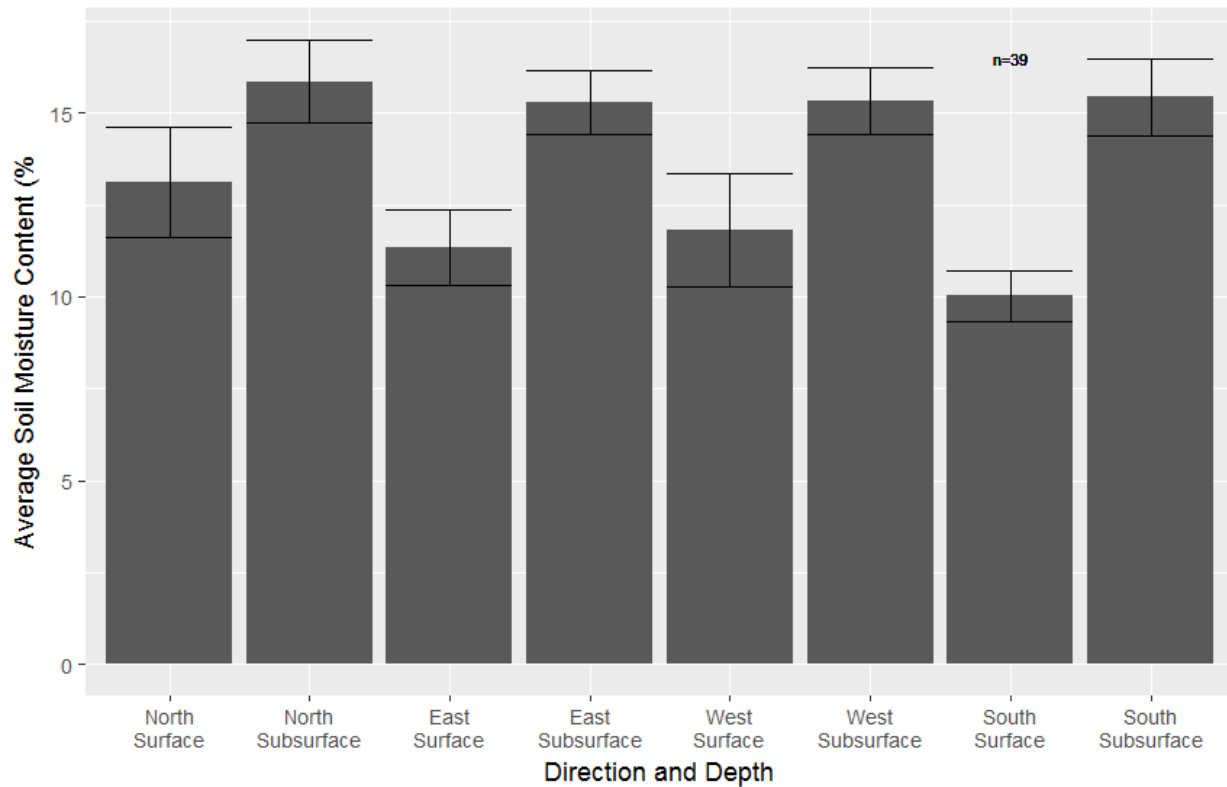


*Figure 33: The effect of direction from juniper tree and depth on soil moisture*

Maps of interpolated surfaces of organic matter, carbon content, nitrogen content,  $\delta^{13}\text{C}$ ,  $\delta^{15}\text{N}$ , and moisture for separate depth increments are shown in Figures 36-47. Interpolations were generated using Empirical Bayesian Kriging because this geospatial method predicted soil properties with relatively low error, visually captured soil variability around juniper trees, and attempted to predict values in unsampled points in grassy areas, where less observations were available. The root-mean-squared-error (RMSE) of predictions produced using Empirical Bayesian Kriging for each variable are shown in Table 6. Inverse distance weighting over-generalized soil properties and did not capture small-scale variability. Simple kriging had high accuracy but only illustrated variability in soil properties in very proximity to juniper trees. Ordinary kriging produced ridged surfaces that matched the lines of the radial sampling transects, rather than the spatial variability known to exist within the data.

The final interpolation maps visualize islands of fertility within the study where carbon content and nitrogen content are elevated through the appearance of circular patterns around trees. Older, larger junipers are accompanied by wider circles of higher carbon, nitrogen, and organic matter content, and lower  $\delta^{13}\text{C}$  and  $\delta^{15}\text{N}$  enrichment. This is expected given that islands of fertility are more pronounced as plant aboveground biomass increases (Jackson and Caldwell, 1993). Predicted moisture had the highest RMSE of any variable, which can be explained by soil water's low spatial autocorrelation (Jackson and Caldwell, 1993). The ANOVA tests suggested that orientation from juniper trees does not create significant variability in soil moisture. The soil moisture maps show that moisture does indeed vary by compass direction from juniper trees, but the compass directions of the highest and lowest soil moisture values are not consistent between trees. The maps of  $\delta^{13}\text{C}$  and  $\delta^{15}\text{N}$  support the conclusion that soil is less enriched in  $\delta^{13}\text{C}$  and  $\delta^{15}\text{N}$  close to juniper trees.

*Table 6: Root-mean-squared-error in predictions of multiple variables generated using Empirical Bayesian Kriging*

Variable	RMSE
Surface organic matter	1.7196
Subsurface organic matter	1.3131
Surface carbon content	1.0918
Subsurface carbon content	0.8125
Surface nitrogen content	0.0605
Subsurface nitrogen content	0.0433
Surface $\delta^{13}\text{C}$	1.2693
Subsurface $\delta^{13}\text{C}$	1.2964
Surface $\delta^{15}\text{N}$	0.7612
Subsurface $\delta^{15}\text{N}$	0.5655
Surface moisture content	2.4790
Subsurface moisture content	2.6698

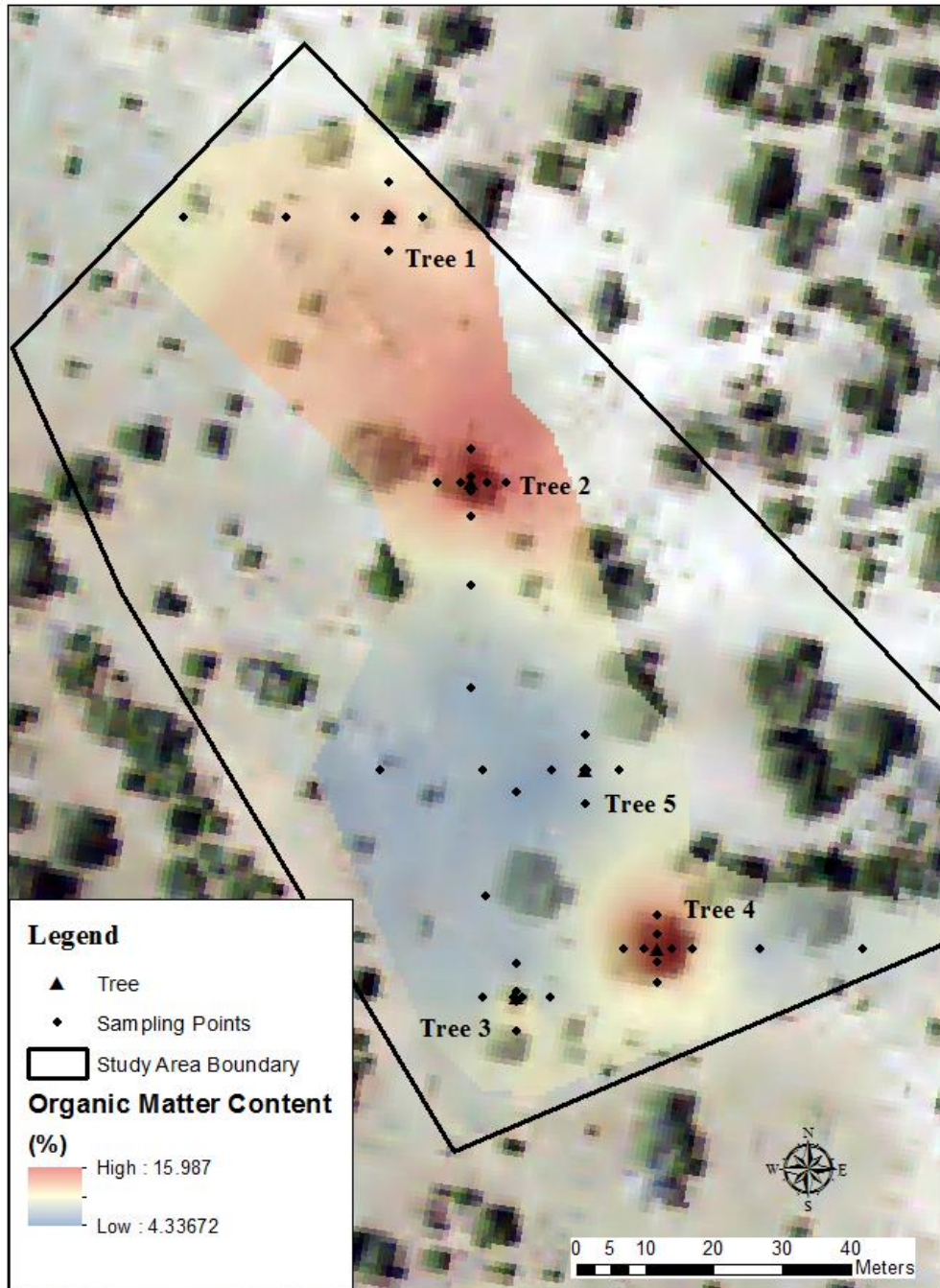


Figure 34: : Surface soil organic matter map

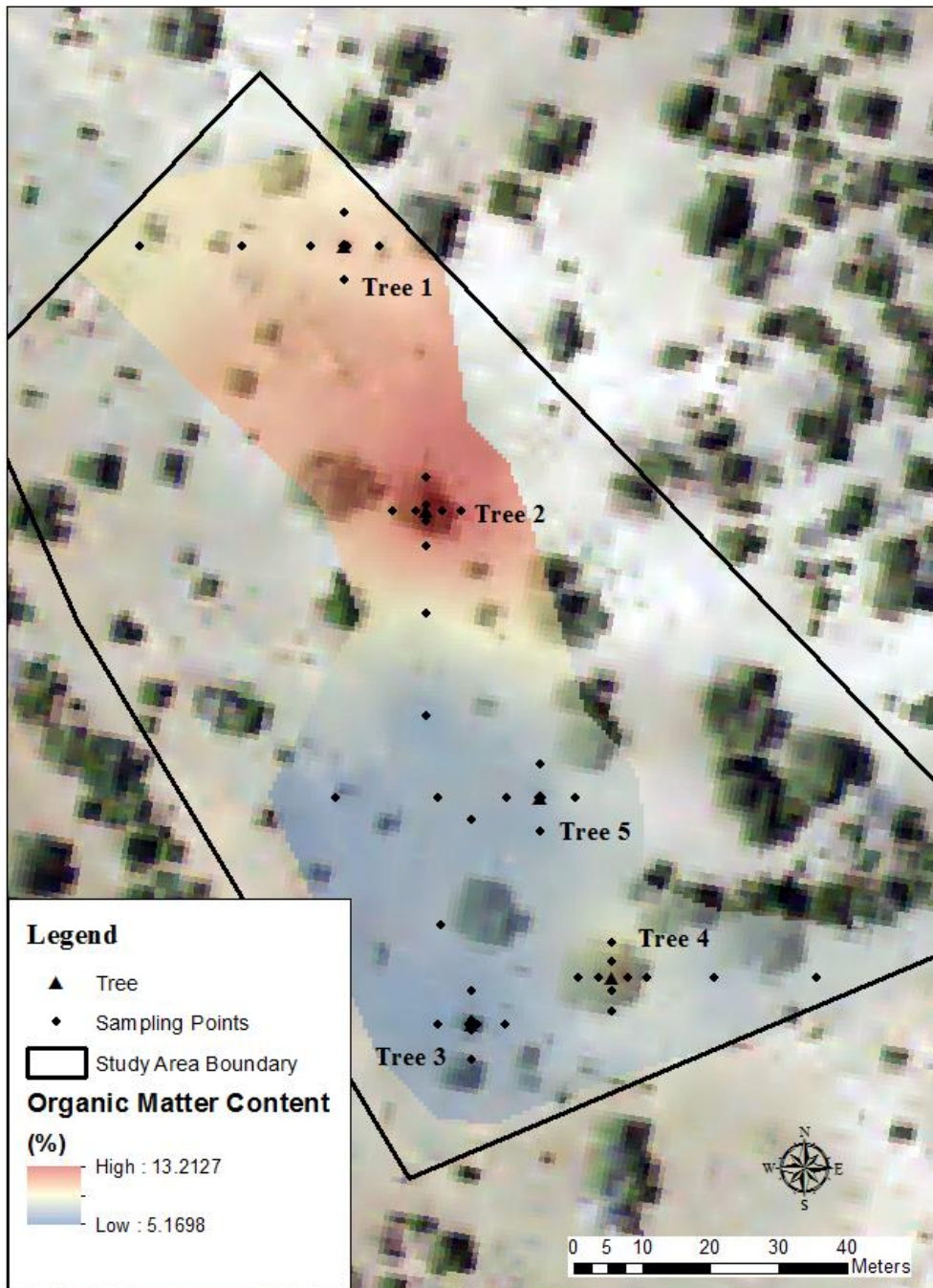


Figure 35: Subsurface soil organic matter map

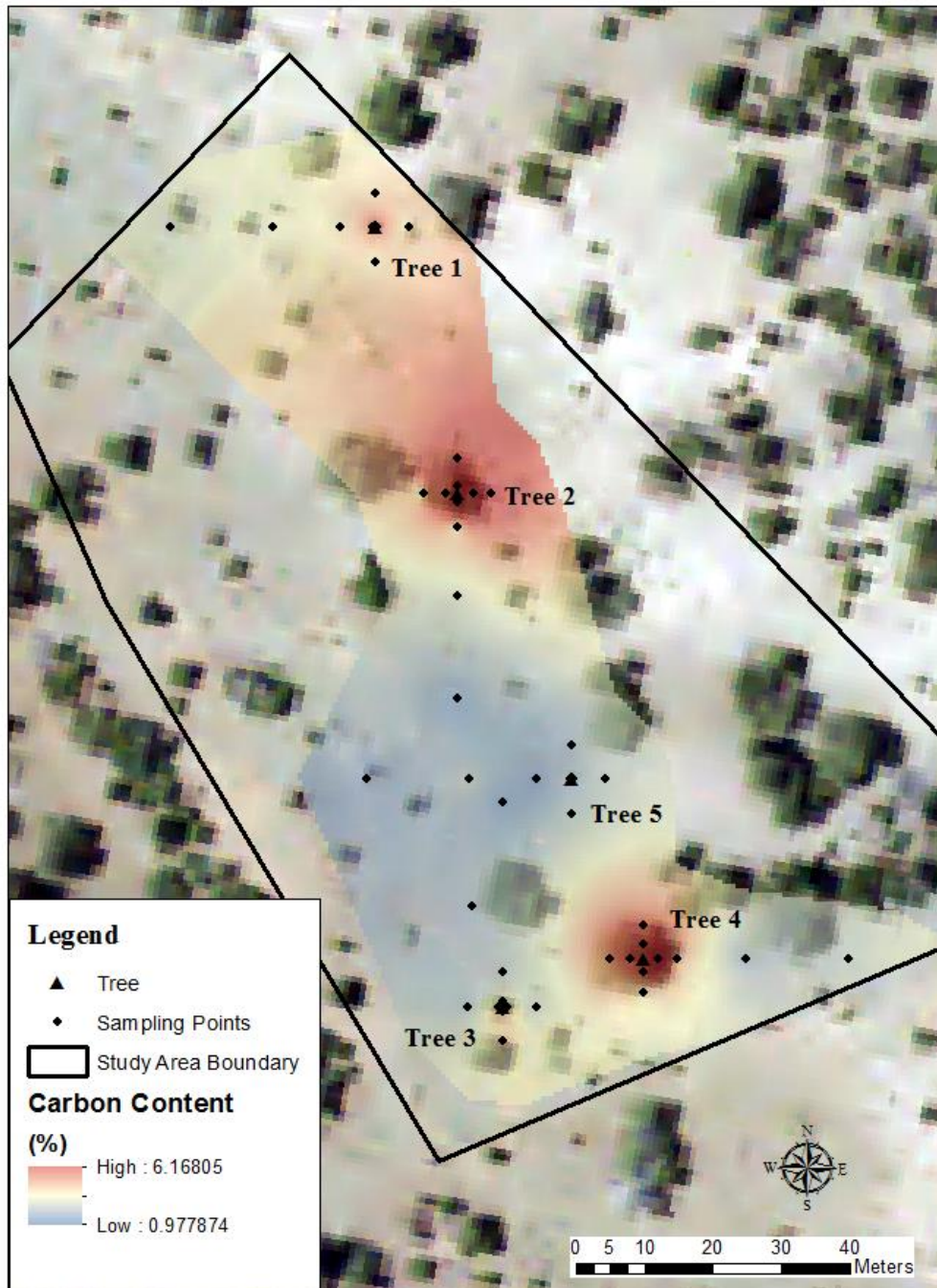


Figure 36: Surface soil carbon map

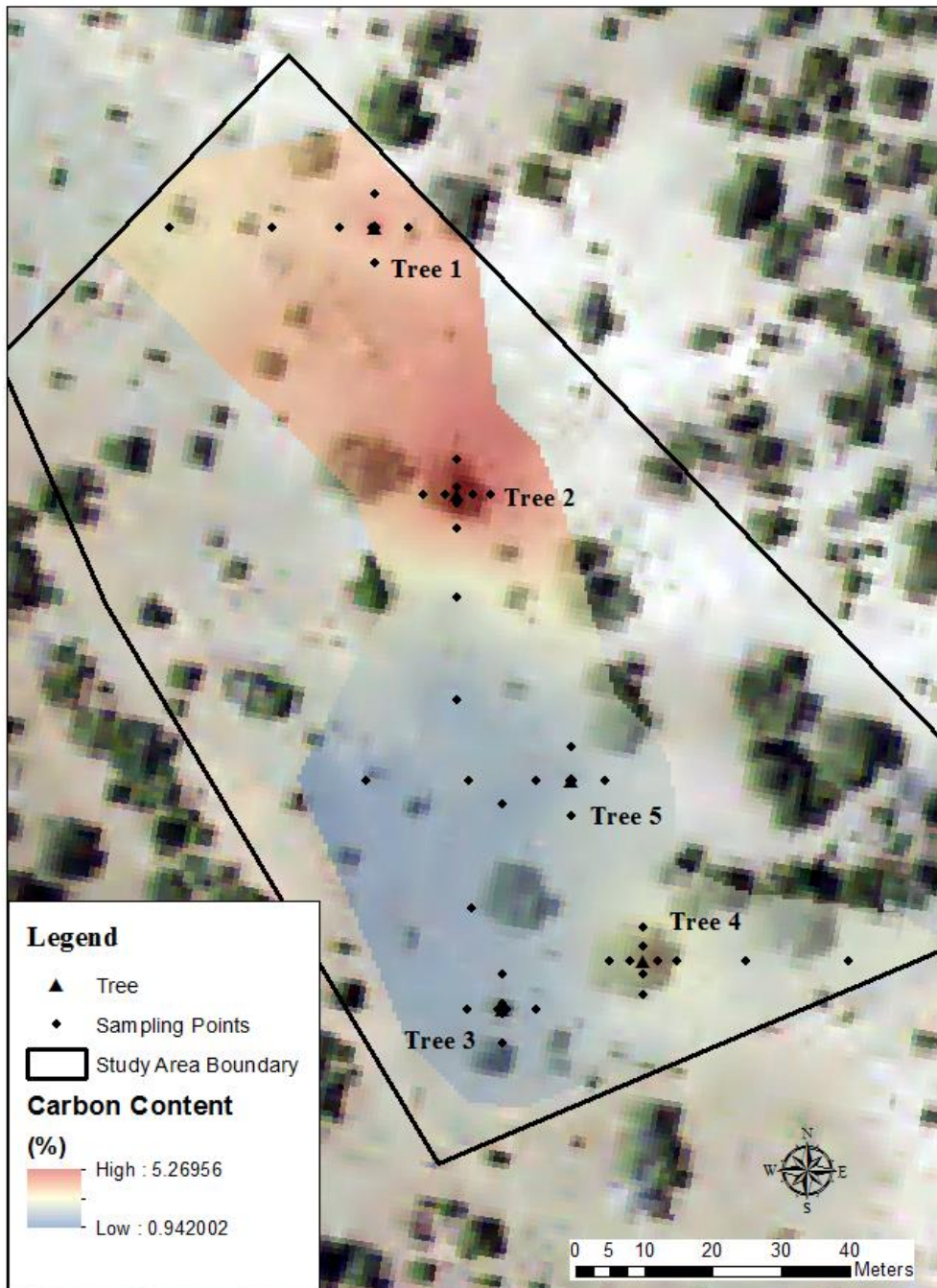


Figure 37: Subsurface soil carbon map

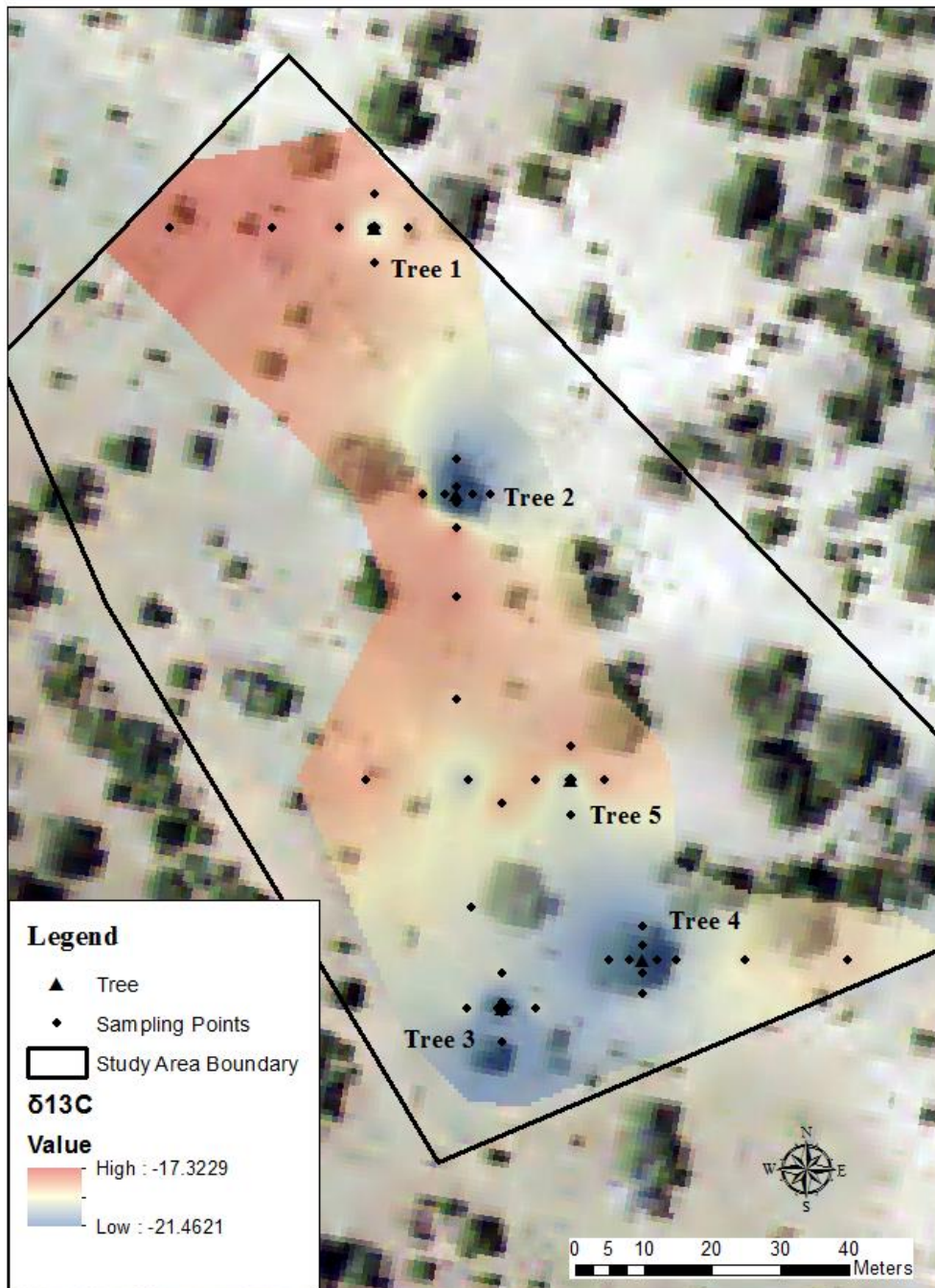


Figure 38: Surface soil  $\delta^{13}\text{C}$  map

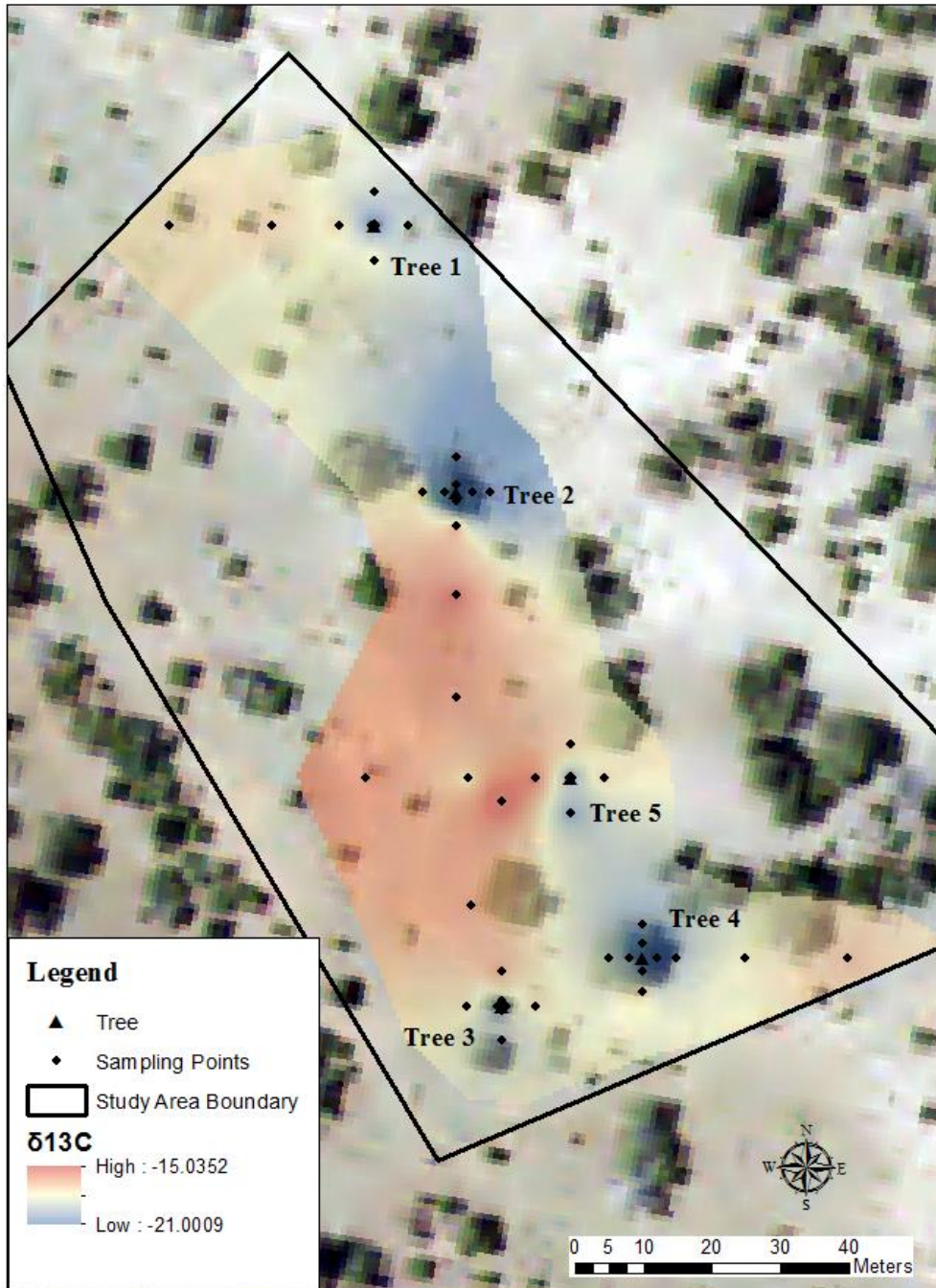


Figure 39: Subsurface soil  $\delta^{13}\text{C}$  map

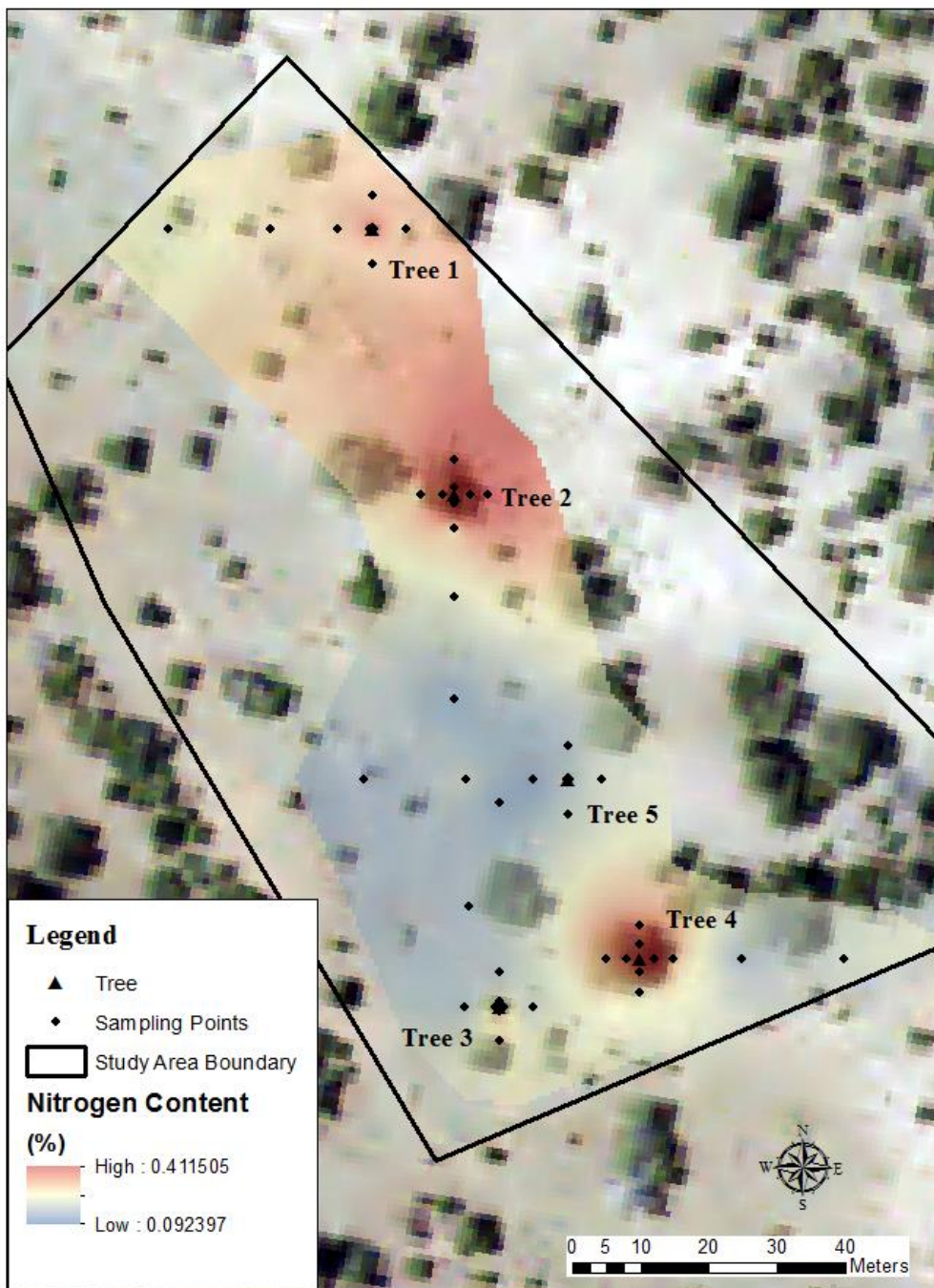


Figure 40: Surface soil nitrogen map

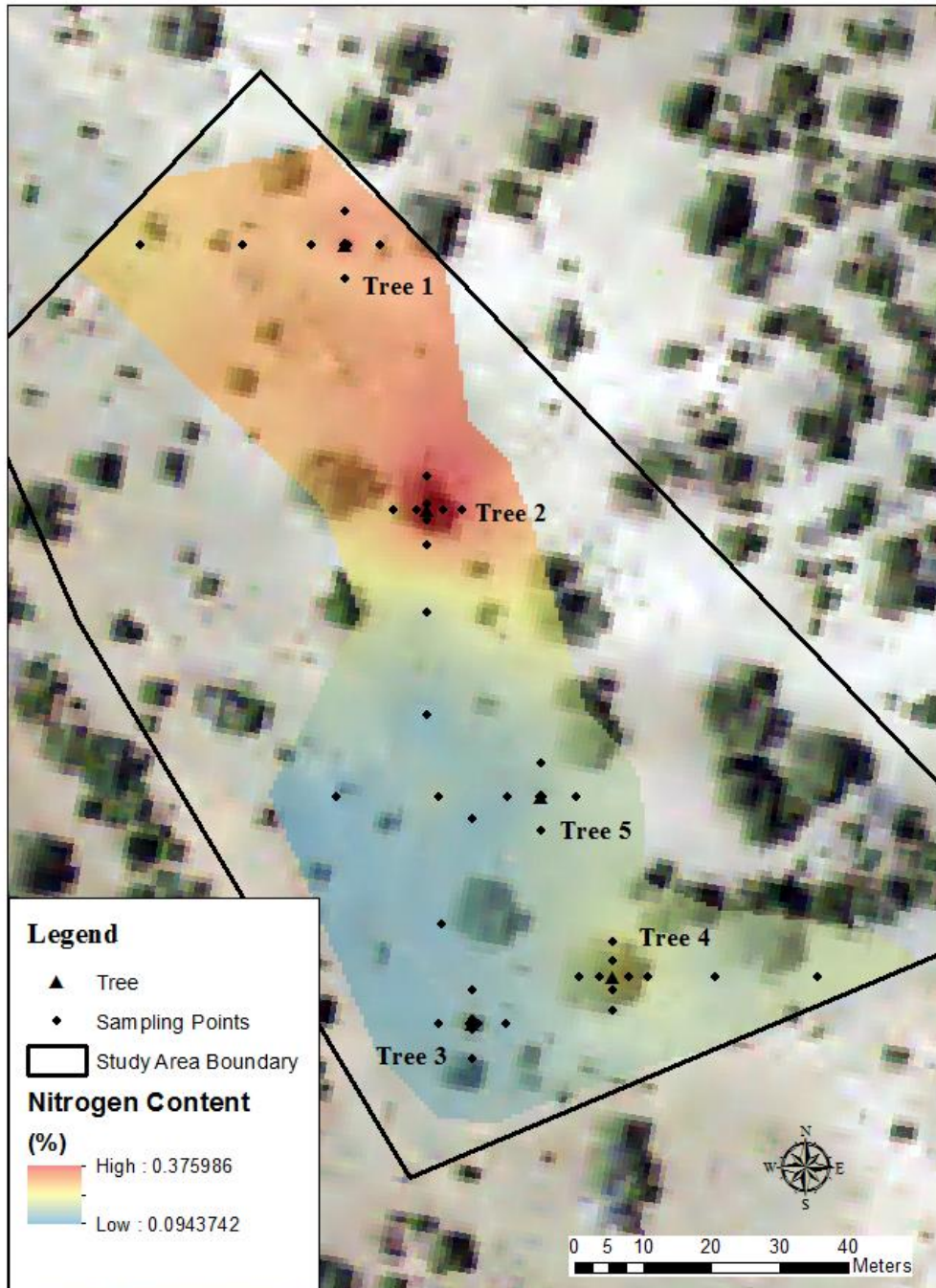


Figure 41: Subsurface soil nitrogen map

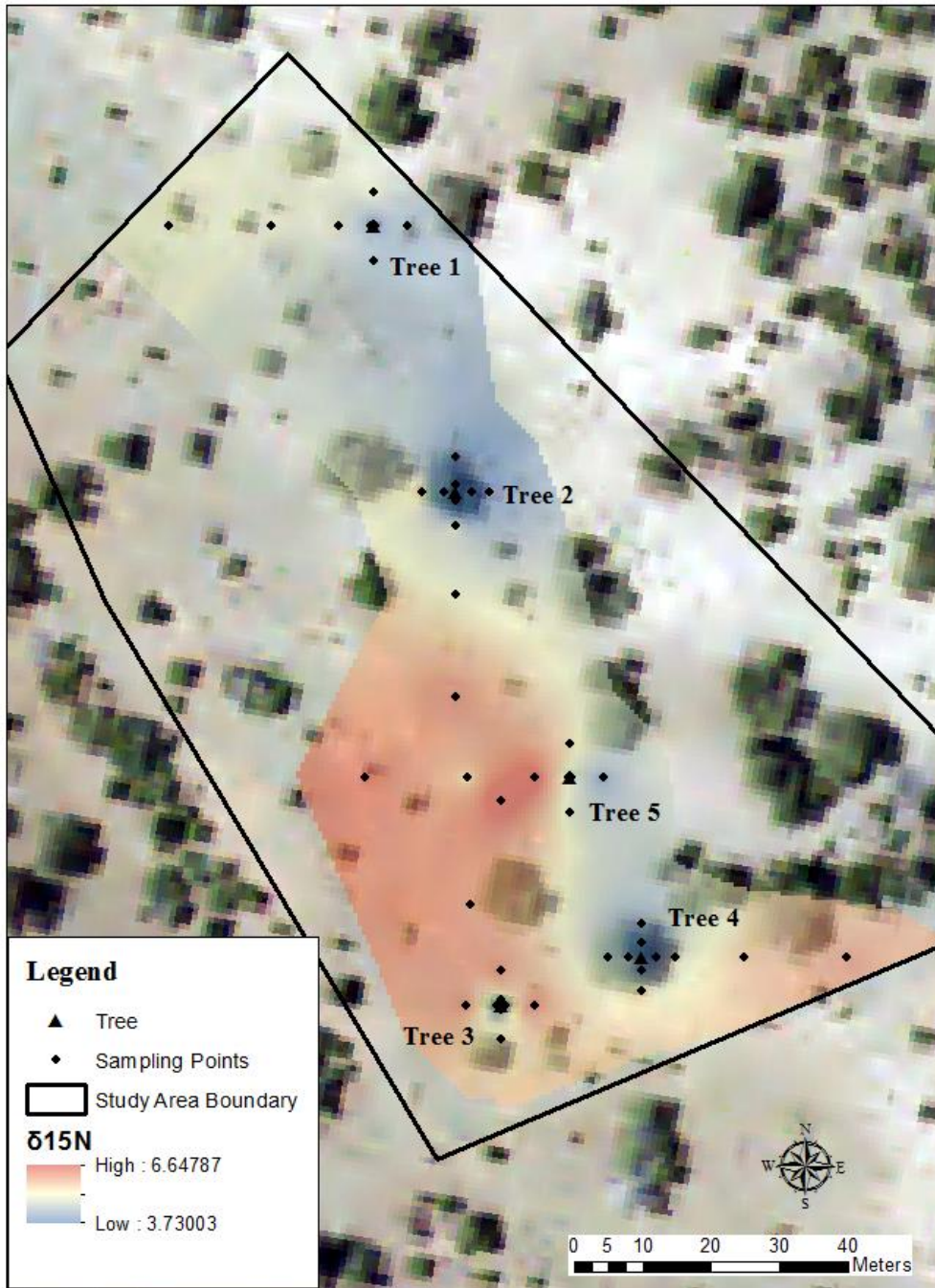


Figure 42: Surface soil  $\delta^{15}\text{N}$  map

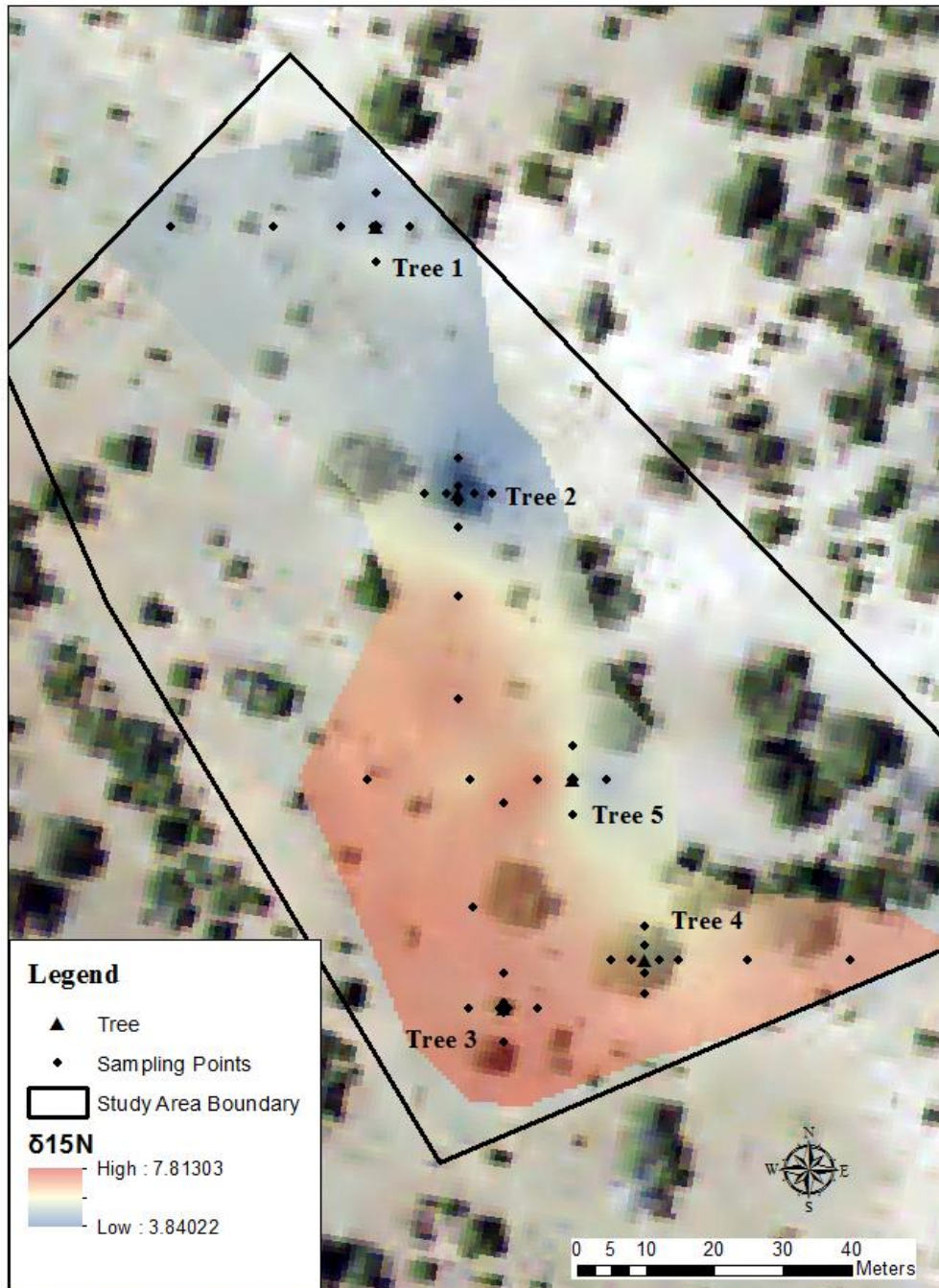


Figure 43: Subsurface soil  $\delta^{15}\text{N}$  map

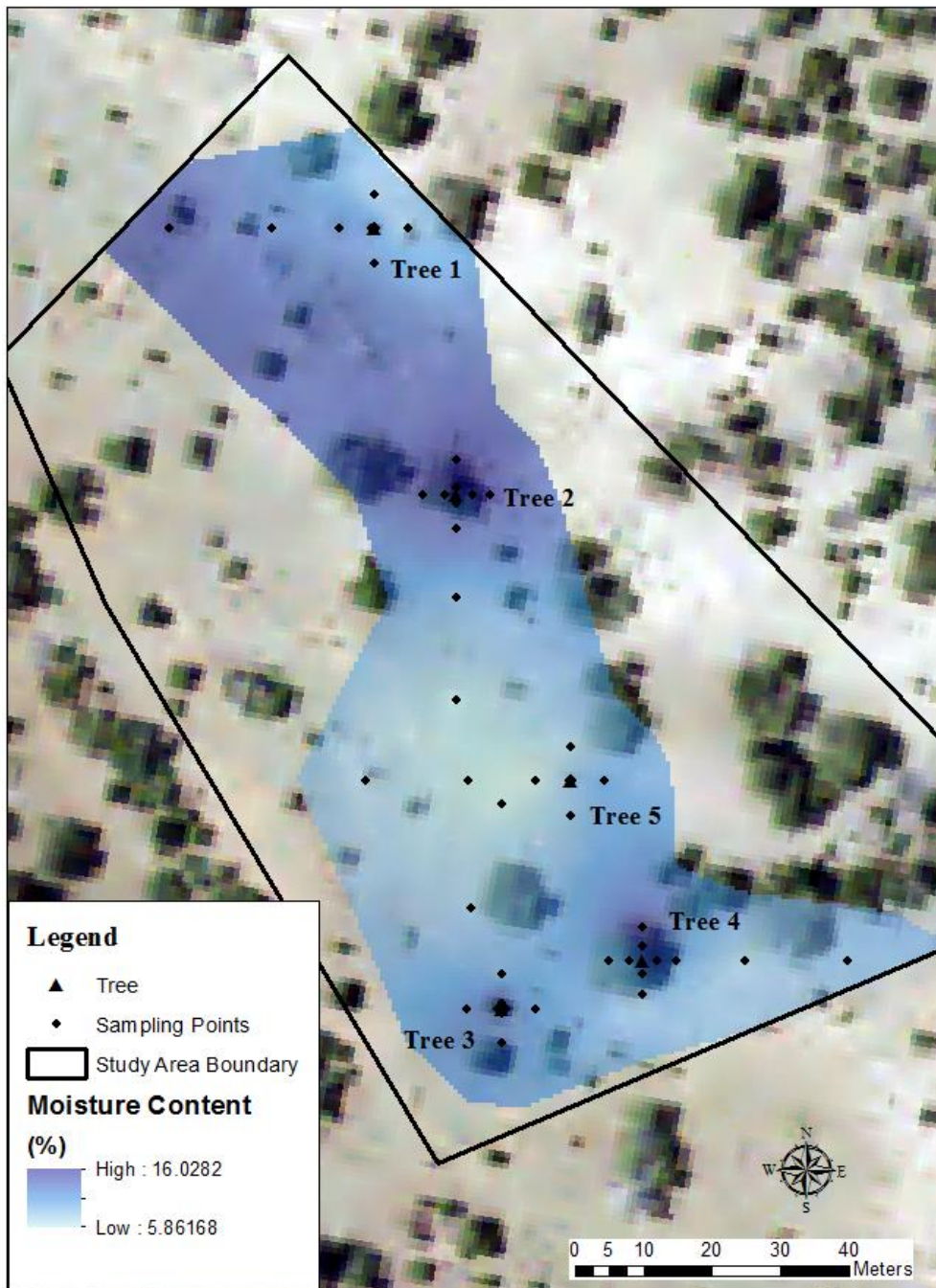


Figure 44: Surface soil moisture map

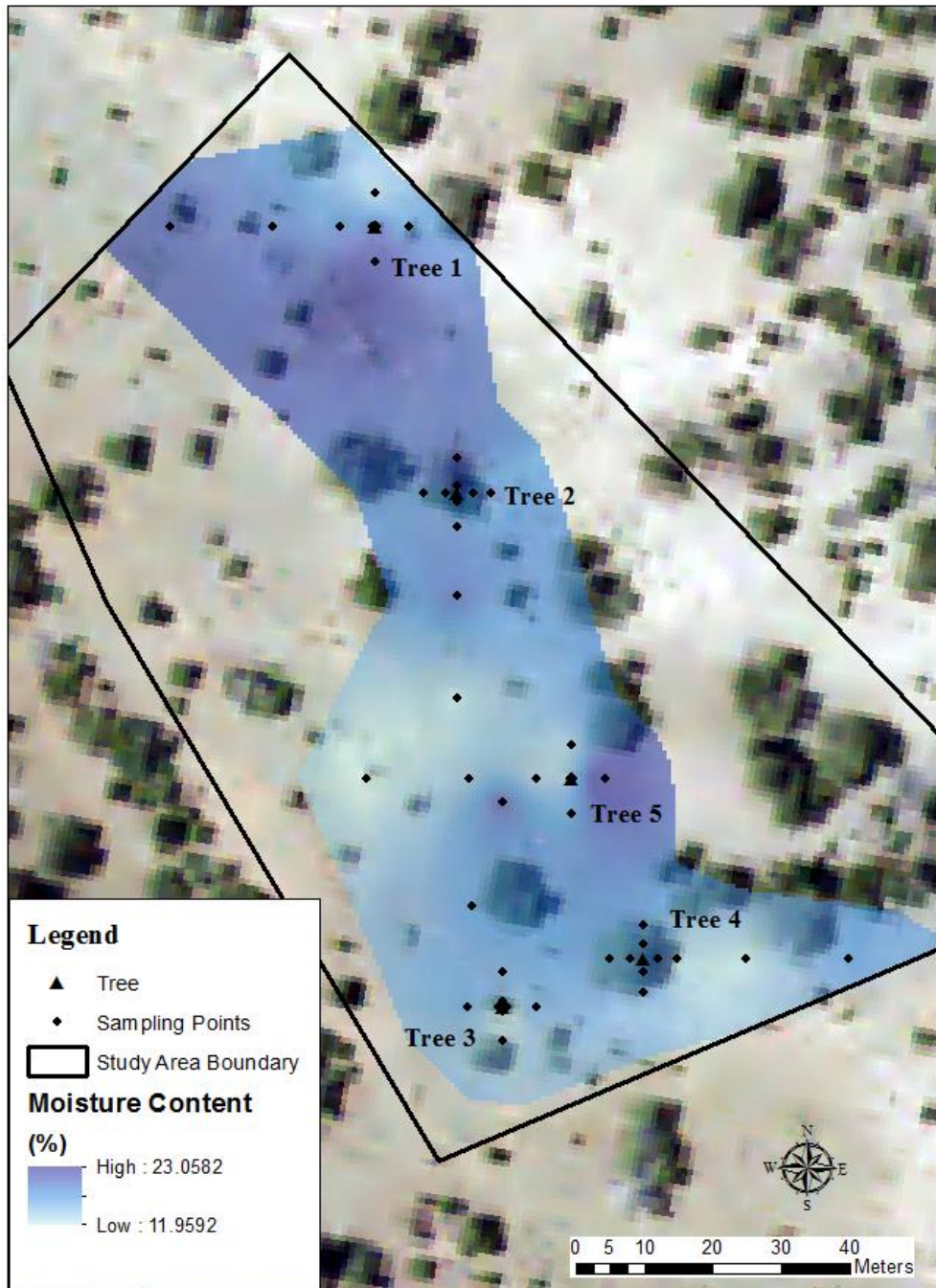


Figure 45: Subsurface soil moisture map

According to the results of the first multivariate linear regression analysis (Model A), distance from juniper trees, canopy diameter, direction from juniper tree, depth, and the interaction between distance and depth all shape soil organic matter content in the study area

(Table 7). Each of these components showed a significant relationship with soil organic matter content. As **distance** from juniper tree increases and depth decreases, organic matter content declines. This decline with distance is more pronounced in surface samples compared to subsurface samples. A broadening of tree canopies is matched by rising organic matter concentrations in the soil. Organic matter accumulates more on north-facing sides of juniper trees compared to south-facing sides. Model A proved to be fairly strong in translating spatial information into soil organic matter content values (Table 8).

*Table 7: Summary of Model A results*

Coefficients	Estimate	Standard Error	p-value
Intercept	1.719984	0.041287	<0.001
Log-transformed distance	-0.038163	0.015073	<0.05
Depth	0.083437	0.042009	<0.05
Canopy diameter	0.037312	0.006653	<0.001
Sin direction	0.056566	0.030411	<0.1
Log-transformed distance : depth	-0.056778	0.021315	<0.01

*Table 8: Accuracy assessment of Model A*

Accuracy measure	Result
Residual standard error	0.2098 on 94 degrees of freedom
Adjusted R-squared	0.4361
F-statistic	16.32 on 5 and 94 DF
AIC	-20.6898

In Model B, distance and canopy area were found to be related to soil organic matter content with high significance (Table 9). As found in Model A, distance from juniper tree and organic matter content are negatively correlated, while canopy area and organic matter content are positively correlated. Surprisingly, these two variables alone generated a model with reasonably high predictive capacity (Table 10). This model is not as powerful as Model A,

however this model does employ variables that can be measured directly from aerial imagery.

*Table 9: Summary of Model B results*

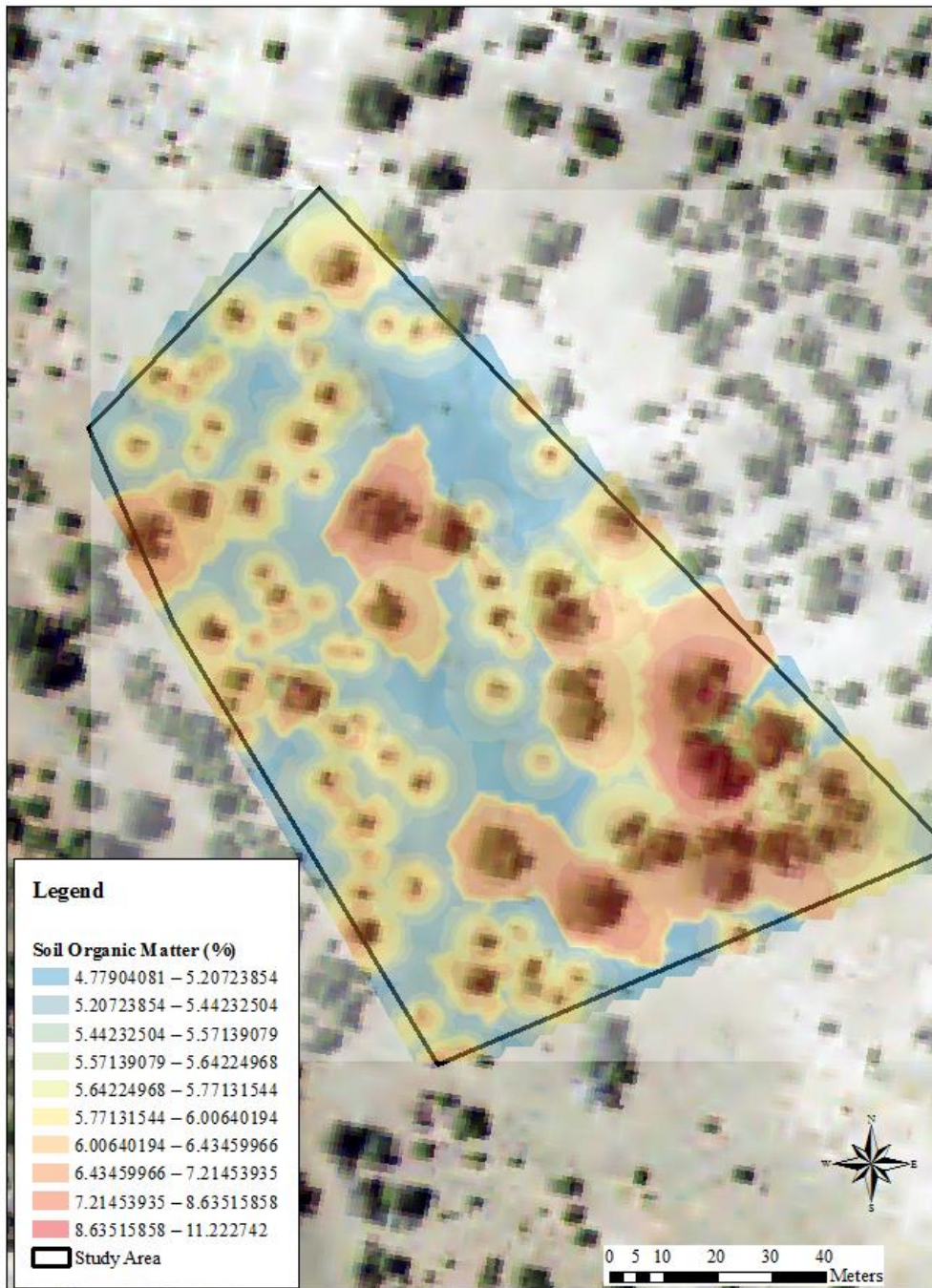
Coefficients	Estimate	Standard Error	p-value
Intercept	1.8360767	0.0449717	<0.001
Log-transformed distance	-0.094804	0.0165542	<0.001
Canopy area	0.0028278	0.0006831	<0.001

*Table 10: Accuracy assessment of Model B*

Accuracy measure	Result
Residual standard error	0.2304 on 47 degrees of freedom
Adjusted R-squared	0.4909
F-statistic	24.63 on 2 and 47 DF
AIC	0.02589901

Combined multivariate linear regression and **interpolation** crafted a map of soil organic matter content that takes **into account the influence of all trees** within the study area (Figure 48). Soil organic matter is highest below juniper trees and lowest under grassy vegetation. Organic matter is most highly concentrated below older, larger trees. The area of influence of juniper trees expands as juniper size increases, as evidenced by the circles of high organic matter content extending farther past the canopies of larger juniper trees compared to that of smaller juniper trees. However, this model only utilized the distances to and canopy areas of the closest tree and does not take into account the combined influence of all neighboring trees.

## Model-Based Soil Organic Matter Predictions



Aerial imagery available from the U.S. Geological Survey.

Figure 46: Map of predicted soil organic matter content using multivariate linear regression and Empirical Bayesian Kriging

## Chapter Five: Discussion

Spatial and temporal patterns in soil properties captured in this study are the manifestation of the linkages between vegetation change and the physical, biological, and chemical characteristics of the world within the soil. The presence of juniper trees in this study site has engendered variations in soil properties across spatial and temporal scales. The spatial patterns of soil properties, namely organic matter content, carbon content,  $\delta^{13}\text{C}$ ,  $\delta^{15}\text{N}$ , nitrogen content, and soil C:N ratios, shaped by the habitation of physical space by juniper trees illustrate that juniper encroachment has modified the accumulation and flow of matter within the site, specifically soil organic carbon stocks, rates of soil organic carbon turnover, and the strength of the soil organic carbon sink. Soil properties under juniper canopies, particularly organic matter content, carbon content, nitrogen content, and soil C:N vary with juniper age. The intensity and breadth of spatial patterns of carbon fluxes are transmuted through time, which means soil carbon responses to juniper encroachment change are not static and are altered in the time dimension.

The high  $\delta^{13}\text{C}$ , high percent carbon, and high C:N of the litter of the two oldest trees relative to the younger trees indicate that litter from younger trees is higher in quality and more readily decomposed (Stockmann et.al., 2013; Yonekura et.al., 2012). The increase in litter C:N with tree age is evidence that the litter of older juniper trees is more recalcitrant than the litter of young juniper trees (Garten and Cooper, 2000; Stockmann et.al., 2013). Considering the high concentration of soil organic matter below juniper canopies and the decline in the soil organic matter content with increasing distance from juniper trees, juniper trees likely provide larger inputs of organic matter than grasses through fallen leaves and root detritus (Fang et al., 2015; McCulley et al., 2004; Throop et al., 2013). Also, in the study site, leafy undergrowth could

often be found clustered below juniper canopies, possibly because the juniper trees provided a microclimate conducive for growth (Koepke et al., 2010; Norton et al., 2012) and/or because of the higher organic matter and nitrogen content of soil adjacent to juniper trees, which reflects the influence of woody encroachment on ecosystem function (Craine et.al., 2015) and nutrient cycling (Bekele and Hudnall, 2005). A portion of the high organic matter content detected below juniper trees could be originating from this vegetation as well. Fallen leaves that are subsequently incorporated into the soil profile are probably a significant contributor to the organic matter pools under juniper trees because under juniper canopies, the surface soil exhibited a higher accumulation of organic matter than the subsurface soil. Conversely, grass roots may contribute more than blades of grass to organic matter pools in soil, given the decrease in organic matter content with depth under grasses. Dead blades of grass may be quickly transported by wind elsewhere without the shelter of juniper trees, or perhaps the decomposition rate of grass is higher at the surface due to increased microbial activity at shallow depth (Fontaine et.al., 2007) or due to the higher decomposability of grass blades relative to their roots. The level of stratification of  $\delta^{13}\text{C}$  with depth is a function of the variability of decomposition rates and organic matter inputs with depth (Garten, 2006). High rates of organic matter inputs from roots can reduce vertical variation in  $\delta^{13}\text{C}$  through the soil profile, thereby obscuring vertical differentiation induced by varying decomposition rates with depth (Garten, 2006). Considering this in light of the patterns of organic matter with depth across the field site, the similarity in stratification ratios of  $\delta^{13}\text{C}$  between soil under juniper trees and soil under grassy areas suggest that differing routes in organic matter input may be driving vertical patterns of organic matter, rather than differences in decomposition rates. Alternatively, increased stability of organic matter with depth (Accoe et.al., 2002; Fontaine et.al., 2007) could explain the

observed pattern in organic matter with depth beyond the juniper canopies.

The organic matter pool measured between the dripline and five-meters from juniper trees likely consists of organic material born from juniper trees as well as grasses, considering the influence of juniper trees extends past the canopy (Figure 48). The lowest organic matter contents were found over five meters from juniper trees, indicating that grasses provide lower inputs of organic matter into soil than juniper trees. The magnification of soil organic matter with increasing tree age suggests that the disparity between soil organic matter below juniper trees and soil organic matter below grasses may be accentuated as time since encroachment increases. The lack of new carbon substrates below the surface soil which stimulate microbial activity can lower carbon mineralization rates and lower decomposition rates at depth (Accoe et.al., 2002), causing an accumulation of carbon. However, high litter inputs at the surface can cause a decline in carbon content with depth (Accoe et.al., 2002; Garten, 2006; Garten and Cooper, 2000). The elevated carbon content in surface soil across the field site likely results from the delivery of leaf litter into the soil profile (Garten and Cooper, 2000).

Considering the reduction in soil carbon content with increasing distance from juniper trees, juniper trees likely generate more litter or lower quality litter than grasses (Stockmann et al., 2013), or create a microclimate unfavorable for microbial activity (Erhagen et al., 2013; Hess and Austin, 2014; Nie et al., 2013; Norton et al., 2012). If juniper trees do indeed generate a higher mass of litter, the soil organic matter content and carbon content of this study area is a function of the rate of input of litter and residues. This is a strong possibility given juniper canopy radius and the organic matter content of surface soil are positively and significantly correlated ( $r= 0.65, p=0.015$ ) and given soil carbon increases with increasing juniper trunk diameter (see Figure 21). This suggests that an increase in aboveground biomass generates a

synonymous increase in litter inputs and a higher flow of organic material from vegetation and into the soil organic matter pool. If juniper trees produce lower quality litter relative to grasses, the soil organic matter content and carbon content of this study area is a function of the differing chemical components and structure of litter originating from the vegetation (Tiwari and Iqbal, 2015). Lower quality litter with higher C:N is more difficult for microbes to decompose and will remain in the soil for a longer period of time compared to higher quality of litter that is readily decomposed by microbes (Stockmann et al., 2013).

Soil  $^{13}\text{C}$  captures the rate of organic carbon turnover in soil, with higher  $\delta^{13}\text{C}$  values stipulating more advanced decomposition as more  $^{13}\text{C}$  is left behind as microbes preferentially use  $^{12}\text{C}$  in respiration (Busari et al., 2016; Garten, 2006; Accoe et.al., 2002). Although the lower  $\delta^{13}\text{C}$  values of soil under juniper canopies could indicate slower turnover rates of soil organic carbon, these low values could also suggest a difference in the  $\delta^{13}\text{C}$  of the plant litter inputs (Accoe et.al., 2002). Grass litter and roots may have inherently higher  $\delta^{13}\text{C}$  values than juniper litter and roots, however grass litter from this field site would need to be isotopically analyzed before this could be concluded with certainty. Such soil  $\delta^{13}\text{C}$  disparities are pronounced in cases of woody encroachment involving the movement of  $\text{C}_3$  woody vegetation onto  $\text{C}_4$  grasslands, as  $\text{C}_3$  vegetation discriminates against  $^{13}\text{CO}_2$  to a greater extent than  $\text{C}_4$  vegetation does (Accoe et.al., 2002).  $\text{C}_3$  vegetation typically has a  $^{13}\text{C}$  signature ranging from -32 to -22, while  $\text{C}_4$  vegetation typically has a  $^{13}\text{C}$  signature ranging from -17 to -9 (Accoe et.al., 2002). *Juniperus monosperma* is  $\text{C}_3$  vegetation and *Bouteloua*, one of the grasses within the site, is  $\text{C}_4$  vegetation (Puttock et.al., 2012). With this in mind, this data likely uncovered the presence of vegetation with different photosynthetic pathways and the strong role vegetation plays in shaping soil chemistry, in addition to vegetation-driven alteration in soil organic carbon turnover.

This pattern in  $\delta^{13}\text{C}$  with distance from juniper trees could also be a result of the rate at which plant organic matter enters the soil organic matter pool, the quality of the litter, or the age of the litter (Accoe et al., 2002; Busari et al., 2016; Garten, 2006). Fresh, labile litter can be identified through the detection of more negative  $\delta^{13}\text{C}$  values (Accoe et.al., 2002). The detection of the most negative  $\delta^{13}\text{C}$  values below juniper trees could be an indication that fresh juniper litter is being amended into the soil at a constant rate or that juniper litter is more labile than grass litter (Busari et al., 2016; Garten, 2006). The former may not be as likely given the similarity in  $\delta^{13}\text{C}$  stratification ratios between soil under grasses and soil under junipers discussed previously. In addition, tree age and soil  $\delta^{13}\text{C}$  are weakly related, therefore soil  $\delta^{13}\text{C}$  is probably not an accurate proxy for litter age. Given the difference in the C:N values of leaf litter and the C:N values of soil, a constant supply of fresh juniper litter is a less likely hypothesis for the observed  $^{13}\text{C}$  patterns, since C:N values of organic matter rise with decomposition (Bekele and Hudnall, 2005). Alternatively, this enrichment in soil  $\delta^{13}\text{C}$  close to juniper trees could simply be reflective of the younger age of juniper trees relative to grasses (Garten, 2006). If soil  $\delta^{13}\text{C}$  is higher than the  $\delta^{13}\text{C}$  of litter inputs, then litter inputs can drive lower soil  $^{13}\text{C}$  values (Accoe et.al., 2002). The higher enrichment in  $\delta^{13}\text{C}$  of the surface soil compared to the subsurface soil indicates more progressed decomposition of organic matter with increasing depth through the discrimination of fungi and other microbes against  $^{13}\text{C}$  (Garten, 2006; Accoe et.al., 2002; Garten and Cooper, 2000).

As soil organic matter residence time increases and decomposition progresses, soil C:N exhibits a decrease (Craine et.al., 2015; Bekele and Hudnall, 2005). However, soil C:N under juniper canopies increases with increasing tree age, which challenges the proposition that decreasing soil C:N over distance from juniper trees is a function of litter age. If litter age is the

main controlling factor for observed C:N patterns, then soil C:N should decrease with increasing tree age. In this case, reduced litter quality and slower decomposition of organic matter may coincide with increasing tree age (Stockmann et.al., 2013). As trunk diameter, thus tree age, increases, litter C:N increases and litter quality declines in this study site. Therefore, juniper encroachment may decelerate soil organic carbon turnover and lengthen soil organic carbon residence times after juniper trees have taken root for a long period of time.

The soil nitrogen is accumulated below juniper canopies and declines with increasing distance from juniper trees. This pattern resembles the islands of fertility hypothesis, which states that trees, through litterfall, root death, and root exudation, increase nutrient levels and enhance nutrient recycling under their canopies (Fontaine et.al, 2007; McCulley et.al., 2004; Stockmann et.al., 2013; Throop et al., 2013). Increased soil nitrogen can elevate litter turnover rates at first, however over time increased nitrogen can inhibit decomposition (Craine et.al., 2015) through a reduction in soil respiration, the restraint of lignolytic enzymes, and changes to the structure of microbial communities (Garten, 2006). Considering the decline in  $\delta^{15}\text{N}$  and the increase in organic matter and carbon with increasing tree age and with decreasing distances to juniper trees, the magnification of nitrogen with increasing tree age may be serving to further hinder microbial decomposition of soil organic carbon.

Litter  $\delta^{15}\text{N}$  is elevated as decomposition progresses because microbes discriminate against  $^{15}\text{N}$  and preferentially consume  $^{14}\text{N}$  when they consume litter and convert organic nitrogen to inorganic forms (Craine et.al., 2015). Specifically, in alkaline arid soils, ammonia volatilization often generates a magnification of  $\delta^{15}\text{N}$  (Craine et.al., 2015).  $\delta^{15}\text{N}$  may decline with initial decomposition and then rise as the conversion of organic nitrogen to inorganic nitrogen accelerates (Craine et.al., 2015). In addition, as decomposition progresses, a decrease

of soil nitrogen occurs (Craine et.al., 2015).

Soil organic matter age increases with depth, resulting in an enrichment of  $\delta^{15}\text{N}$  because the organic matter has remained in the soil long enough to reach a more advanced stage of decomposition (Craine et.al., 2015). This explains the enrichment in  $\delta^{15}\text{N}$  with increasing depth at all distance increments. The higher stratification of  $\delta^{15}\text{N}$  in soil under juniper trees may indicate a higher loss of nitrogen from the soil system through nitrate leaching and ammonia volatilization (Bekele and Hudnall, 2005), but this increased stratification may also indicate that surface  $\delta^{15}\text{N}$  values are capturing the  $\delta^{15}\text{N}$  of litter and roots entering the soil, while subsurface  $\delta^{15}\text{N}$  values are capturing decomposition processes (Craine et.al., 2015).

Considering the enrichment of  $\delta^{15}\text{N}$  and the reduction of soil nitrogen with increasing distance from juniper trees, organic matter decomposition is likely proceeding at a faster rate in grassy areas compared to soil under juniper trees. However, higher  $\delta^{15}\text{N}$  values accompanied by lower C:N values may indicate that organic matter has remained in soil for longer periods of time, thereby giving microbes a larger window of time in which to decompose organic matter and assimilate it into their biomass (Craine et.al., 2015). Considering soil  $\delta^{15}\text{N}$  and soil C:N show an inverse relationship over distance, the enrichment of  $^{15}\text{N}$  in grassy areas may be reflective of the higher age of the grasses compared to more recently settled junipers. However, the disassociation between juniper age and soil  $\delta^{15}\text{N}$  suggests that vegetation age is not the only factor driving patterns in soil  $\delta^{15}\text{N}$ . Therefore, a decrease in the rate of organic matter turnover under juniper trees is still a potential hypothesis for observed soil  $\delta^{15}\text{N}$  values.

If soil C:N ratios are an accurate proxy of organic matter decomposition, then perhaps juniper trees must be established in soil for longer periods of time before a change in decomposition rates can be realized. A change in  $\delta^{15}\text{N}$  post-encroachment is not instantaneous

and requires time before it manifests into a detectable vegetation-driven pedogenesis (Bekele and Hudnall, 2005). However, if litter residence time is indeed the determinant for  $\delta^{15}\text{N}$  enrichment in soil, then soil under older trees should be more enriched in  $\delta^{15}\text{N}$ . Considering the absence of this trend, differing rates of decomposition between soil under juniper trees and soil under grasses could still be the dominant determinant of soil organic carbon fluxes in the study area. Soil  $\delta^{15}\text{N}$  has significantly diverged from juniper litter  $\delta^{15}\text{N}$  (see Table 2) and soil  $\delta^{15}\text{N}$  can show nitrogen cycling across centuries (Craine et.al., 2015), therefore the soil  $\delta^{15}\text{N}$  data in this study may have captured long-term spatial patterns of organic matter turnover external of organic matter residence times. The long-term view of nitrogen dynamics created through soil  $\delta^{15}\text{N}$  analysis may also explain the lack of correlation between juniper tree age and soil  $\delta^{15}\text{N}$  if the time spans between the establishments of each tree in chronosequence are at a higher resolution than the resolution associated with soil  $\delta^{15}\text{N}$  dynamics. Without an estimate of organic matter residence times, the effect of woody plant encroachment on the rate of organic matter decomposition cannot be determined with complete certainty. However, the spatial heterogeneity in  $\delta^{15}\text{N}$  driven by the vegetation in the study site does show with certainty that woody plant encroachment in this area has shaped nitrogen cycling (Bekele and Hudnall, 2005).

In this study site, percent moisture, percent nitrogen,  $\delta^{13}\text{C}$ ,  $\delta^{15}\text{N}$ , and pH were most highly and significantly correlated with organic matter content. Carbon mineralization is limited by soil moisture (Norton et.al., 2012) and temperature (Gartent and Cooper, 2000). Trees reduce rates of evapotranspiration and produce a cooling effect through their interception of incoming sunlight (Gea-Izquierdo et.al., 2009). In addition, trees decrease the intensity of temperature fluctuations (Gea-Izquierdo et.al., 2009). The temperature and moisture regulation provided by trees may inhibit microbial activity or perhaps create an environment conducive for the growth

of understory vegetation which could provide additional inputs of plant material to the soil organic matter pool. The relationship between organic matter and pH is unexpected considering the accumulation of organic matter typically results in acidification as the organic matter is decomposed (Jobbagy and Jackson, 2003). However, the highest organic matter content and potentially lowest rates of decomposition were found under juniper canopies. This slow decomposition could restrict the release of organic acids and carbonic acids.

The absence of a trend in pH with increasing distance from juniper trees was unexpected. The transition from grassland to forest typically results in acidification of the soil through the generation of carbonic acids from microbial respiration, the release of organic acids from litter and through decomposition, and the removal of exchangeable base cations as the cations are incorporated into biomass, litter, and soil (Jobbagy and Jackson, 2003). Considering vegetation type did not alter pH in this study site, climate and parent material are likely the dominant drivers of pH. In wet and cold environments, pH is lower due to the accrual of organic material which readily decomposes and releases organic acids into the soil (Fabian et.al., 2014). The soil in the study site is underlain by basalt and limestone bedrock (Northern Arizona University, 2014), and carbonate-derived soil is inherently high (basic) in pH (Fabian et.al., 2014).

Variations in soil moisture with compass direction from juniper trees were expected given trees modify rates of evapotranspiration through differential shading related to orientation (Gea-Izquierado et.al., 2009). These variations in soil moisture would have also driven changes in organic matter content, carbon content,  $\delta^{13}\text{C}$ , and  $\delta^{15}\text{N}$  because moisture availability influences carbon turnover (Norton et.al., 2012). Although ANOVA did not detect significant variability in soil moisture generated by compass direction, the lowest soil moisture values were found in the surface soil on the south sides of juniper trees, which coincides with another study

which found that the southwest sides of trees receive the most insolation (Gea-Izquierado et al., 2009).

The soil properties maps produced for this study area substantiate the power of maps in conveying variations in soil properties across space. Juniper encroachment modifies the characteristics of a space, and soil mapping allows for the visualization of how a space is transformed below the surface. Although the graphs produced for this study did reveal a significant change in soil properties between grasslands and juniper woodlands and a decline in the influence of juniper trees on soil properties with greater distance from juniper trees, the maps allow for the investigation of variations in soil properties at spatial scales determined by the viewer, within the bounds of detail established by the resolution of the raster datasets and extent of the study area. In addition, the maps validated the presence of islands of fertility within the study site and illustrated how these islands expand in extent and deepen in richness as tree age increases. The map generated through a combination of multivariate linear regression and geostatistical analysis shows that an understanding how ecosystem processes operate across space allows for the enhanced prediction of soil organic carbon fluxes. Dissassembling the complex, interacting factors that drive soil organic carbon content and simplifying the nature of these relationships into quantitative terms allows for the possibility of discovery beyond the constraints of direct *in situ* and *in vitro* measurements. These maps enable viewers to see what cannot be seen with the naked eye and can only be detected through instrumentation and analysis. The goal of the production of these maps was to capture the spatial variability of soil organic carbon within the study site. These maps not only identified the amplification of soil organic carbon pools under and adjacent to juniper canopies; the soil  $\delta^{15}\text{N}$  map shows the flow of carbon through the microbial community and into the atmosphere.

In this study area, juniper trees magnify soil organic carbon stocks through the accumulation of organic matter, carbon, and nitrogen below their canopies. The enlargement of the soil organic carbon pool with increasing tree age evidenced by the amplification of soil organic matter, carbon, and surface nitrogen and the expansion of islands of fertility captured in the soil maps is a strong indication that as time since encroachment increases and juniper trees mature, soil organic carbon pools expand. In other words, juniper encroachment produces a positive effect on soil organic carbon pool size, and this effect becomes stronger as juniper woodlands become more established on grasslands in this study area.

The increased input of organic carbon delivered into the soil by juniper trees is not matched by an equivalent loss of organic carbon from the soil to the atmosphere. On the contrary, if a difference in decomposition rates between soil under juniper trees and soil under grasses is the dominant mechanism behind observed soil  $\delta^{15}\text{N}$  and C:N values, then juniper trees encourage slower rates of organic carbon turnover compared to grasses. This means that the large flux of carbon from juniper trees to soil is likely greater in magnitude than the flux of carbon from the soil to the atmosphere, therefore juniper trees introduce a net positive change in soil organic carbon storage. Furthermore, the increase in litter C:N and soil C:N under juniper canopies with greater juniper tree maturity suggests that organic carbon turnover rates become progressively slower as tree age increases. Therefore, the net positive balance of soil organic carbon becomes more pronounced as juniper trees become long-term residents of areas previously dominated by grasslands. Given the accumulation of soil organic carbon and the decreased rate of decomposition of organic carbon produced by juniper trees in this study site, juniper encroachment may increase the carbon sink strength of soil in Northern Arizona, thereby mitigating climate change.

## **Chapter Five: Conclusions**

Matter flows differently within and around woody vegetation and grasses (Bekele and Hudnall, 2005). Woody plants and grasses capture nutrients differently, have different nutrient requirements, and devote acquired nutrients to different parts of their biomasses (Bekele and Hudnall, 2005). In addition, their litter and roots are cycled back into the soil at different rates (Bekele and Hudnall, 2005). The movement of woody plants into grasslands alters landscapes and soil in terms of the spatial patterns of matter and energy (Jobbagy and Jackson, 2003; Bekele and Hudnall, 2006). Juniper trees introduced new spatial patterns of soil organic matter, carbon,

and nitrogen in this study site through the creation of islands of fertility. Distance and juniper age cause significant variability in multiple soil properties, including carbon, nitrogen, organic matter, and  $\delta^{15}\text{N}$ . Direction from juniper trees did not create significant variability in soil properties; the effect of direction on soil properties varied between juniper trees. Under juniper canopies, soil organic matter, carbon, and nitrogen content were heightened, reflecting increased litter and root inputs to the soil. Soil organic carbon pools and nitrogen pools are enlarged under juniper canopies. This increase in pool size can induce positive impacts on ecosystem function through the increased availability of the building blocks of life. Future studies should endeavor to sample deeper into the soil profile to fully capture the range of microbial activity acting at various depths and to ensure that the majority of the soil carbon pool in the top meter of soil is represented.

As the influence of juniper trees on soil properties weakened with increased distance from juniper canopies, increasing enrichment of  $\delta^{15}\text{N}$  occurred. Although this enrichment could point to longer residence times of grass-derived organic matter due to the earlier establishment of grasses relative to juniper trees, the absence of an enrichment of  $\delta^{15}\text{N}$  with increasing juniper age suggests that  $\delta^{15}\text{N}$  values may indicate rates of organic matter decomposition more than vegetation age. In addition, litter C:N and soil C:N rose with increasing tree age, which shows that the organic matter becomes more recalcitrant, therefore more stable, with increasing tree age. Soil under grasses was more enriched in  $\delta^{13}\text{C}$  compared to soil under juniper canopies. This site contained a mix of *Juniperus monosperma*, a C<sub>3</sub> vegetation type, and grasses belonging to the genus *Bouteloua*, a C<sub>4</sub> vegetation type, therefore soil  $\delta^{13}\text{C}$  values reflected differences in the  $\delta^{13}\text{C}$  litter resulting from the utilization of different photosynthetic pathways between these two vegetation types, in addition to diminished rates of organic carbon turnover under juniper trees.

This divergence in  $\delta^{13}\text{C}$  between soil under juniper trees and soil under grasses suggests that the sampling design did successfully capture soil properties within two vegetation types, thereby supporting the efficacy of the sampling design. However, in future work, soil samples should be taken at farther distances from juniper trees than allowed within this site to ensure that zones completely independent from juniper influence are also studied. Future studies should also analyze  $\delta^{13}\text{C}$  of grasses to trace  $\delta^{13}\text{C}$  changes in the transition of organic matter from vegetation to soil organic matter pools. Soil  $\delta^{15}\text{N}$ , soil C:N and litter C:N patterns suggest that rates organic carbon turnover are lower under juniper trees. Considering the accumulation of organic material and the slower rates of carbon turnover under juniper canopies, juniper trees likely increase the carbon sink strength of soil in Northern Arizona.

Mapping of soil properties is a powerful tool to capture ecosystem processes occurring at multiple spatial scales within a study site. The maps produced in this study elucidated the creation of islands of fertility under juniper canopies. Furthermore, the maps illustrated the profound level of variability in soil properties on very small spatial scales and allowed comparisons between soil properties and distance and directions from juniper trees to be revealed simultaneously. Future studies should aim to obtain a higher density of sampling points within grassy areas in order to study variability in soil properties within grasslands and to improve the accuracy of soil organic carbon stock across entire field sites.

Juniper encroachment is driven by human interference into the natural world. Human beings have a powerful influence on the course of nature and strongly shape the landscapes they inhabit. This study has shown that anthropogenically-driven vegetation change in Northern Arizona has resounded in the world below the surface of those landscapes, altering the chemical, physical, and biological structures of that universe. If juniper encroachment has indeed

magnified soil organic carbon stocks, slowed the delivery of CO<sub>2</sub> from the soil to the atmosphere, and strengthened the carbon sink strength of the soil in Northern Arizona, then juniper encroachment has produced a negative feedback to climate change. If this theory holds true, the rise in atmospheric carbon dioxide concentrations precipitated by human activity may be partially diminished by vegetation change instigated by the resulting climate change. This would posit nature as a guardian of human life, serving to lessen the consequences of our decisions even as it itself is irreversibly shaped by our choices.

However, the scope of this study is spatially small, both in the distance encompassed and depth reached into the earth, and temporally limited, as space and juniper tree age were the only proxies for time. Widening the scope of this study spatially and temporally may reveal soil organic carbon pool responses that disprove this theory. Although this study has elucidated soil responses to juniper encroachment on the landscape-scale in Northern Arizona, the findings of this study are only small drops in the ocean of literature on this topic that is slowly forming as we uncover the linkages between plants, soil, and human life, and should be considered as such in any land-use management decisions.

## References

- Accoe, F., Boeckx, P., Cleemput, O. V., Hofman, G., Zhang, Y., & Guanxiong, C. (2002). Evolution of the  $\delta^{13}\text{C}$  signature related to total carbon contents and carbon decomposition rate constants in a soil profile under grassland. *Rapid Communications in Mass Spectrometry*, 16(23), 2184-2189.

- Bekele, A., & Hudnall, W. H. (2005). Response of soil d15N and nutrients to eastern red cedar (*juniperus virginiana*) encroachment into a relict calcareous prairie. *Plant & Soil*, 271(1/2), 143-155.
- Bekele, A., & Hudnall, W. H. (2006). spatial variability of soil chemical properties of a prairie–forest transition in louisiana. *Plant & Soil*, 280(1/2), 7-21.
- Bragazza, L., Bardgett, R. D., Mitchell, E. A. D., & Buttler, A. (2015). Linking soil microbial communities to vascular plant abundance along a climate gradient. *New Phytologist*, 205(3), 1175-1176-1182.
- Brockway, D. G., Gatewood, R. G., & Paris, R. B. (2002). Restoring grassland savannas from degraded pinyon-juniperwoodlands: Effects of mechanical overstory reduction and slash treatment alternatives. *Journal of Environmental Management*, 64(2), 179-180-197.
- Busari, M. A., Salako, F. K., & Tuniz, C. (2016). Stable isotope technique in the evaluation of tillage and fertilizer effects on soil carbon and nitrogen sequestration and water use efficiency. *European Journal of Agronomy*, 73, 98-99-106.
- Chatterjee, A., Lal, R., Wielopolski, L., Martin, M. Z., & Ebinger, M. H. (2009). Evaluation of different soil carbon determination methods. *Critical Reviews in Plant Sciences*, 28(3), 164-165-178.
- Chen, C., Hu, K., Li, H., Yun, A., & Li, B. (2015). Three-dimensional mapping of soil organic carbon by combining kriging method with profile depth function. *Plos One*, 10(6), 1-2-15.

Chen, F. (2015). The diversity changes of soil microbial communities stimulated by climate, soil type and vegetation type analyzed via a functional gene array. *World Journal of Microbiology & Biotechnology*, 31(11), 1755-1756-1763.

Chen, Z., Yu, G., Ge, J., Wang, Q., Zhu, X., & Xu, Z. (2015). Roles of climate, vegetation and soil in regulating the spatial variations in ecosystem carbon dioxide fluxes in the northern hemisphere. *Plos One*, 10(4), 1-2-14.

Cihacek, L. J., Foss, L. A., & Jacobson, K. A. (2015). Comparison of soil sampling devices for soil bulk density determination for carbon sequestration monitoring. *Communications in Soil Science and Plant Analysis*, 46(2), 180-181-184.

Craine, J., Brookshire, E., Cramer, M., Hasselquist, N., Koba, K., Marin-Spiotta, E., et al. (2015). Ecological interpretations of nitrogen isotope ratios of terrestrial plants and soils. *Plant & Soil*, 396(1/2), 1-26.

Croft, H. (2012). On the use of remote sensing techniques for monitoring spatio-temporal soil organic carbon dynamics in agricultural systems. *Catena (Giessen)*, 94, 64-65-74.

Davidson, E. A., & Janssens, I. A. (2006). Temperature sensitivity of soil carbon decomposition and feedbacks to climate change. *Nature*, 440(7081), 165-166-173.

de Paul Obade, V., & Lal, R. (2013). Assessing land cover and soil quality by remote sensing and geographical information systems (GIS). *Catena*, 104, 77-78-92.

Erhagen, B., Öquist, M., Sparrman, T., Haei, M., Ilstedt, U., Hedenström, M., et al. (2013). Temperature response of litter and soil organic matter decomposition is determined by

chemical composition of organic material. *Global Change Biology*, 19(12), 3858-3859-3871.

Fabian, C., Reimann, C., Fabian, K., Birke, M., Baritz, R., & Haslinger, E. (2014). GEMAS: Spatial distribution of the pH of european agricultural and grazing land soil. *Applied Geochemistry*, 47, 207-216.

Fang, X., Chen, F., Wan, S., Yang, Q., & Shi, J. (2015). Topsoil and deep soil organic carbon concentration and stability vary with aggregate size and vegetation type in subtropical china. *Plos One*, 10(9), 1-2-17.

Fontaine, S., Barot, S., Barré, P., Bdioui, N., Mary, B., & Rumpel, C. (2007). Stability of organic carbon in deep soil layers controlled by fresh carbon supply. *Nature*, 450(7167), 277-278-280.

Garten Jr, C. T. (2006). Relationships among forest soil C isotopic composition, partitioning, and turnover times. *Canadian Journal of Forest Research*, 36(9), 2157-2167.

Garten Jr., C. T., & Cooper, L. W. (2000). Climate controls on forest soil C isotope ratios in the southern Appalachian mountains. *Ecology*, 81(4), 1108-1119.

Gea-Izquierdo, G., Montero, G., & Cañellas, I. (2009). Changes in limiting resources determine spatio-temporal variability in tree–grass interactions. . *Agroforestry Systems*, 76(2), 375-387.

- He, Y., Trumbore, S. E., Torn, M. S., Harden, J. W., Vaughn, L. J. S., Allison, S. D., et al. (2016). Radiocarbon constrains imply reduced carbon intake by soils during the 21st century. *Science*, 353(6306), 1419-1424.
- Hess, L. J. T., & Austin, A. T. (2014). Pinus ponderosa alters nitrogen dynamics and diminishes the climate footprint in natural ecosystems of patagonia. *Journal of Ecology*, 102, 610-611-621.
- Hurteau, M. D., Stoddard, M. T., & Fule, P., Z. (2011). The carbon costs of mitigating high-severity wildfire in southwestern ponderosa pine. *Global Change Biology*, 17, 1516-1517-1521.
- Jackson, R. B., & Caldwell, M. M. (1993). Geostatistical patterns of plant heterogeneity around individual perennial plants. *Journal of Ecology*, 81, 683-684-692.
- Jobbagy, E. G., & Jackson, R. B. (2000). The vertical distribution of soil organic carbon and its relation to climate and vegetation. *Ecological Applications*, 10.2, 423-424-436.
- Jobbágy, E. G., & Jackson, R. B. (2003). patterns and mechanisms of soil acidification in the conversion of grasslands to forests. *Biogeochemistry*, 64(2), 205-229.
- Johnson, D. D., & Miller, R. F. (2006). Structure and development of expanding western juniper woodlands as influenced by two topographic variables. *Forest Ecology and Management*, 229(1), 7-15.
- Johnson, D. W., & Curtis, P. S. (2001). Effects of forest management on soil C and N storage: Meta analysis. *Forest Ecology and Management*, 140(2), 227-238.

- Johnson, N. C., Wilson, G. W. T., Bowker, M. A., Wilson, J. A., & Miller, R. M. (2010). Resource limitation is a driver of local adaptation in mycorrhizal symbioses. *Proceedings of the National Academy of Sciences of the United States of America*, 107(5), 2093-2094-2098.
- Koepke, D. F., Kolb, T. E., & Adams, H. D. (2010). Variation in woody plant mortality and dieback from severe drought among soils, plant groups, and species within a northern arizona ecotone. *Oecologia*, 163(4), 1079-1080-1090.
- Kucuker, M. A., Guney, M., Oral, H. V., Copty, N. K., & Onay, T. T. (2015). Impact of deforestation on soil carbon stock and its spatial distribution in the western black sea regional of turkey. *Journal of Environmental Management*, 147, 227-228-235.
- Kumar, S., Lal, R., & Liu, D. (2012). A geographically weighted regression kriging approach for mapping soil organic carbon stock. *Geoderma*, 189-190, 627-628-634.
- Lal, R. (2004). Soil carbon sequestration impacts on climate change and food security. *Science*, 304(5677), 1623-1624-1627.
- Lal, R. (2004). Soil carbon sequestration to mitigate climate change. *Geoderma*, 123(1/2), 1-2-22.
- Lark, R. M. (2012). Towards soil geostatistics. *Spatial Statistics*, , 92-93-99.
- Malone, B. P., McBratney, A. B., Minasny, B., & Laslett, G. M. (2009). Mapping continuous depth functions of soil carbon storage and available water capacity. *Geoderma*, 154(1/2), 138-139-152.

Manning, P., Vries, F. T., Tallowin, J. R. B., Smith, R., Mortimer, S. R., Pilgrim, E. S., et al. (2015). Simple measures of climate, soil properties and plant traits predict national-scale grassland soil carbon stocks. *Journal of Applied Ecology*, 52(5), 1188-1189-1196.

McCulley, R. L., Archer, S. R., Boutton, T. W., Hons, E. M., & Zuberer, D. A. (2004). Soil respiration and nutrient cycling in wooded communities developing in grassland. *Ecology*, 36(11), 2804-2805-2817.

Miller, B. A., Koszinski, S., Hierold, W., Rogasik, H., Schröder, B., Van Oost, K., et al. (2016). Towards mapping soil carbon landscapes: Issues of sampling scale and transferability. *Soil & Tillage Research*, 156, 194-195-208.

Nie, M., Pendall, E., Bell, C., Gasch, C. K., Raut, S., Tamang, S., et al. (2013). Positive climate feedbacks of soil microbial communities in a semi-arid grassland. *Ecology Letter*, 16(2), 234-235-241.

Northern Arizona University. (2014). *Southwest experimental garden array: Blue chute*. Retrieved February, 2017, from <http://www.sega.nau.edu/gardens/blue-chute>

Norton, U., Saetre, P., Hooker, T. D., & Stark, J. M. (2012). Vegetation and moisture controls on soil carbon mineralization in semiarid environments. *Soil Science Society of America Journal*, 76(3), 1038-1039-1047.

Olson, K. R., & Al-Kaisi, M. M. (2015). The importance of soil sampling depth for accurate account of soil organic carbon sequestration, storage, retention and loss. *Catena*, 125, 33-34-37.

- Overby, S. T., Owen, S. M., Hart, S. C., Neary, D. G., & Johnson, N. C. (2015). Soil microbial community resilience with tree thinning in a 40-year-old experimental ponderosa pine forest. *Applied Soil Ecology*, 93, 1-2-10.
- Parker, C. L. (2009). *Evaluating juniper cover change from 1936-1997 in the wupatki area using repeat aerial Photography*. Unpublished Masters, Northern Arizona University,
- Puttock, A., Dungait, J. A. J., Bol, R., Dixon, E. R., Macleod, C. J. A., & Brazier, R. E. (2012). Stable carbon isotope analysis of fluvial sediment fluxes over two contrasting **C4-C3** semi-arid **vegetation** transitions. *Rapid Communications in Mass Spectrometry*, 26(20), 2386-2392.
- Scott, R. L., Huxman, T. E., Williams, D. G., & Goodrich, D. C. (2006). Ecohydrological impacts of woody-plant encroachment: Seasonal patterns of water and carbon dioxide exchange within a semiarid riparian environment. . *Global Change Biology*, 12(2), 311-324.
- Simón, N., Montes, F., Díaz-Pinés, E., Benavides, R., Roig, S., & Rubio, A. (2013). Spatial distribution of the soil organic carbon pool in a holm oak dehesa in spain. *Plant Soil*, 366(1/2), 537-538-549.
- Stockmann, U., Adams, M. A., Crawford, J. W., Field, D. J., Henakaarchchi, N., Jenkins, M., et al. (2013). The knowns, known unknowns and unknowns of sequestration of soil organic carbon. *Agriculture, Ecosystems, and Envriionment*, 164, 80-81-99.

The Intergovernmental Panel on Climate Change. (2003). *Good practice guidance for land use, land-use change and forestry*. Publishers Institute for Global Environmental Strategies, Japan: Institute of Global Environmental Strategies (IGES) for the IPCC.

Throop, H., Lajtha, K., & Kramer, M. (2013). Density fractionation and  $^{13}\text{C}$  reveal changes in soil carbon following woody encroachment in a desert ecosystem. *Biogeochemistry*, 112(1-3), 409-410-422.

Tiwari, S. C., & Iqbal, S. (2015). Sequestration of soil organic carbon pool under different natural forest vegetation covers in achanakmar, chhattisgarh. *International Journal of Multidisciplinary Approach & Studies*, 2(2), 57-58-62.

United States Department of Agriculture Farm Service Agency. *National agriculture imagery program*. Retrieved September, 2016, from <https://earthexplorer.usgs.gov/>

Wagle, P., Xiao, X., Scott, R. L., Kolb, T. E., Cook, D. R., Brunsell, N., et al. (2015). Biophysical controls on carbon and water vapor fluxes across a grassland climatic gradient in the united states. *Agricultural and Forest Meteorology*, 214, 293-294-305.

Wang, J., Yang, R., & Bai, Z. (2015). Spatial variability and sampling optimization of soil organic carbon and total nitrogen for minesoils of the loess plateau using geostatistics. *Ecological Engineering*, 82, 159-160-164.

Winowiecki, L. (2016). Effects of land cover on ecosystem services in tanzania: A spatial assessment of soil organic carbon. *Geoderma*, 263, 274-275-283.

Xiang, H., Zhang, J., & Zhu, Q. (2015). A scientometric analysis of worldwide soil carbon stocks research from 2000 to 2014. *Current Science*, 109(3), 513-514-519.

Yonekura, Y., Ohta, S., Kiyono, Y., Aksa, D., Morisada, K., Tanaka, N., et al. (2012). Dynamics of soil carbon following destruction of tropical rainforest and the subsequent establishment of imperata grassland in indonesian borneo using stable carbon isotopes. *Global Change Biology*, 18(8), 683-684-699.

Yusuf, H. M., Treydte, A. C., & Sauerborn, J. (2015). Managing semi-arid rangelands for carbon storage: Grazing and woody encroachment effects on soil carbon and nitrogen. *Plos One*, 10(10), 1-2-18.

Zelikova, T. J., Housman, D. C., Grote, E. E., Neher, D. A., & Belnap, J. (2012). Warming and increased precipitation frequency on the colorado plateau: Implications for biological soil crusts and soil processes. *Plant Soil*, 355(1/2), 265-266-282.

Zhang, K., Dang, H., Zhang, Q., & Cheng, X. (2015). Soil carbon dynamics following land-use change varied with temperature and precipitation gradients: Evidence from stable isotopes. *Global Change Biology*, 21(7), 2762-2763-2772.

## Appendix A

### **R script for statistical analyses:**

```
#install.packages("readr")
library(readr)

setwd("F:/Thesis")
SoilCarbon = read.csv("F:/SoilDataFinal.csv")
LitterData = read.csv("F:/LitterData.csv")

head(SoilCarbon)
dim(SoilCarbon) #OAR: 100 x 35
class(SoilCarbon) #data.frame

head(LitterData)
dim(LitterData) #OAR: 4 x 7
class(LitterData) #data.frame

#OAR: load the necessary packages
#install.packages("ggplot2")
#install.packages("gridExtra")
library(ggplot2)
library(gridExtra)

#OAR: load the necessary functions
load("correlation.R")
load("pValue.R")
load("averagesStEr.R")
load("avgSE.R")
load("linReg.R")
load("rmse.R")
load("averagesDistBins.R")
load("avgSETenBins.R")
load("diameterGraphs.R")
load("predictedValues.R")

#plot litter CN against tree diameter
litter.CN = ggplot(data=LitterData, aes(x=LitterData$Diameter, y=LitterData$CN)) +
  geom_bar(stat="identity") + labs(x="Trunk Diameter (cm)", y= "Litter C:N") + geom_text(x= 0,
y = 47,label="n=4")
litter.CN

#make data frames for only surface and only bottom
surface.samples.index = which(SoilCarbon$DepthKey == "S")
```

```

bottom.samples.index = which(SoilCarbon$DepthKey == "B")

surface.samples = SoilCarbon[surface.samples.index,]
bottom.samples = SoilCarbon[bottom.samples.index,]

#Create histograms for each variable

percentOMHist = ggplot(data=SoilCarbon, aes(x=SoilCarbon$PercentOM)) +
  geom_histogram(binwidth = 1) + labs(x="Organic Matter (%)",
                                    y="Frequency") + geom_text(x = 16, y = 21, label = "n=100")
percentOMHist

percentMoistureHist = ggplot(data=SoilCarbon,
                               aes(x=SoilCarbon$PercentMoisture)) + geom_histogram(binwidth = 2.5) +
  labs(x= "Soil Moisture (%)", y="Frequency") + geom_text(x = 22, y = 23, label = "n=99")
percentMoistureHist

percentCarbonHist = ggplot(data=SoilCarbon, aes(x=SoilCarbon$PercentC)) +
  geom_histogram(binwidth = 0.5) + labs(x= "Soil Carbon (%)", y="Frequency") + geom_text(x =
6.5, y = 21, label = "n=100")
percentCarbonHist

percentNitrogenHist = ggplot(data=SoilCarbon,
                               aes(x=SoilCarbon$PercentN)) + geom_histogram(binwidth=0.025) +
  labs(x="Soil Nitrogen (%)", y="Frequency") + geom_text(x = 0.43, y = 13.5, label = "n=100")
percentNitrogenHist

pHHist = ggplot(data=SoilCarbon, aes(x=SoilCarbon$pH)) + geom_histogram(binwidth=0.2) +
  labs(x="Soil pH", y="Frequency") + geom_text(x = 6.8, y = 30.5, label = "n=100")
pHHist

clayHist = ggplot(data=SoilCarbon, aes(x=SoilCarbon$Clay)) + geom_histogram(binwidth=1) +
  labs(x="Percent Clay", y="Frequency") + geom_text(x = 28.5, y = 13, label = "n=100")
clayHist

siltHist = ggplot(data=SoilCarbon, aes(x=SoilCarbon$Silt)) + geom_histogram(binwidth=1.5) +
  labs(x="Percent Silt", y="Frequency") + geom_text(x = 72, y = 17, label = "n=100")
siltHist

veryFineSandHist = ggplot(data=SoilCarbon, aes(x=SoilCarbon$VeryFineSand)) +
  geom_histogram(binwidth=1) + labs(x="Percent Very Fine Sand", y="Frequency") +
  geom_text(x = 15, y = 22, label = "n=100")
veryFineSandHist

fineSandHist = ggplot(data=SoilCarbon, aes(x=SoilCarbon$FineSand)) +
  geom_histogram(binwidth=1) + labs(x="Percent Fine Sand", y="Frequency") + geom_text(x =

```

```

7.6, y = 33, label = "n=100")
fineSandHist

mediumSandHist = ggplot(data=SoilCarbon, aes(x=SoilCarbon$MediumSand)) +
  geom_histogram(binwidth=1) + labs(x="Percent Medium Sand", y="Frequency") + geom_text(x =
  5.5, y = 73, label = "n=100")
mediumSandHist

#graph organic matter, carbon and nitrogen under the tree for all directions and depth increments
#surface samples
underTreeNorthSurface = which(SoilCarbon$Distance=="0" &
  SoilCarbon$Direction == "N" & SoilCarbon$DepthKey == "S")
underTreeSouthSurface = which(SoilCarbon$Distance=="0" &
  SoilCarbon$Direction == "S" & SoilCarbon$DepthKey == "S")
underTreeEastSurface = which(SoilCarbon$Distance=="0" &
  SoilCarbon$Direction == "E" & SoilCarbon$DepthKey == "S")
underTreeWestSurface = which(SoilCarbon$Distance=="0" &
  SoilCarbon$Direction == "W" & SoilCarbon$DepthKey == "S")
#subsurface samples
underTreeNorthSub = which(SoilCarbon$Distance=="0" &
  SoilCarbon$Direction == "N" & SoilCarbon$DepthKey == "B")
underTreeSouthSub = which(SoilCarbon$Distance=="0" &
  SoilCarbon$Direction == "S" & SoilCarbon$DepthKey == "B")
underTreeEastSub = which(SoilCarbon$Distance=="0" & SoilCarbon$Direction
  == "E" & SoilCarbon$DepthKey == "B")
underTreeWestSub = which(SoilCarbon$Distance=="0" & SoilCarbon$Direction
  == "W" & SoilCarbon$DepthKey == "B")

#OM by direction under tree (distance = 0)
c.labels = c("North Surface", "North Subsurface", "East Surface", "East Subsurface", "West
Surface",
  "West Subsurface", "South Surface",
  "South Subsurface")
om.direction.graph = avgSE(SoilCarbon$PercentOM, c.labels,
  underTreeNorthSurface, underTreeNorthSub, underTreeEastSurface,
  underTreeEastSub, underTreeWestSurface, underTreeWestSub, underTreeSouthSurface,
  underTreeSouthSub, "Direction and Depth", "Average Organic Matter Content
(%)") + geom_text(x = 7.5, y = 11, label = "n=40")
om.direction.graph

#C by direction under tree (distance = 0)
c.direction.graph = avgSE(SoilCarbon$PercentC, c.labels,
  underTreeNorthSurface, underTreeNorthSub, underTreeEastSurface,
  underTreeEastSub, underTreeWestSurface, underTreeWestSub, underTreeSouthSurface,
  underTreeSouthSub, "Direction and Depth", "Average Carbon Content (%)") +

```

```

geom_text(x = 7.5, y = 4.6, label = "n=40")
c.direction.graph

#N by direction under tree (distance = 0)
n.direction.graph = avgSE(SoilCarbon$PercentN, c.labels,
                           underTreeNorthSurface, underTreeNorthSub, underTreeEastSurface,
                           underTreeEastSub, underTreeWestSurface, underTreeWestSub, underTreeSouthSurface,
                           underTreeSouthSub, "Direction and Depth", "Average Nitrogen Content (%)") +
geom_text(x = 7.5, y = 0.31, label = "n=40")
n.direction.graph

#C isotope abundance by direction under tree (distance = 0)
Ciso.direction.graph = avgSE(SoilCarbon$d13C, c.labels,
                           underTreeNorthSurface, underTreeNorthSub, underTreeEastSurface,
                           underTreeEastSub, underTreeWestSurface, underTreeWestSub, underTreeSouthSurface,
                           underTreeSouthSub, "Direction and Depth", "Average Natural Abundance of
                           13C") + geom_text(x = 7.75, y = -20.5, label = "n=40")
Ciso.direction.graph

#N isotope abundance by direction under tree (distance = 0)

Niso.direction.graph = avgSE(SoilCarbon$d15N, c.labels,
                           underTreeNorthSurface, underTreeNorthSub, underTreeEastSurface,
                           underTreeEastSub, underTreeWestSurface, underTreeWestSub, underTreeSouthSurface,
                           underTreeSouthSub, "Direction and Depth", "Average Natural Abundance of
                           15N") + geom_text(x = 1, y = 6.2, label = "n=40")
Niso.direction.graph

#CN ratio by direction under tree (distance = 0)
CN.direction.graph = avgSE(SoilCarbon$CNRatio, c.labels,
                           underTreeNorthSurface, underTreeNorthSub, underTreeEastSurface,
                           underTreeEastSub, underTreeWestSurface, underTreeWestSub, underTreeSouthSurface,
                           underTreeSouthSub, "Direction and Depth", "Average C:N Ratio") +
geom_text(x = 7.75, y = 14, label = "n=40")
CN.direction.graph

#soil moisture by direction under tree (distance = 0)
moisture.direction.graph = avgSE(SoilCarbon$PercentMoisture,
                           c.labels, underTreeNorthSurface, underTreeNorthSub,
                           underTreeEastSurface, underTreeEastSub, underTreeWestSurface,
                           underTreeWestSub, underTreeSouthSurface,
                           underTreeSouthSub, "Direction and Depth", "Average Soil Moisture Content
                           (%)") + geom_text(x = 7, y = 16.5, label = "n=39")
moisture.direction.graph

#pH by direction under tree (distance = 0)

```

```

pH.direction.graph = avgSE(SoilCarbon$pH, c.labels,
                           underTreeNorthSurface, underTreeNorthSub, underTreeEastSurface,
                           underTreeEastSub, underTreeWestSurface, underTreeWestSub, underTreeSouthSurface,
                           underTreeSouthSub, "Direction and Depth", "pH") + geom_text(x = 7.75, y =
8.25, label = "n=40")
pH.direction.graph

#clay by direction under tree (distance =0)
clay.direction.graph = avgSE(SoilCarbon$Clay, c.labels,
                             underTreeNorthSurface, underTreeNorthSub, underTreeEastSurface,
                             underTreeEastSub, underTreeWestSurface, underTreeWestSub, underTreeSouthSurface,
                             underTreeSouthSub, "Direction and Depth", "Percent Clay") + geom_text(x = 7,
y = 24.5, label = "n=40")
clay.direction.graph

silt.direction.graph = avgSE(SoilCarbon$Silt, c.labels,
                             underTreeNorthSurface, underTreeNorthSub, underTreeEastSurface,
                             underTreeEastSub, underTreeWestSurface, underTreeWestSub, underTreeSouthSurface,
                             underTreeSouthSub, "Direction and Depth", "Percent Silt") + geom_text(x =
7.5, y = 70, label = "n=40")
silt.direction.graph

#find indices for each direction/depth for distance = 5m
fiveMetersNorthSurface = which(SoilCarbon$AdjustedDistance <=5 &
SoilCarbon$AdjustedDistance >0 &
SoilCarbon$Direction == "N" & SoilCarbon$DepthKey == "S")
fiveMetersNorthSub = which(SoilCarbon$AdjustedDistance <=5 &
SoilCarbon$AdjustedDistance >0 &
SoilCarbon$Direction == "N" & SoilCarbon$DepthKey == "B")
fiveMetersSouthSurface = which(SoilCarbon$AdjustedDistance <=5 &
SoilCarbon$AdjustedDistance >0 &
SoilCarbon$Direction == "S" & SoilCarbon$DepthKey == "S")
fiveMetersSouthSub = which(SoilCarbon$AdjustedDistance <=5 &
SoilCarbon$AdjustedDistance >0 &
SoilCarbon$Direction == "S" & SoilCarbon$DepthKey == "B")
fiveMetersEastSurface = which(SoilCarbon$AdjustedDistance <=5 &
SoilCarbon$AdjustedDistance >0 &
SoilCarbon$Direction == "E" & SoilCarbon$DepthKey == "S")
fiveMetersEastSub = which(SoilCarbon$AdjustedDistance <=5 & SoilCarbon$AdjustedDistance
>0 &
SoilCarbon$Direction == "E" & SoilCarbon$DepthKey == "B")
fiveMetersWestSurface = which(SoilCarbon$AdjustedDistance <=5 &
SoilCarbon$AdjustedDistance >0 &
SoilCarbon$Direction == "W" & SoilCarbon$DepthKey == "S")
fiveMetersWestSub = which(SoilCarbon$AdjustedDistance <=5 &

```

```

SoilCarbon$AdjustedDistance >0 &
  SoilCarbon$Direction == "W" & SoilCarbon$DepthKey == "B")
#OM by direction/depth for 5m
om.5m.graph = avgSE(SoilCarbon$PercentOM, c.labels,
  fiveMetersNorthSurface, fiveMetersNorthSub, fiveMetersEastSurface,
  fiveMetersEastSub,
  fiveMetersWestSurface, fiveMetersWestSub, fiveMetersSouthSurface,
  fiveMetersSouthSub, "Direction and Depth",
  "Average Organic Matter Content (%)") + geom_text(x = 7.5, y = 7.5, label =
  "n=40")
om.5m.graph

#C for direction/depth for 5m
c.5m.graph = avgSE(SoilCarbon$PercentC, c.labels,
  fiveMetersNorthSurface, fiveMetersNorthSub, fiveMetersEastSurface,
  fiveMetersEastSub,
  fiveMetersWestSurface, fiveMetersWestSub, fiveMetersSouthSurface,
  fiveMetersSouthSub, "Direction and Depth",
  "Average Soil Carbon Content (%)") + geom_text(x = 7.5, y = 2.6, label = "n=40")
c.5m.graph

#N for direction/depth for 5m
n.5m.graph = avgSE(SoilCarbon$PercentN, c.labels,
  fiveMetersNorthSurface, fiveMetersNorthSub, fiveMetersEastSurface,
  fiveMetersEastSub,
  fiveMetersWestSurface, fiveMetersWestSub, fiveMetersSouthSurface,
  fiveMetersSouthSub, "Direction and Depth",
  "Average Soil Nitrogen Content (%)") + geom_text(x = 7.5, y = 0.21, label = "n=40")
n.5m.graph

#moisture for direction/depth for 5m
moisture.fiveM.west.ss = which(SoilCarbon$AdjustedDistance <=5 &
  SoilCarbon$AdjustedDistance >0 &
  SoilCarbon$Direction == "W" & SoilCarbon$DepthKey == "S" &
  !is.na(SoilCarbon$PercentMoisture))
moisture.5m.graph = avgSE(SoilCarbon$PercentMoisture, c.labels,
  fiveMetersNorthSurface, fiveMetersNorthSub, fiveMetersEastSurface,
  fiveMetersEastSub,
  fiveMetersWestSurface, moisture.fiveM.west.ss, fiveMetersSouthSurface,
  fiveMetersSouthSub, "Direction and Depth",
  "Average Soil Moisture Content (%)") + geom_text(x = 7, y = 17.5, label =
  "n=39")
moisture.5m.graph

#C isotopes for direction/depth for 5m
cIso.5m.graph = avgSE(SoilCarbon$d13C, c.labels,

```

```

fiveMetersNorthSurface, fiveMetersNorthSub, fiveMetersEastSurface,
fiveMetersEastSub,
    fiveMetersWestSurface, fiveMetersWestSub, fiveMetersSouthSurface,
    fiveMetersSouthSub, "Direction and Depth",
    "Average Natural Abundance of 13C") + geom_text(x = 7.75, y = -19, label =
"n=40")
cIso.5m.graph

#N isotopes for direction/depth for 5m
nIso.5m.graph = avgSE(SoilCarbon$d15N, c.labels,
    fiveMetersNorthSurface, fiveMetersNorthSub, fiveMetersEastSurface,
fiveMetersEastSub,
    fiveMetersWestSurface, fiveMetersWestSub, fiveMetersSouthSurface,
    fiveMetersSouthSub, "Direction and Depth",
    "Average Natural Abundance of 15N") + geom_text(x = 7, y = 6.8, label = "n=40")
nIso.5m.graph

#CN for direction/depth for 5m
CN.5m.graph = avgSE(SoilCarbon$CNRatio, c.labels,
    fiveMetersNorthSurface, fiveMetersNorthSub, fiveMetersEastSurface,
fiveMetersEastSub,
    fiveMetersWestSurface, fiveMetersWestSub, fiveMetersSouthSurface,
    fiveMetersSouthSub, "Direction and Depth",
    "Average C:N Ratio") + geom_text(x = 7.75, y = 12.3, label = "n=40")
CN.5m.graph

#pH for direction/depth for 5m
pH.5m.graph = avgSE(SoilCarbon$pH, c.labels,
    fiveMetersNorthSurface, fiveMetersNorthSub, fiveMetersEastSurface,
fiveMetersEastSub,
    fiveMetersWestSurface, fiveMetersWestSub, fiveMetersSouthSurface,
    fiveMetersSouthSub, "Direction and Depth",
    "pH") + geom_text(x = 7.75, y = 8.1, label = "n=40")
pH.5m.graph

#clay by direction in intercanopy
clay.5m.graph = avgSE(SoilCarbon$Clay, c.labels,
    fiveMetersNorthSurface, fiveMetersNorthSub, fiveMetersEastSurface,
fiveMetersEastSub,
    fiveMetersWestSurface, fiveMetersWestSub, fiveMetersSouthSurface,
    fiveMetersSouthSub, "Direction and Depth", "Percent Clay") + geom_text(x =
7.5, y = 25, label = "n=40")
clay.5m.graph

silt.5m.graph = avgSE(SoilCarbon$Silt, c.labels,
    fiveMetersNorthSurface, fiveMetersNorthSub, fiveMetersEastSurface,

```

```

fiveMetersEastSub,
  fiveMetersWestSurface, fiveMetersWestSub, fiveMetersSouthSurface,
  fiveMetersSouthSub, "Direction and Depth", "Percent Silt") + geom_text(x =
7.75, y = 70, label = "n=40")
silt.5m.graph

#find indices for each distance/depth
zeroMetersSurface = which(soilCarbon.30m.transects.all$AdjustedDistance == 0 &
                           soilCarbon.30m.transects.all$DepthKey == "S")
zeroMetersSub = which(soilCarbon.30m.transects.all$AdjustedDistance == 0 &
                      soilCarbon.30m.transects.all$DepthKey
                      == "B")
fiveMetersSurface = which(soilCarbon.30m.transects.all$AdjustedDistance > 0 &
                           soilCarbon.30m.transects.all$AdjustedDistance <= 5 &
                           soilCarbon.30m.transects.all$DepthKey == "S")
fiveMetersSub = which(soilCarbon.30m.transects.all$AdjustedDistance > 0 &
                      soilCarbon.30m.transects.all$AdjustedDistance <= 5 &
                      soilCarbon.30m.transects.all$DepthKey
                      == "B")
fifteenMetersSurface = which(soilCarbon.30m.transects.all$Distance > 5 &
                               soilCarbon.30m.transects.all$DepthKey == "S")
fifteenMetersSub = which(soilCarbon.30m.transects.all$Distance > 5 &
                           soilCarbon.30m.transects.all$DepthKey == "B")

distance.labels = c("Surface Under Canopy", "Subsurface\nUnder Canopy", "Surface
Dripline\nonto 5 Meters",
                   "Subsurface Dripline\nonto 5 Meters", "Surface Beyond\n5 Meters", "Subsurface
Beyond\n5 Meters")
#OM for distances and depths
om.distance.graph = avgSEBins(soilCarbon.30m.transects.all$PercentOM, distance.labels,
                               zeroMetersSurface, zeroMetersSub, fiveMetersSurface, fiveMetersSub,
                               fifteenMetersSurface, fifteenMetersSub, "Distance and Depth", "Average
Organic Matter Content
(%)") + geom_text(x = 5.75, y = 9, label = "n=40")
om.distance.graph

#c for distances and depths

c.distance.graph = avgSEBins(soilCarbon.30m.transects.all$PercentC, distance.labels,
                               zeroMetersSurface, zeroMetersSub, fiveMetersSurface, fiveMetersSub,
                               fifteenMetersSurface, fifteenMetersSub, "Distance and Depth", "Average Soil
C Content (%)") + geom_text(x = 5.75, y = 3.4, label = "n=40")
c.distance.graph

#n for distances and depths
n.distance.graph = avgSEBins(soilCarbon.30m.transects.all$PercentN, distance.labels,
                               zeroMetersSurface, zeroMetersSub, fiveMetersSurface, fiveMetersSub,

```

```

fifteenMetersSurface, fifteenMetersSub, "Distance and Depth", "Average Soil
N Content (%))" + geom_text(x = 5.75, y = 0.26, label = "n=40")
n.distance.graph

```

```

#C isotopes for distances and depths
cIso.distance.graph = avgSEBins(soilCarbon.30m.transects.all$d13C, distance.labels,
                                zeroMetersSurface, zeroMetersSub, fiveMetersSurface, fiveMetersSub,
                                fifteenMetersSurface, fifteenMetersSub, "Distance and Depth", "Average
Natural Abundance of 13C") + geom_text(x = 6, y = -19, label = "n=40")
cIso.distance.graph

```

```

#N isotopes for distances and depths
nIso.distance.graph = avgSEBins(soilCarbon.30m.transects.all$d15N, distance.labels,
                                zeroMetersSurface, zeroMetersSub, fiveMetersSurface, fiveMetersSub,
                                fifteenMetersSurface, fifteenMetersSub, "Distance and Depth", "Average
Natural Abundance of 15N") + geom_text(x = 0.75, y = 7, label = "n=40")
nIso.distance.graph

```

```

#CN for distances and depths
CN.distance.graph = avgSEBins(soilCarbon.30m.transects.all$CN, distance.labels,
                                zeroMetersSurface, zeroMetersSub, fiveMetersSurface, fiveMetersSub,
                                fifteenMetersSurface, fifteenMetersSub, "Distance and Depth", "Average C:N
of Soil") + geom_text(x = 5.75, y = 13, label = "n=40")
CN.distance.graph

```

```

pH.distance.graph = avgSEBins(soilCarbon.30m.transects.all$pH, distance.labels,
                                zeroMetersSurface, zeroMetersSub, fiveMetersSurface, fiveMetersSub,
                                fifteenMetersSurface, fifteenMetersSub, "Distance and Depth", "Average pH")
+ geom_text(x = 5.9, y = 8.1, label = "n=40")
pH.distance.graph

```

```

clay.distance.graph = avgSEBins(soilCarbon.30m.transects.all$Clay, distance.labels,
                                zeroMetersSurface, zeroMetersSub, fiveMetersSurface, fiveMetersSub,
                                fifteenMetersSurface, fifteenMetersSub, "Distance and Depth", "Average
Clay Content (%))" + geom_text(x = 5.9, y = 25.5, label = "n=40")
clay.distance.graph

```

```

silt.distance.graph = avgSEBins(soilCarbon.30m.transects.all$Silt, distance.labels,
                                zeroMetersSurface, zeroMetersSub, fiveMetersSurface, fiveMetersSub,
                                fifteenMetersSurface, fifteenMetersSub, "Distance and Depth", "Average
Silt Content (%))" + geom_text(x = 5.9, y = 67, label = "n=40")
silt.distance.graph

```

```

veryFinesand.distance.graph = avgSEBins(soilCarbon.30m.transects.all$VeryFineSand,
distance.labels,
zeroMetersSurface, zeroMetersSub, fiveMetersSurface, fiveMetersSub,
fifteenMetersSurface, fifteenMetersSub, "Distance and Depth", "Average
Very Fine Sand Content (%)") + geom_text(x = 5.9, y = 67, label = "n=40")
veryFinesand.distance.graph

noFineSand = which(soilCarbon.30m.transects.all$FineSand==0)
Finesand.distance.graph = avgSEBins(soilCarbon.30m.transects.all$FineSand, distance.labels,
zeroMetersSurface, zeroMetersSub, fiveMetersSurface, fiveMetersSub,
fifteenMetersSurface, fifteenMetersSub, "Distance and Depth",
"Average Fine Sand Content (%)") + geom_text(x = 5.9, y = 67, label = "n=40")
Finesand.distance.graph

Mediumsand.distance.graph = avgSEBins(soilCarbon.30m.transects.all$MediumSand,
distance.labels,
zeroMetersSurface, zeroMetersSub, fiveMetersSurface, fiveMetersSub,
fifteenMetersSurface, fifteenMetersSub, "Distance and Depth",
"Average Medium Sand Content (%)") + geom_text(x = 5.9, y = 67, label = "n=40")
Mediumsand.distance.graph

#do distance for strat ratios
stratRatio.15n.dist.graph = avgSEStrat(soilCarbon.30m.transects.all$StratificationRatio15N,
c("Under Canopy", "Dripline to Five Meters", "Beyond Five Meters"), zeroMetersSurface,
fiveMetersSurface, fifteenMetersSurface, "Distance from Juniper Tree", "Average Stratification
Ratio of 15N") + geom_text(x = 3.3, y = 0.96, label = "n=40")
stratRatio.15n.dist.graph

stratRatio.13c.dist.graph = avgSEStrat(soilCarbon.30m.transects.all$StratificationRatio13C,
c("Under Canopy", "Dripline to Five Meters", "Beyond Five Meters"), zeroMetersSurface,
fiveMetersSurface, fifteenMetersSurface, "Distance from Juniper Tree", "Average Stratification
Ratio of 13C") + geom_text(x = 3.3, y = 1.18, label = "n=40")
stratRatio.13c.dist.graph
length(soilCarbon.30m.transects.all$StratificationRatio13C)#pretty much the same

#see which variables best explain soil OM
#moisture
noMoisureData = which(is.na(SoilCarbon$PercentMoisture))
moisture.soil.om.r = correlation(SoilCarbon$PercentMoisture[-noMoisureData],
SoilCarbon$PercentOM[-noMoisureData])
moisture.soil.om.r#0.2911719

```

```

moisture.soil.om.p = pValue(SoilCarbon$PercentMoisture[-noMoisureData],
                           SoilCarbon$PercentOM[-noMoisureData])
#nitrogen
nitrogen.soil.om.r = correlation(SoilCarbon$PercentN,
                                  SoilCarbon$PercentOM)
nitrogen.soil.om.r #0.9464142
nitrogen.soil.om.p = pValue(SoilCarbon$PercentN, SoilCarbon$PercentOM)

#clay (will not be testing this further- value is very small)
tinyFrac.soil.om.r = correlation(SoilCarbon$Clay,
                                  SoilCarbon$PercentOM)
tinyFrac.soil.om.r #0.08001233

#silt fraction (will not be testing this further- value is very small)
silt.soil.om.r = correlation(SoilCarbon$Silt,
                             SoilCarbon$PercentOM)
silt.soil.om.r #-0.05972373

#very fine sand fraction
veryFineSand.soil.om.r = correlation(SoilCarbon$VeryFineSand,
                                       SoilCarbon$PercentOM)
veryFineSand.soil.om.r #-0.2244806
veryFineSand.soil.om.p = pValue(SoilCarbon$VeryFineSand,
                                 SoilCarbon$PercentOM)

#fine sand fraction
FineSand.Soil.om.r = correlation(SoilCarbon$FineSand,
                                  SoilCarbon$PercentOM)
FineSand.Soil.om.r #0.1279845
FineSand.Soil.om.p = pValue(SoilCarbon$FineSand,
                            SoilCarbon$PercentOM)

#Medium sand fraction
MediumSand.om.r =
  correlation(SoilCarbon$MediumSand,
              SoilCarbon$PercentOM)
MediumSand.om.r #0.2072566
MediumSand.om.p = pValue(SoilCarbon$MediumSand,
                         SoilCarbon$PercentOM)

#pH
pH.om.r = correlation(SoilCarbon$pH, SoilCarbon$PercentOM)
pH.om.r #0.3918284
pH.om.p = pValue(SoilCarbon$pH, SoilCarbon$PercentOM)

#carbon isotope
d13C.om.r =correlation(SoilCarbon$d13C, SoilCarbon$PercentOM)
d13C.om.r
d13C.om.p = pValue(SoilCarbon$d13C, SoilCarbon$PercentOM)

```

```

#nitrogen isotope
d15N.om.r = correlation(SoilCarbon$d15N, SoilCarbon$PercentOM)
d15N.om.r
d15N.om.p = pValue(SoilCarbon$d15N, SoilCarbon$PercentOM)

#graph of predictors for soil OM
factors.corrs.om.df = data.frame(Factor = c("Percent Moisture", "Percent Nitrogen", "d13C",
"d15N", "Very Fine Sand", "Fine Sand",
"Medium Sand", "pH"), Correlation.Coefficient
= rbind(Percent.Moisture = moisture.soil.om.r, Percent.Nitrogen =
nitrogen.soil.om.r, d13C = d13C.om.r, d15N = d15N.om.r,
Very.Fine.Sand = veryFineSand.soil.om.r, Fine.Sand
= FineSand.Soil.om.r, Medium.Sand =
MediumSand.om.r, soil.pH = pH.om.r), p.Value =
rbind(Percent.Moisture = moisture.soil.om.p, Percent.Nitrogen =
nitrogen.soil.om.p, d13C = d13C.om.p, d15N =
d15N.om.p, Very.Fine.Sand = veryFineSand.soil.om.p, Fine.Sand
= FineSand.Soil.om.p, Medium.Sand =
MediumSand.om.p, soil.pH = pH.om.p))
factors.corrs.om.df

#levels(factors.corrs.om.df$Factor) = c("Fifty\nMicron\nFraction"

factors.corrs.om.plot = ggplot(data=factors.corrs.om.df, aes(x=Factor, y =
Correlation.Coefficient, fill = p.Value<0.01)) + geom_bar(stat ="identity") +
labs(title="Correlation and Significance Between Multiple Factors and Soil Organic Matter
Content", x="Factor", y="Correlation Coefficient (r)") + scale_x_discrete(limits =
factors.corrs.om.df[,1])
factors.corrs.om.plot

#see which variables best explain soil C
#moisture
moisture.soil.c.r = correlation(SoilCarbon$PercentMoisture[-noMoisureData],
SoilCarbon$PercentC[-noMoisureData])
moisture.soil.c.r #0.1552082
moisture.soil.c.p = pValue(SoilCarbon$PercentMoisture[-noMoisureData],
SoilCarbon$PercentC[-noMoisureData])
#nitrogen
nitrogen.soil.c.r = correlation(SoilCarbon$PercentN,
SoilCarbon$PercentC)
nitrogen.soil.c.r #0.9865819
nitrogen.soil.c.p = pValue(SoilCarbon$PercentN, SoilCarbon$PercentC)

#tinyfraction (will not be testing this further- value is very small)
#tinyFrac.soil.c.r = correlation(SoilCarbon$TinyFraction, SoilCarbon$PercentC)

```

```

#tinyFrac.soil.c.r #0.0005906371
#2 micron fractdion (will not be testing this further- value is very small)
#twoMicron.soil.c.r = correlation(SoilCarbon$TwoMicronFraction,SoilCarbon$PercentC)
#twoMicron.soil.c.r #-0.07327602

#very fine sand fraction
very.fine.sand.soil.c.r = correlation(SoilCarbon$VeryFineSand,
                                         SoilCarbon$PercentC)
very.fine.sand.soil.c.r #-0.1854455
very.fine.sand.soil.c.p = pValue(SoilCarbon$VeryFineSand,
                                   SoilCarbon$PercentC)

#fine sand fraction
fineSand.c.r = correlation(SoilCarbon$FineSand,
                            SoilCarbon$PercentC)
fineSand.c.r #0.168455
fineSand.c.p = pValue(SoilCarbon$FineSand,
                      SoilCarbon$PercentC)

#medium sand fraction
medium.sand.c.r =
  correlation(SoilCarbon$MediumSand,
              SoilCarbon$PercentC)
medium.sand.c.r #0.306582
medium.sand.c.p =
  pValue(SoilCarbon$MediumSand, SoilCarbon$PercentC)

#pH
pH.c.r = correlation(SoilCarbon$pH, SoilCarbon$PercentC)
pH.c.r #0.3776242
pH.c.p = pValue(SoilCarbon$pH, SoilCarbon$PercentC)

#carbon isotope
d13C.c.r =correlation(SoilCarbon$d13C, SoilCarbon$PercentC)
d13C.c.r #-.7387485
d13C.c.p = pValue(SoilCarbon$d13C, SoilCarbon$PercentC)

#nitrogen isotope
d15N.c.r = correlation(SoilCarbon$d15N, SoilCarbon$PercentC)
d15N.c.r #-.8070099
d15N.c.p = pValue(SoilCarbon$d15N, SoilCarbon$PercentC)

#graph of predictors for carbon
#graph of predictors for soil OM
factors.corrs.c.df = data.frame(Factor = c("Percent Moisture", "Percent Nitrogen", "d13C",
                                             "d15N", "Very Fine Sand", "Fine Sand",
                                             "Medium Sand", "pH"), Correlation.Coefficient
                                             = rbind(Percent.Moisture = moisture.soil.c.r, Percent.Nitrogen =

```

```

nitrogen.soil.c.r, d13C = d13C.c.r, d15N = d15N.c.r, Very.Fine.Sand =
very.fine.sand.soil.c.r, Fine.Sand
= fineSand.c.r, Medium.Sand =
medium.sand.c.r,
soil.pH = pH.c.r), p.Value = rbind(Percent.Moisture = moisture.soil.c.p,
Percent.Nitrogen = nitrogen.soil.c.p, d13C =
d13C.c.p, d15N = d15N.c.p, Very.Fine.Sand = very.fine.sand.soil.c.p, Fine.Sand
= fineSand.c.p, Medium.Sand =
medium.sand.c.p, soil.pH = pH.c.p))

factors.corrs.c.df
#levels(factors.corrs.c.df$Factor) = c("Fifty\nMicron\nFraction", "Hundred\nMicron\nFraction",
"Percent\nMoisture", "Percent\nNitrogen", "pH", "Two Hundred\nMicron\nFraction")
factors.corrs.c.plot = ggplot(data=factors.corrs.c.df, aes(x=Factor, y =
Correlation.Coefficient, fill = p.Value<0.01)) +
geom_bar(stat =
"identity") +
labs(title="Correlation and Significance Between Multiple Factors and Soil Carbon Content",
x="Factor", y="Correlation Coefficient (r)") + scale_x_discrete(limits = factors.corrs.c.df[,1])
factors.corrs.c.plot

#distance as a predictive variable
#pull out samples along long (30-m) transects
zhaad.transect.bottom = which(SoilCarbon$Tree=="T1" & SoilCarbon$Direction=="W" &
SoilCarbon$DepthKey == "B")
zhaad.transect.surface = which(SoilCarbon$Tree=="T1" & SoilCarbon$Direction=="W" &
SoilCarbon$DepthKey == "S")
zhaad.transect.all = which(SoilCarbon$Tree=="T1" & SoilCarbon$Direction=="W")

elijah.transect.bottom = which(SoilCarbon$Tree=="T2" & SoilCarbon$Direction=="S" &
SoilCarbon$DepthKey == "B")
elijah.transect.surface = which(SoilCarbon$Tree=="T2" & SoilCarbon$Direction=="S" &
SoilCarbon$DepthKey == "S")
elijah.transect.all = which(SoilCarbon$Tree=="T2" & SoilCarbon$Direction=="S")

larry.transect.bottom = which(SoilCarbon$Tree=="T3" & SoilCarbon$Direction=="N" &
SoilCarbon$DepthKey == "B")
larry.transect.surface = which(SoilCarbon$Tree=="T3" & SoilCarbon$Direction=="N" &
SoilCarbon$DepthKey == "S")
larry.transect.all = which(SoilCarbon$Tree=="T3" & SoilCarbon$Direction=="N")

athena.transect.bottom = which(SoilCarbon$Tree=="T4" & SoilCarbon$Direction=="E" &
SoilCarbon$DepthKey == "B")
athena.transect.surface = which(SoilCarbon$Tree=="T4" & SoilCarbon$Direction=="E" &
SoilCarbon$DepthKey == "S")
athena.transect.all = which(SoilCarbon$Tree=="T4" & SoilCarbon$Direction=="E")

```

```

borris.transect.bottom = which(SoilCarbon$Tree=="T5" & SoilCarbon$Direction=="W" &
SoilCarbon$DepthKey == "B")
borris.transect.surface = which(SoilCarbon$Tree=="T5" & SoilCarbon$Direction=="W" &
SoilCarbon$DepthKey == "S")
borris.transect.all = which(SoilCarbon$Tree=="T5" & SoilCarbon$Direction=="W")

soilCarbon.30m.transects.all = SoilCarbon[c(zhaad.transect.all, elijah.transect.all,
larry.transect.all, athena.transect.all, borris.transect.all),]

soilCarbon.30m.transects.surface = SoilCarbon[c(zhaad.transect.surface, elijah.transect.surface,
larry.transect.surface, athena.transect.surface, borris.transect.surface),]
soilCarbon.30m.transects.surface

#distance predicting d15N
d15N.distance.surface.plot = ggplot(data=SoilCarbon[c(zhaad.transect.surface,
elijah.transect.surface, larry.transect.surface, athena.transect.surface, borris.transect.surface),],
aes(x=SoilCarbon$AdjustedDistance[c(zhaad.transect.surface, elijah.transect.surface,
larry.transect.surface, athena.transect.surface, borris.transect.surface)],
y=SoilCarbon$d15N[c(zhaad.transect.surface, elijah.transect.surface, larry.transect.surface,
athena.transect.surface, borris.transect.surface)])) + geom_point()
d15N.distance.surface.plot

#distance predicting percent carbon
distance.c.r = correlation(SoilCarbon$AdjustedDistance, SoilCarbon$PercentC)
distance.c.r #-0.5038028
distance.c.p = pValue(SoilCarbon$AdjustedDistance, SoilCarbon$PercentC)

#distance predicting d13C
distance.d13c.r = correlation(SoilCarbon$AdjustedDistance, SoilCarbon$d13C)
distance.d13c.r #0.5659629
distance.d13c.p = pValue(SoilCarbon$AdjustedDistance, SoilCarbon$d13C)
distance.d13c.p #3.791003e-10

#distance predicting d15N
distance.d15n.r = correlation(SoilCarbon$AdjustedDistance, SoilCarbon$d15N)
distance.d15n.r #0.4406547
distance.d15n.p = pValue(SoilCarbon$AdjustedDistance, SoilCarbon$d15N)
distance.d15n.p #6.74116e-07

head(SoilCarbon)

#ggplot(data=SoilCarbon, aes(x=SoilCarbon$AdjustedDistance, y=SoilCarbon$d15N)) +
geom_point()
underTree.samples = SoilCarbon[which(SoilCarbon$Distance=="0"),]
underTree.samples.surface =
SoilCarbon[which(SoilCarbon$Distance=="0"&SoilCarbon$DepthKey=="S"),]

```

```

underTree.samples.subsurface =
SoilCarbon[which(SoilCarbon$Distance=="0"&SoilCarbon$DepthKey=="B"),]

anovaTest.direction.depth.om = aov(underTree.samples$PercentOM ~
underTree.samples$Direction*underTree.samples$DepthKey, data=underTree.samples)
summary(anovaTest.direction.depth.om)

#ANOVA for distance and depth for 13C
anovaTest.distance.depth.d13C = aov(soilCarbon.30m.transects.all$d13C ~
soilCarbon.30m.transects.all$DistanceBins)
summary(anovaTest.distance.depth.d13C)

#ANOVA for distance and depth for 15N
anovaTest.distance.depth.d15N = aov(soilCarbon.30m.transects.all$d15N ~
soilCarbon.30m.transects.all$DistanceBins)
summary(anovaTest.distance.depth.d15N)

#ANOVA for tree and depth for 15N (for only under tree)
anovaTest.tree.depth.d15N = aov(underTree.samples$d15N ~
underTree.samples$TrunkDiameter)
summary(anovaTest.tree.depth.d15N)

#ANOVA for tree and depth for 13C (for only under tree)
anovaTest.tree.depth.d13C = aov(underTree.samples$d13C ~
underTree.samples$TrunkDiameter)
summary(anovaTest.tree.depth.d13C)

anovaTest.tree.C = aov(underTree.samples$PercentC ~ underTree.samples$TrunkDiameter)
summary(anovaTest.tree.C)

anovaTest.tree.N = aov(underTree.samples$PercentN ~ underTree.samples$TrunkDiameter)
summary(anovaTest.tree.N)

anovaTest.tree.om = aov(underTree.samples$PercentOM ~ underTree.samples$TrunkDiameter)
summary(anovaTest.tree.om)

anovaTest.tree.moisture = aov(underTree.samples$PercentMoisture ~
underTree.samples$TrunkDiameter)
summary(anovaTest.tree.moisture)

anovaTest.tree.pH = aov(underTree.samples$pH ~ underTree.samples$TrunkDiameter)
summary(anovaTest.tree.pH)

anovaTest.tree.clay = aov(underTree.samples$Clay ~ underTree.samples$TrunkDiameter)
summary(anovaTest.tree.clay)

```

```
anovaTest.tree.silt = aov(underTree.samples$Silt ~ underTree.samples$TrunkDiameter)
summary(anovaTest.tree.silt)
```

```
anovaTest.tree.VeryFineSand = aov(underTree.samples$VeryFineSand ~
underTree.samples$TrunkDiameter)
summary(anovaTest.tree.VeryFineSand)
```

#ANOVA for distances

```
anovaTest.dist.d15N = aov(soilCarbon.30m.transects.all$d15N ~
soilCarbon.30m.transects.all$DistanceBins)
summary(anovaTest.dist.d15N)
```

```
anovaTest.dist.d13C = aov(soilCarbon.30m.transects.all$d13C ~
soilCarbon.30m.transects.all$DistanceBins)
summary(anovaTest.dist.d13C)
```

```
anovaTest.dist.C = aov(soilCarbon.30m.transects.all$PercentC ~
soilCarbon.30m.transects.all$DistanceBins)
summary(anovaTest.dist.C)
```

```
anovaTest.dist.N = aov(soilCarbon.30m.transects.all$PercentN ~
soilCarbon.30m.transects.all$DistanceBins)
summary(anovaTest.dist.N)
```

```
anovaTest.dist.om = aov(soilCarbon.30m.transects.all$PercentOM ~
soilCarbon.30m.transects.all$DistanceBins)
summary(anovaTest.dist.om)
```

```
anovaTest.dist.moisture = aov(soilCarbon.30m.transects.all$PercentMoisture ~
soilCarbon.30m.transects.all$DistanceBins)
summary(anovaTest.dist.moisture)
```

```
anovaTest.dist.pH = aov(soilCarbon.30m.transects.all$pH ~
soilCarbon.30m.transects.all$DistanceBins)
summary(anovaTest.dist.pH)
```

```
anovaTest.dist.clay = aov(soilCarbon.30m.transects.all$Clay ~
soilCarbon.30m.transects.all$DistanceBins)
summary(anovaTest.dist.clay)
```

```
anovaTest.dist.silt = aov(soilCarbon.30m.transects.all$Silt ~
soilCarbon.30m.transects.all$DistanceBins)
summary(anovaTest.dist.silt)
```

```
anovaTest.dist.VeryFineSand = aov(soilCarbon.30m.transects.all$VeryFineSand ~
soilCarbon.30m.transects.all$DistanceBins)
```

```

summary(anovaTest.dist.VeryFineSand)

anovaTest.dist.stratRatio.surface.d13C =
aov(soilCarbon.30m.transects.surface$StratificationRatio13C ~
soilCarbon.30m.transects.surface$DistanceBins)
summary(anovaTest.dist.stratRatio.surface.d13C)

anovaTest.dist.stratRatio.surface.d15N =
aov(soilCarbon.30m.transects.surface$StratificationRatio15N ~
soilCarbon.30m.transects.surface$DistanceBins)
summary(anovaTest.dist.stratRatio.surface.d15N)

#ANOVA for directions
anovaTest.dir.d15N = aov(underTree.samples$d15N ~ underTree.samples$Direction)
summary(anovaTest.dir.d15N)

anovaTest.dir.d13C = aov(underTree.samples$d13C ~ underTree.samples$Direction)
summary(anovaTest.dir.d13C)

anovaTest.dir.C = aov(underTree.samples$PercentC ~ underTree.samples$Direction)
summary(anovaTest.dir.C)

anovaTest.dir.N = aov(underTree.samples$PercentN ~ underTree.samples$Direction)
summary(anovaTest.dir.N)

anovaTest.dir.om = aov(underTree.samples$PercentOM ~ underTree.samples$Direction)
summary(anovaTest.dir.om)

anovaTest.dir.moisture = aov(underTree.samples$PercentMoisture ~
underTree.samples$Direction)
summary(anovaTest.dir.moisture)

anovaTest.dir.pH = aov(underTree.samples$pH ~ underTree.samples$Direction)
summary(anovaTest.dir.pH)

anovaTest.dir.clay = aov(underTree.samples$Clay ~ underTree.samples$Direction)
summary(anovaTest.dir.clay)

anovaTest.dir.silt = aov(underTree.samples$Silt ~ underTree.samples$Direction)
summary(anovaTest.dir.silt)

anovaTest.dir.VeryFineSand = aov(underTree.samples$VeryFineSand ~
underTree.samples$Direction)
summary(anovaTest.dir.VeryFineSand)

```

```

anovaTest.direction.stratRatio.surface.d13C =
aov(underTree.samples.surface$StratificationRatio13C ~ underTree.samples.surface$Direction)
summary(anovaTest.direction.stratRatio.surface.d13C)

anovaTest.direction.stratRatio.surface.d15N =
aov(underTree.samples.surface$StratificationRatio15N ~ underTree.samples.surface$Direction)
summary(anovaTest.direction.stratRatio.surface.d15N)

#ANOVA for tree for stratification ratio of 13C (for only surface under tree)
anovaTest.tree.direction.stratRatio.surface.d13C =
aov(underTree.samples.surface$StratificationRatio13C ~
underTree.samples.surface$TrunkDiameter)
summary(anovaTest.tree.direction.stratRatio.surface.d13C)

#ANOVA for tree for stratification ratio of 15N (for only surface under tree)
anovaTest.tree.direction.stratRatio.surface.d15N =
aov(underTree.samples.surface$StratificationRatio15N ~
underTree.samples.surface$TrunkDiameter)
summary(anovaTest.tree.direction.stratRatio.surface.d15N)

#ANOVA for stratification ratio for 13C for distance
anovaTest.distance.stratRatio.13c =
aov(soilCarbon.30m.transects.surface$StratificationRatio13C ~
soilCarbon.30m.transects.surface$DistanceBins)
summary(anovaTest.distance.stratRatio.13c) #F 1.291 #p 0.301

#ANOVA for stratification ratio for 15N for distance
anovaTest.distance.stratRatio.15N =
aov(soilCarbon.30m.transects.surface$StratificationRatio15N ~
soilCarbon.30m.transects.surface$DistanceBins)
summary(anovaTest.distance.stratRatio.15N) #F:10.48 p: 0.00108

#ANOVA between pH and distance + depth
anovaTest.distance.pH =
aov(soilCarbon.30m.transects.all$pH~soilCarbon.30m.transects.all$DistanceBins, data =
soilCarbon.30m.transects.all)
summary(anovaTest.distance.pH) #not significant

#ANOVA between pH and distance only for surface
anovaTest.distance.pH.surface =
aov(soilCarbon.30m.transects.surface$pH~soilCarbon.30m.transects.surface$DistanceBins,
data=soilCarbon.30m.transects.surface)
summary(anovaTest.distance.pH.surface) #not significant F:0.366, P: 0.699

#test out canopy radius on soil properties of surface samples below tree
noCanopy.radius.surface = which(is.na(underTree.samples.surface$CanopyRadius))

```

```

noCanopy.radius.surface
#as canopy radius increases, OM increases
canopyRadius.OM.r = correlation(underTree.samples.surface$CanopyRadius[-noCanopy.radius.surface], underTree.samples.surface$PercentOM[-noCanopy.radius.surface])
canopyRadius.OM.r #0.6510502
canopyRadius.OM.p = pValue(underTree.samples.surface$CanopyRadius[-noCanopy.radius.surface], underTree.samples.surface$PercentOM[-noCanopy.radius.surface])
canopyRadius.OM.p #0.01504178

boxplot(underTree.samples.surface$PercentOM[-noCanopy.radius.surface]~underTree.samples.surface$CanopyRadius[-noCanopy.radius.surface], main="Canopy Radius vs. Surface Soil Properties Under Juniper Trees", xlab="Canopy Radius(cm)", ylab="Percent Organic Matter")

canopyRadius.moisture.r = correlation(underTree.samples.surface$CanopyRadius[-noCanopy.radius.surface], underTree.samples.surface$PercentMoisture[-noCanopy.radius.surface])
canopyRadius.moisture.r #0.3661681
canopyRadius.moisture.p = pValue(underTree.samples.surface$CanopyRadius[-noCanopy.radius.surface], underTree.samples.surface$PercentMoisture[-noCanopy.radius.surface])
canopyRadius.moisture.p #0.09123132 no bueno

canopyRadius.15N.r = correlation(underTree.samples.surface$CanopyRadius[-noCanopy.radius.surface], underTree.samples.surface$d15N[-noCanopy.radius.surface])
canopyRadius.15N.r #-0.5751552
canopyRadius.15N.p = pValue(underTree.samples.surface$CanopyRadius[-noCanopy.radius.surface], underTree.samples.surface$d15N[-noCanopy.radius.surface])
canopyRadius.15N.p #0.0228193

ggplot(data=underTree.samples.surface[-noCanopy.radius.surface], aes(x=CanopyRadius, y = PercentOM)) + geom_point()

#if 15N decreases with tree age, then it's not litter residence time, but the litter itself that is causing a slower turnover
diameter.underTree.15N.plot = ggplot(data=underTree.samples.surface,
aes(x=underTree.samples.surface$TrunkDiameter, y=underTree.samples.surface$d15N)) +
geom_point()
diameter.underTree.15N.r = correlation(underTree.samples.surface$TrunkDiameter, underTree.samples.surface$d15N)
diameter.underTree.15N.r #-0.4541911
diameter.underTree.15N.p = pValue(underTree.samples.surface$TrunkDiameter, underTree.samples.surface$d15N)
diameter.underTree.15N.p #0.07500771

```

```

diameter.underTree.15Nb.r = correlation(underTree.samples.subsurface$TrunkDiameter,
underTree.samples.subsurface$d15N)
diameter.underTree.15Nb.r #-0.0248327
diameter.underTree.15Nb.p = pValue(underTree.samples.subsurface$TrunkDiameter,
underTree.samples.subsurface$d15N)
diameter.underTree.15Nb.p #0.4708769

#diameter.underTree.13c.plot = ggplot(data=underTree.samples.surface,
aes(x=underTree.samples.surface$TrunkDiameter, y=underTree.samples.surface$d15N)) +
geom_point()
diameter.underTree.13c.r = correlation(underTree.samples.surface$TrunkDiameter,
underTree.samples.surface$d15N)
diameter.underTree.13c.r #-0.4541911
diameter.underTree.13c.p = pValue(underTree.samples.surface$TrunkDiameter,
underTree.samples.surface$d15N)
diameter.underTree.13c.p #0.07500771

boxplot(underTree.samples.surface$d15N~underTree.samples.surface$TrunkDiameter,
main="Juniper Trunk Diameter vs. Natural Abundance of 15N", xlab="Trunk Diameter (m)",
ylab="15N")

borris.surface = which(underTree.samples.surface$Tree == "T5")
zhaad.surface = which(underTree.samples.surface$Tree == "T1")
larry.surface = which(underTree.samples.surface$Tree == "T3")
elijah.surface = which(underTree.samples.surface$Tree == "T2")
athena.surface = which(underTree.samples.surface$Tree == "T4")

borris.sub = which(underTree.samples.subsurface$Tree == "T5")
zhaad.sub = which(underTree.samples.subsurface$Tree == "T1")
larry.sub = which(underTree.samples.subsurface$Tree == "T3")
elijah.sub = which(underTree.samples.subsurface$Tree == "T2")
athena.sub = which(underTree.samples.subsurface$Tree == "T4")

diameter.CN.plot = diameters(underTree.samples$CNRatio, "Increasing Tree Age", "Average
C:N of Soil", "Average C:N of Soil as a Function of Juniper Age")
diameter.CN.plot

diameter.15N.plot = diameters(underTree.samples$d15N, "Increasing Tree Age", "Average
Natural Abundance of 15N of Soil", "Average Natural Abundance of 15N of Soil as a Function of
Juniper Age") + geom_text(x=9.75, y = 7.2, label= "n=40")
diameter.15N.plot

diameter.13C.plot = diameters(underTree.samples$d13C, "Increasing Tree Age", "Average
Natural Abundance of 13C of Soil", "Average Natural Abundance of 13C of Soil as a Function of
Juniper Age")

```

diameter.13C.plot

```
diameter.c.plot = diameters(underTree.samples$PercentC, "Increasing Tree Age", "Average Carbon Content of Soil (%)", "Average Natural Abundance of 13C of Soil as a Function of Juniper Age")
diameter.c.plot
```

```
diameter.n.plot = diameters(underTree.samples$PercentN, "Increasing Tree Age", "Average Nitrogen Content of Soil (%)", "Average Natural Abundance of 13C of Soil as a Function of Juniper Age")
diameter.n.plot
```

```
diameter.om.plot = diameters(underTree.samples$PercentOM, "Increasing Tree Age", "Average Organic Matter Content of Soil (%)", "Average Natural Abundance of 13C of Soil as a Function of Juniper Age") + geom_text(x=9.75, y = 14, label= "n=40")
diameter.om.plot
```

```
diameter.15n.stratRatio.plot = stratRatioDiam(underTree.samples$StratificationRatio15N, "Increasing Tree Age", "Average Stratification Ratio of 15N in Soil (%)", "Average Natural Abundance of 13C of Soil as a Function of Juniper Age") + geom_text(x=5, y = 1, label= "n=40")
diameter.15n.stratRatio.plot
```

```
#diameter.13c.stratRatio.plot = stratRatioDiam(underTree.samples$StratificationRatio13C, "Increasing Tree Age", "Average Stratification Ratio of 13C in Soil (%)", "Average Natural Abundance of 13C of Soil as a Function of Juniper Age")
#diameter.13c.stratRatio.plot
```

```
diameter.underTree.CN.plot = ggplot(data=underTree.samples.surface,
aes(x=underTree.samples.surface$TrunkDiameter, y=underTree.samples.surface$CN)) +
geom_point()
diameter.underTree.CN.plot
diameter.underTree.CN.r = correlation(underTree.samples.surface$TrunkDiameter, underTree.samples.surface$CN)
diameter.underTree.CN.r #0.7142968
diameter.underTree.CN.p = pValue(underTree.samples.surface$TrunkDiameter, underTree.samples.surface$CN)
diameter.underTree.CN.p #0.005078203
```

```
diameter.underTree.Ns.r = correlation(underTree.samples.surface$TrunkDiameter, underTree.samples.surface$PercentN)
diameter.underTree.Ns.r #0.6143001
diameter.underTree.Ns.p = pValue(underTree.samples.surface$TrunkDiameter, underTree.samples.surface$PercentN)
diameter.underTree.Ns.p #0.03767225
```

```

diameter.underTree.Nb.r = correlation(underTree.samples.subsurface$TrunkDiameter,
underTree.samples.subsurface$PercentN)
diameter.underTree.Nb.r #0.2165229
diameter.underTree.Nb.p = pValue(underTree.samples.subsurface$TrunkDiameter,
underTree.samples.subsurface$PercentN)
diameter.underTree.Nb.p #0.2479814

diameter.underTree.15N.plot = ggplot(data=underTree.samples.surface,
aes(x=underTree.samples.surface$TrunkDiameter,
y=underTree.samples.surface$StratificationRatio15N)) + geom_point()
diameter.underTree.15N.plot
diameter.underTree.stratRatio.15N.r = correlation(underTree.samples.surface$TrunkDiameter,
underTree.samples.surface$StratificationRatio15N)
diameter.underTree.stratRatio.15N.r #-0.47462
diameter.underTree.stratRatio.15N.p = pValue(underTree.samples.surface$TrunkDiameter,
underTree.samples.surface$StratificationRatio15N)
diameter.underTree.stratRatio.15N.p #0.03469739

diameter.underTree.c13.r = correlation(underTree.samples.surface$TrunkDiameter,
underTree.samples.surface$d13C)
diameter.underTree.c13.r #0.7142968
diameter.underTree.c13.p = pValue(underTree.samples.surface$TrunkDiameter,
underTree.samples.surface$d13C)
diameter.underTree.c13.p

dist.15N.linReg = bValue(soilCarbon.30m.transects.surface$AdjustedDistance,
soilCarbon.30m.transects.surface$d15N)
dist.15N.linReg
dist.15N.surface.yHats = predictions(soilCarbon.30m.transects.surface$AdjustedDistance,
soilCarbon.30m.transects.surface$d15N)
dist.15N.surface.yHats
dist.15N.surface.rmse = rmse(soilCarbon.30m.transects.surface$d15N, dist.15N.surface.yHats)
dist.15N.surface.rmse

SoilCarbonLog = read.csv("F:/SoilDataFinal3.csv")

m1 = lm(PercentOM ~ AdjustedDistance + CanopyArea + Sin + Cos, data = SoilCarbon)
summary(m1)

m2 = lm(PercentOM ~ AdjustedDistance + CanopyArea + Sin, data = SoilCarbon)
summary(m2)

m3 = lm(PercentOM ~ AdjustedDistance + CanopyMaxDiameter + Sin, data = SoilCarbon)
summary(m3)

```

```
m4 = lm(PercentOM ~ log(AdjustedDistance) + CanopyMaxDiameter + Sin, data =
SoilCarbonLog)
summary(m4)
```

```
m5 = lm(log(PercentOM) ~ log(AdjustedDistance) + CanopyMaxDiameter + Sin, data =
SoilCarbonLog)
summary(m5)
```

```
hist(log(SoilCarbonLog$AdjustedDistance))
hist(SoilCarbon$PercentOM)
hist(m3$residuals)
hist(m4$residuals)
hist(m5$residuals)
```

```
AIC(m3)
AIC(m4)
AIC(m5)
```

```
m6 = lm(log(PercentOM) ~ log(AdjustedDistance) + CanopyMaxDiameter + Sin + DepthKey,
data = SoilCarbonLog)
summary(m6)
```

```
mean(SoilCarbon$PercentOM[which(SoilCarbon$DepthKey == "S")])
mean(SoilCarbon$PercentOM[which(SoilCarbon$DepthKey == "B")])
```

```
AIC(m6)
```

```
m7 = lm(log(PercentOM) ~ log(AdjustedDistance) + CanopyMaxDiameter*DepthKey + Sin,
data = SoilCarbonLog)
summary(m7)
AIC(m7)
```

```
m8 = lm(log(PercentOM) ~ log(AdjustedDistance)*DepthKey +
CanopyMaxDiameter*DepthKey + Sin*DepthKey, data = SoilCarbonLog)
summary(m8)
AIC(m8)
```

```
m9 = lm(log(PercentOM) ~ log(AdjustedDistance)*DepthKey +
CanopyMaxDiameter*DepthKey + Sin, data = SoilCarbonLog)
summary(m9)
AIC(m9)
```

```
m10 = lm(log(PercentOM) ~ log(AdjustedDistance)*DepthKey + CanopyMaxDiameter + Sin,
data = SoilCarbonLog)
summary(m10)
AIC(m10)
```

```

m11 = lm(log(PercentOM) ~ log(AdjustedDistance) + CanopyArea + Sin, data =
SoilCarbonLog[which(SoilCarbonLog$DepthKey == "S"),])
summary(m11)
AIC(m11)
hist(m11$residuals)

m12 = lm(log(PercentOM) ~ log(AdjustedDistance) + CanopyArea, data =
SoilCarbonLog[which(SoilCarbonLog$DepthKey == "S"),])
summary(m12)
AIC(m12)

correlation = function(X,Y){
  rValue = cor(X,Y)
  return(rValue)
}

avgStEr = function(data, locs, set1, set2, set3, set4, set5, set6, set7,
set8, xlabel, ylabel){
  #OM calculations
  names.df = data.frame(ncol=1, nrow=8)
  names.df = data.frame(locs)
  averages.df = data.frame(ncol=1, nrow=8)
  averages.df = data.frame(rbind((mean(data[set1])/sqrt(length(data[set1]))),
(mean(data[set2])/sqrt(length(data[set2]))),
(mean(data[set3])/sqrt(length(data[set3]))),
(mean(data[set4])/sqrt(length(data[set4]))), (mean(data[set5])/sqrt(length(data[set5]))),
(mean(data[set6])/sqrt(length(data[set6]))),
(mean(data[set7])/sqrt(length(data[set7]))),
(mean(data[set8])/sqrt(length(data[set8])))))
  stdev.df = data.frame (ncol=1, nrow=8)
  stdev.df = data.frame(rbind(sd(data[set1]), sd(data[set2]),
sd(data[set3]), sd(data[set4]), sd(data[set5]), sd(data[set6]),
sd(data[set7]), sd(data[set8])))
  averages.final.df = data.frame(ncol=3, nrow=8)
  averages.final.df = data.frame(cbind(names.df, averages.df, stdev.df))
  #OM graph
  limits= aes(ymax = averages.final.df[,2] + averages.final.df[,3], ymin
= averages.final.df[,2] - averages.final.df[,3])
  averagegraph = ggplot(data=averages.final.df,
  aes(x=averages.final.df[,1], y=averages.final.df[,2])) +
  geom_bar(stat="identity") + geom_errorbar(limits) + labs(x= xlabel,
y=ylabel)
  return(averagegraph)
}

```

```

pValue = function(X,Y){
  #OAR: find the correlation between two data sets (assumes Y is already transposed)
  correlate = cor(X,Y)
  #OAR: use autocorrelation to find out the effective degrees of freedom for the two given data
  sets
  source("ar1.R")
  EffN = length(X) * (1 - ar1(X)*ar1(Y))/(1+ar1(X)*ar1(Y))
  EffDf = EffN-2
  #OAR: calculate the t-value for X
  if(EffDf>0){
    tVal = correlate * sqrt((EffDf/(1-correlate^2)))
    #OAR: calculate the p-value for NegEx detrended data and temperature
    pVal = pt(-abs(tVal), df=EffDf)
  }
  if(EffDf<0){
    tVal = correlate * sqrt((EffN/(1-correlate^2)))
    #OAR: calculate the p-value for NegEx detrended data and temperature
    pVal = pt(-abs(tVal), df=EffN)
  }

  return(pVal)
}

regression=function(X,Y){
  XX=t(X)%*%X
  XY=t(X)%*%Y
  B=solve(XX)%*%XY
  yHat = X %*% B
  return(yHat)
}

avgSEBins = function(data, locs, set1, set2, set3, set4, set5, set6, xlabel, ylabel){
  #OM calculations
  names.df = data.frame(ncol=1, nrow=6)
  names.df = data.frame(locs)
  averages.df = data.frame(ncol=1, nrow=6)
  averages.df = data.frame(rbind(mean(data[set1]), mean(data[set2]),
    mean(data[set3]), mean(data[set4]), mean(data[set5]), mean(data[set6])))
  stdev.df = data.frame (ncol=1, nrow=6)
  stdev.df = data.frame(rbind((sd(data[set1])/sqrt(length(data[set1]))),
    (sd(data[set2])/sqrt(length(data[set2]))),
    (sd(data[set3])/sqrt(length(data[set3]))),
    (sd(data[set4])/sqrt(length(data[set4]))), (sd(data[set5])/sqrt(length(data[set5]))),
    (sd(data[set6])/sqrt(length(data[set6])))))

  averages.final.df = data.frame(ncol=3, nrow=6)
}

```

```

averages.final.df = data.frame(cbind(names.df, averages.df, stdev.df))
#OM graph
errors= aes(ymax = averages.final.df[,2] + averages.final.df[,3], ymin
           = averages.final.df[,2] - averages.final.df[,3])
averagegraph = ggplot(data=averages.final.df,
                      aes(x=averages.final.df[,1], y=averages.final.df[,2])) +
  geom_bar(stat="identity") + geom_errorbar(errors) + labs(x= xlabel,
                                                       y=ylabel) + scale_x_discrete(limits = averages.final.df[,1])
return(averagegraph)
}

avgSE = function(data, locs, set1, set2, set3, set4, set5, set6, set7,
                 set8, xlabel, ylabel){
  #OM calculations
  names.df = data.frame(ncol=1, nrow=8)
  names.df = data.frame(locs)
  averages.df = data.frame(ncol=1, nrow=8)
  averages.df = data.frame(rbind(mean(data[set1]), mean(data[set2]),
                                  mean(data[set3]), mean(data[set4]), mean(data[set5]), mean(data[set6]),
                                  mean(data[set7]), mean(data[set8])))
  stdev.df = data.frame (ncol=1, nrow=8)
  stdev.df = data.frame(rbind((sd(data[set1])/sqrt(length(data[set1]))),
                               (sd(data[set2])/sqrt(length(data[set2]))),
                               (sd(data[set3])/sqrt(length(data[set3]))),
                               (sd(data[set4])/sqrt(length(data[set4]))), (sd(data[set5])/sqrt(length(data[set5]))),
                               (sd(data[set6])/sqrt(length(data[set6]))),
                               (sd(data[set7])/sqrt(length(data[set7]))),
                               (sd(data[set8])/sqrt(length(data[set8])))))
  averages.final.df = data.frame(ncol=3, nrow=8)
  averages.final.df = data.frame(cbind(names.df, averages.df, stdev.df))
  #OM graph
  errors= aes(ymax = averages.final.df[,2] + averages.final.df[,3], ymin
             = averages.final.df[,2] - averages.final.df[,3])
  averagegraph = ggplot(data=averages.final.df,
                        aes(x=averages.final.df[,1], y=averages.final.df[,2])) +
    geom_bar(stat="identity") + geom_errorbar(errors) + labs(x= xlabel,
                                                          y=ylabel) + scale_x_discrete(limits = averages.final.df[,1])
  return(averagegraph)
}

diameters = function(data, xlabel, ylabel, mainTitle){

borris.surface = which(underTree.samples$Tree == "T5" & underTree.samples$DepthKey ==
  "S")
zhaad.surface = which(underTree.samples$Tree == "T1" & underTree.samples$DepthKey ==
  "S")
}

```

```

larry.surface = which(underTree.samples$Tree == "T3" & underTree.samples$DepthKey ==
"S")
elijah.surface = which(underTree.samples$Tree == "T2" & underTree.samples$DepthKey ==
"S")
athena.surface = which(underTree.samples$Tree == "T4" & underTree.samples$DepthKey ==
"S")

borris.sub = which(underTree.samples$Tree == "T5" & underTree.samples$DepthKey == "B")
zhaad.sub = which(underTree.samples$Tree == "T1" & underTree.samples$DepthKey == "B")
larry.sub = which(underTree.samples$Tree == "T3" & underTree.samples$DepthKey == "B")
elijah.sub = which(underTree.samples$Tree == "T2" & underTree.samples$DepthKey == "B")
athena.sub = which(underTree.samples$Tree == "T4" & underTree.samples$DepthKey == "B")

myLabels = c("Surface Soil\nTree 5", "Subsurface Soil\nTree 5", "Surface Soil\nTree 1",
"Subsurface Soil\nTree 1", "Surface Soil\nTree 3", "Subsurface Soil\nTree 3", "Surface
Soil\nTree 2", "Subsurface Soil\nTree 2", "Surface Soil\nTree 4", "Subsurface Soil\nTree 4")
names.df = data.frame(ncol=1, nrow=10)
names.df = data.frame(myLabels)
averages.df = data.frame(ncol=1, nrow=10)
averages.df = data.frame(rbind(mean(data[borris.surface]), mean(data[borris.sub]),
mean(data[zhaad.surface]), mean(data[zhaad.sub]), mean(data[larry.surface]),
mean(data[larry.sub]),
mean(data[elijah.surface]), mean(data[elijah.sub]),
mean(data[athena.surface]), mean(data[athena.sub])))
stdev.df = data.frame (ncol=1, nrow=10)
stdev.df = data.frame(rbind((sd(data[borris.surface])/sqrt(length(data[borris.surface]))),
(sd(data[borris.sub])/sqrt(length(data[borris.sub]))),
(sd(data[zhaad.surface])/sqrt(length(data[zhaad.surface]))),
(sd(data[zhaad.sub])/sqrt(length(data[zhaad.sub]))),
(sd(data[larry.surface])/sqrt(length(data[larry.surface]))),
(sd(data[larry.sub])/sqrt(length(data[larry.sub]))),
(sd(data[elijah.surface])/sqrt(length(data[elijah.surface]))),
(sd(data[elijah.sub])/sqrt(length(data[elijah.sub]))),
(sd(data[athena.surface])/sqrt(length(data[athena.surface]))),
(sd(data[athena.sub])/sqrt(length(data[athena.sub]))))

averages.final.df = data.frame(ncol=3, nrow=10)
averages.final.df = data.frame(cbind(names.df, averages.df, stdev.df))
#OM graph
errors= aes(ymax = averages.final.df[,2] + averages.final.df[,3], ymin
= averages.final.df[,2] - averages.final.df[,3])
averagegraph = ggplot(data=averages.final.df,
aes(x=averages.final.df[,1], y=averages.final.df[,2])) +
geom_bar(stat="identity") + geom_errorbar(errors) + labs(x= xlabel,
y=ylabel) + scale_x_discrete(limits = averages.final.df[,1])
return(averagegraph)

```

```

}

#OAR: This function calculates the root mean squared given the expected values and the actual
values.
#-----
rmse = function(Y,YHat){
#OAR: calculate all of the residuals (Y-Yhat)
E = matrix(,nrow=length(Y))
for(i in 1:length(Y)){
  E=Y-YHat
}
#OAR: calculate the sum of squares, divide by the degrees of freedom, and find the square root
of the result.
ss = t(E) %*% E
ssdivDf= ss/(length(Y)-2)
answer = sqrt(ssdivDf)
return(answer)
}

avgSEStrat = function(data, locs, set1, set2, set3, xlabel, ylabel){
  names.df = data.frame(ncol=1, nrow=3)
  names.df = data.frame(locs)
  averages.df = data.frame(ncol=1, nrow=3)
  averages.df = data.frame(rbind(mean(data[set1]), mean(data[set2]),
    mean(data[set3])))
  stdev.df = data.frame (ncol=1, nrow=3)
  stdev.df = data.frame(rbind((sd(data[set1])/sqrt(length(data[set1]))),
    (sd(data[set2])/sqrt(length(data[set2]))),
    (sd(data[set3])/sqrt(length(data[set3])))))
  averages.final.df = data.frame(ncol=3, nrow=3)
  averages.final.df = data.frame(cbind(names.df, averages.df, stdev.df))
#OM graph
errors= aes(ymax = averages.final.df[,2] + averages.final.df[,3], ymin
  = averages.final.df[,2] - averages.final.df[,3])
averagegraph = ggplot(data=averages.final.df,
  aes(x=averages.final.df[,1], y=averages.final.df[,2])) +
  geom_bar(stat="identity") + geom_errorbar(errors) + labs(x= xlabel,
  y=ylabel) + scale_x_discrete(limits = averages.final.df[,1])
return(averagegraph)
}

stratRatioDiam = function(data, xlabel, ylabel, mainTitle){

  borris.surface = which(underTree.samples$Tree == "T5" & underTree.samples$DepthKey ==
    "S")
  zhaad.surface = which(underTree.samples$Tree == "T1" & underTree.samples$DepthKey ==
    "S")
}

```

```

"S")
larry.surface = which(underTree.samples$Tree == "T3" & underTree.samples$DepthKey ==
"S")
elijah.surface = which(underTree.samples$Tree == "T2" & underTree.samples$DepthKey ==
"S")
athena.surface = which(underTree.samples$Tree == "T4" & underTree.samples$DepthKey ==
"S")

myLabels = c("Tree 5", "Tree 1", "Tree 3", "Tree 2", "Tree 4")
names.df = data.frame(ncol=1, nrow=5)
names.df = data.frame(myLabels)
averages.df = data.frame(ncol=1, nrow=5)
averages.df = data.frame(rbind(mean(data[borris.surface]),
                               mean(data[zhaad.surface]), mean(data[larry.surface]),
                               mean(data[elijah.surface]), mean(data[athena.surface])))
stdev.df = data.frame (ncol=1, nrow=5)
stdev.df = data.frame(rbind((sd(data[borris.surface])/sqrt(length(data[borris.surface]))),
                           (sd(data[zhaad.surface])/sqrt(length(data[zhaad.surface]))),
                           (sd(data[larry.surface])/sqrt(length(data[larry.surface]))),
                           (sd(data[elijah.surface])/sqrt(length(data[elijah.surface]))),
                           (sd(data[athena.surface])/sqrt(length(data[athena.surface])))))

averages.final.df = data.frame(ncol=3, nrow=5)
averages.final.df = data.frame(cbind(names.df, averages.df, stdev.df))
#OM graph
errors= aes(ymax = averages.final.df[,2] + averages.final.df[,3], ymin
           = averages.final.df[,2] - averages.final.df[,3])
averagegraph = ggplot(data=averages.final.df,
                      aes(x=averages.final.df[,1], y=averages.final.df[,2])) +
  geom_bar(stat="identity") + geom_errorbar(errors) + labs(x= xlabel,
                                                       y=ylabel) + scale_x_discrete(limits = averages.final.df[,1])
return(averagegraph)

```